FACULTY OF SCIENCE AND TECHNOLOGY

MASTER'S THESIS

Study programme/specialisation: Biological Chemistry	Spring semester, 2018 Confidential
Author: Samantha Pamela Goonewardene	..... (signature of author)
Faculty supervisor: Krista Kaster External supervisor: Danila Shutemov, ConocoPhillips	
Title of master's thesis: Culture-dependent versus Culture-independent Methods for Quantifying Sulphate-Reducing Bacteria in Injection and Produced Water from the Greater Ekofisk Area	
Credits: 60 ECTS	
Keywords: qPCR, PCR, MPN, SRB, GAB, MIC, Injection water, Produced water	Number of pages: 89 + supplemental material: 11 Stavanger, 26.05.18

Abstract

Planktonic and sessile bacteria, in particular sulphate-reducing bacteria (SRB), in the petroleum industry can be damaging to top-side facilities, pipelines and reservoirs. Development of microbial influenced corrosion (MIC), loss of production through reservoir souring, generation of H_2S gas and degradation of petroleum products, are some of the main concerns, due to the growth of deleterious microorganisms. These problems can be reduced through appropriate bacteriological monitoring and management.

This study has compared the culture-dependent most probable number (MPN) method with the culture-independent quantitative PCR (qPCR) method, for quantifying SRB in injection and produced water from the Greater Ekofisk Area. Further, a qPCR protocol for absolute quantification of SRB was developed. In addition, detection of general aerobic bacteria (GAB) was performed using MPN. Injection and produced water samples were taken over a period of 7 months from the offshore installations Eldfisk 2/7B, Eldfisk 2/7E, Ekofisk 2/4VB and Ekofisk 2/4J.

The final standard curve used for quantification was developed with plasmid DNA containing the PCR insert of the dissimilatory sulphite reductase B (dsrB) gene from produced water. SRB was detected by qPCR using dsrB specific primers and the limit of detection (LOD) was 10^3 dsrB copies/µl. qPCR quantified SRB in both injection (10^5-10^6 copies/µl) and produced water (10^7-10^8 copies/µl). SRB was not detected by MPN, whereas GAB was detected in both injection and produced water.

Results in this study documents that qPCR is more suitable for detection and quantification of SRB compared to the MPN method and could be beneficial for application at Ekofisk. With the developed qPCR assay, quantitative and objective bacteriological results at Ekofisk can be obtained within a few hours, rather than 30 days as with the MPN method currently applied. Injection water from Ekofisk 2/4VB indicates higher bacterial numbers, and measures should be taken to reduce the microbial flora, to further prevent MIC. Except for Ekofisk 2/4VB, other sampling locations for injection water did not show any signs of bacterial growth, indicating a highly efficient injection water treatment system.

Acknowledgements

I would like to thank my internal supervisor at the University of Stavanger, Assoc. Prof. Krista Kaster, for project description, advice, practical guidance and academic feedback. I would also like to thank my external supervisor at ConocoPhillips, Danila Shutemov, for coordinating water sampling, providing information about injection water treatment systems and academic feedback.

In addition, I would like to thank Trond M. Schei, ConocoPhillips, for introducing me to the company.

Table of contents

List of figures

List of tables

Abbreviations and Acronyms

BLAST - Basic Local Alignment Search Tool
Cq - Quantification cycle
DNA - Deoxyribonucleic acid
DsrA - Dissimilatory sulphite reductase A
DsrB - Dissimilatory sulphite reductase B
DSHPSP - Downstream High Pressure Separator
DSLPSP - Downstream Low Pressure Separator
DS UV - Downstream Ultraviolet
DS DA - Downstream Deaerator
dsDNA - double stranded DNA
EOR - Enhanced Oil Recovery
EPS - Extracelluar Polymeric Substance
GAB - General Aerobic Bacteria
hNRB - Heterotrophic Nitrate-reducing Bacteria
IOR - Improved Oil Recovery
IRIS - International Research Institute of Stavanger
KPI – Key Performance Indicator
LOD – Limit of Detection
MIC - Microbiologically Influenced Corrosion
MPB - Modified Postgate B
MPN - Most Probable Number
MMM - Molecular Microbiological Methods
mRNA - messenger RNA
NCBI – National Center for Biotechnology Information
NTC - No Template Control
PAH - Polyaromatic Hydrocarbon
PDB - Phenol Red Dextrose Broth
PCR - Polymerase Chain Reaction
qPCR - Quantitative Polymerase Chain Reaction
RNA - Ribonucleic Acid
RpoB – RNA Polymerase subunit B
RT-qPCR – Reverse Transcriptase qPCR
soNRB - Sulphide-Oxidizing Nitrate-reducing Bacteria
SRB - Sulphate-reducing Bacteria
SRM – Sulphate-reducing Microorganisms
SRP - Sulphate-reducing Prokaryotes
ssDNA - single stranded DNA
THPS – Tetrakishydroxymethyl phosphonium sulphate
US FF - Upstream Fine filters
WH - Wellhead
USHPSP - Upstream High Pressure Separator
USLPSP - Upstream Low Pressure Separator

1. Introduction

The petroleum industry is often faced with challenges related to a diverse microbial flora within water systems, which can raise concerns regarding microbial influenced corrosion (MIC), degradation of petroleum products, safety due to H_2S gas, loss of production and damage to reservoirs through souring (Skovhus et al., 2012). Both planktonic and sessile microbes are present in the water systems (Spark and Mutch, 2002), which can cause corrosion in anoxic environments and may lead to high economic costs for the petroleum industry (Enning et al., 2012). Sulphate-reducing bacteria (SRB) are one of the main contributors, and the estimated cost for MIC by SRB alone is approximately 100 million US dollars in the US every year (Jhobalia et al., 2005). In addition, general aerobic bacteria (GAB)/facultative anaerobic acid-producing heterotrophic bacteria can also be damaging to oil systems by contributing to corrosion (Spark and Mutch, 2002) by polymer precipitation and acid production (Alkindi et al., 2007). Thus, it is important to monitor both SRB and GAB to avoid downstream contamination of water injection systems (Spark and Mutch, 2002). Regular monitoring includes enumeration of SRB, inspection of metal surfaces and water analysis. Water analysis only gives an indication of SRB numbers, because only planktonic microorganisms are identified (Hurst et al., 2007).

Culture-dependent and culture-independent methods are the two main approaches used to detect the presence of bacteria. A widely used culture-dependent method is the most probable number (MPN) (Smits et al., 2004). Culture-dependent methods are considered conventional but are laborious and time-consuming due to slow growth of bacteria (up to 30 days) and are not very accurate regarding quantity and the types of bacteria present (Ben-Dov et al., 2007). Merely 0.001-15% of the viable bacteria can be cultured by conventional methods (Larsen et al., 2008).

A more rapid and accurate method for monitoring and quantifying bacteria is necessary to detect bacteria that might be involved in MIC and reservoir souring, and culture-*independent* methods such as qPCR meet these requirements. The petroleum industry is therefore looking into the development of culture-independent methods to quantify and identify bacteria that may be associated with reservoir souring or MIC (Larsen et al., 2008). Quantitative polymerase chain reaction (qPCR) is a well-known culture-independent method within the field of molecular microbiological methods (MMM) and can quantify the number of microorganisms present (Larsen et al., 2010; Larsen et al., 2011).

A comparison of the MPN method with the qPCR method for quantifying SRB in injection water and produced water from the Greater Ekofisk Area was performed. A qPCR protocol for absolute quantification of the functional dsrB gene in SRB was developed in this study. In addition, general aerobic bacteria (GAB) detection was performed using MPN.

2. Objectives

The *primary* objective of this thesis is to compare the culture-dependent MPN method with the culture-independent qPCR method, for quantification of SRB in injection water and produced water from the Greater Ekofisk Area, operated by ConocoPhillips. The *secondary* objective is to develop a qPCR protocol for absolute quantification of SRB. Water samples were taken over a period of 7 months (September 2017 to March 2018). All laboratory experiments were conducted at the Department of Chemistry, Bioscience and Environmental Engineering, University of Stavanger.

3. Background

This chapter will give a general overview of water injection treatment, SRB and their influence with regards to MIC, corrosion prevention using biocides and finally, theory regarding methods used in this thesis for quantification of SRB and GAB.

3.1 Microbial populations and nutrients in the oil reservoir

Microbial populations in reservoir waters are generally not very high and can vary from a few cells to 10^4 bacteria/ml. The low densities may be due to nutrient limitations or other biological parameters. The major limiting nutrient in oil reservoirs is phosphorus, whereas nitrogen is found in abundance. Dissolved oxygen is not found in the oil reservoir, causing anaerobic microorganisms to grow. Sulphate and carbonate are found at varying concentrations in the stratal waters and can be used as growth substrates for different metabolic processes such as sulphate reduction, fermentation, methanogenesis and homoacetogenensis. During sulphate reduction and fermentation, electron donors derive from organic molecules. Thus, organic compounds such as acetate, along with formate, butyrate, propionate and benzoate are often detected in many oil reservoirs and can be used for microbial growth (Ollivier and Magot, 2005).

3.2 Oil recovery mechanisms

The three main steps in oil recovery include primary, secondary and tertiary recovery. During primary recovery, the reservoir pressure is high enough for oil and gas to drift to the surface, however, as production continues, the reservoir pressure drops progressively, and secondary recovery becomes necessary. Approximately 10% of oil is produced by primary recovery. Secondary recovery consists of water injection (into the aquifer) or injection of gas (into the gas cap), to uphold the reservoir pressure for increased oil recovery. Finally, tertiary recovery involves improved oil recovery (IOR) which includes processes such as enhanced oil recovery (EOR). EOR aims to increase oil production by improving oil flow and sweep in the reservoir (Ollivier and Magot, 2005).

3.3 Water injection

Seawater injection is a common procedure on offshore installations in the North Sea (Hoffmann and Spark, 2012) and involves injecting water into the reservoir through an injection well. It is vital that injection water is of high quality and therefore it is treated on offshore installations prior to injection. Treatments involve chlorination, filtration, UV sterilization and the removal of oxygen to eliminate unwanted material that may have adverse effects in the reservoir. Inadequate treatment of injected water can lead to formation damage, which may result in reduced production (Rochon et al., 1996). After treatment, water free of solids and oil, where microorganisms have been significantly reduced, and is non-scaling, is injected into the reservoir using high pressure and occasionally high temperatures (Patton, 1990; Hoffmann and Spark, 2012). Chemical composition, dissolved gases, corrosivity, suspended solids, oil content and bacteria are some aspects of injection water that need to be monitored and controlled (Patton, 1990).

A typical water injection system includes seawater pumps, filters, UV sterilizer, vacuum deaerators, injection booster pumps, injection pump accumulator, water injection pumps and seawater injection well (Hoffmann and Spark, 2012). SRB and GAB growth is most prevalent in and around the vacuum deaerator towers and in the injection wells (Spark and Mutch, 2002). Figure 3.1 shows a simplified seawater injection treatment system. Deaerated seawater contains high concentrations of sulphate, around 2700 mg/l, making it possible for sulphate-reducing prokaryotes (SRP) to grow and thrive within seawater injection systems. Both thermophilic and mesophilic sulphate reducers can be present in injection systems. Sulphate is present in high enough concentrations in injection water to stimulate the growth of SRB, whereas carbon, phosphorus and nitrogen are present in low concentrations in seawater (Hoffmann and Spark, 2012).

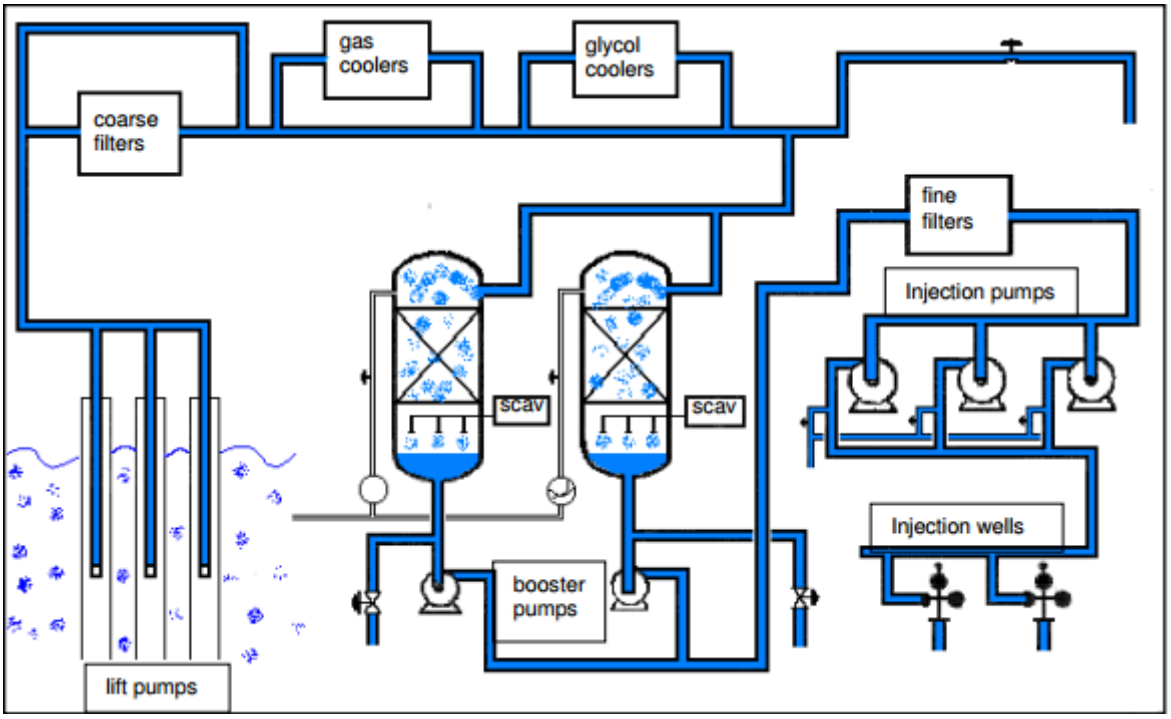

Figure 3.1: Simplified illustration of a seawater injection treatment system (Hoffmann and Spark, 2012).

3.3.1 ConocoPhillips water injection treatment system

Seawater is lifted by 3 seawater pumps to Ekofisk 2/4K (from 17 m depth) and 4 seawater pumps to Eldfisk 2/7E (from 50 m depth). Hypochlorite is then added at the seawater intake, and the water passes through fine filters that remove particles larger than 2 µm. To aid the filtration, flocculant is added continuously upstream the fine filters, and biocide is injected in batches upstream the fine filters to remove organics that survived the hypochlorite treatment. Following filtration, water is sterilized by UV-radiation. Afterwards, water is passed through two vacuum deaerator towers, which reduce foaming during water injection into the reservoir. Downstream the vacuum deaerator towers, a second batch of biocide is injected. In addition, antifoam is added to improve deaeration. The water is now ready to be injected into the reservoir (ConocoPhillips, 2018). A simplified flow diagram of the Ekofisk 2/4K water injection treatment system is shown in figure 3.2.

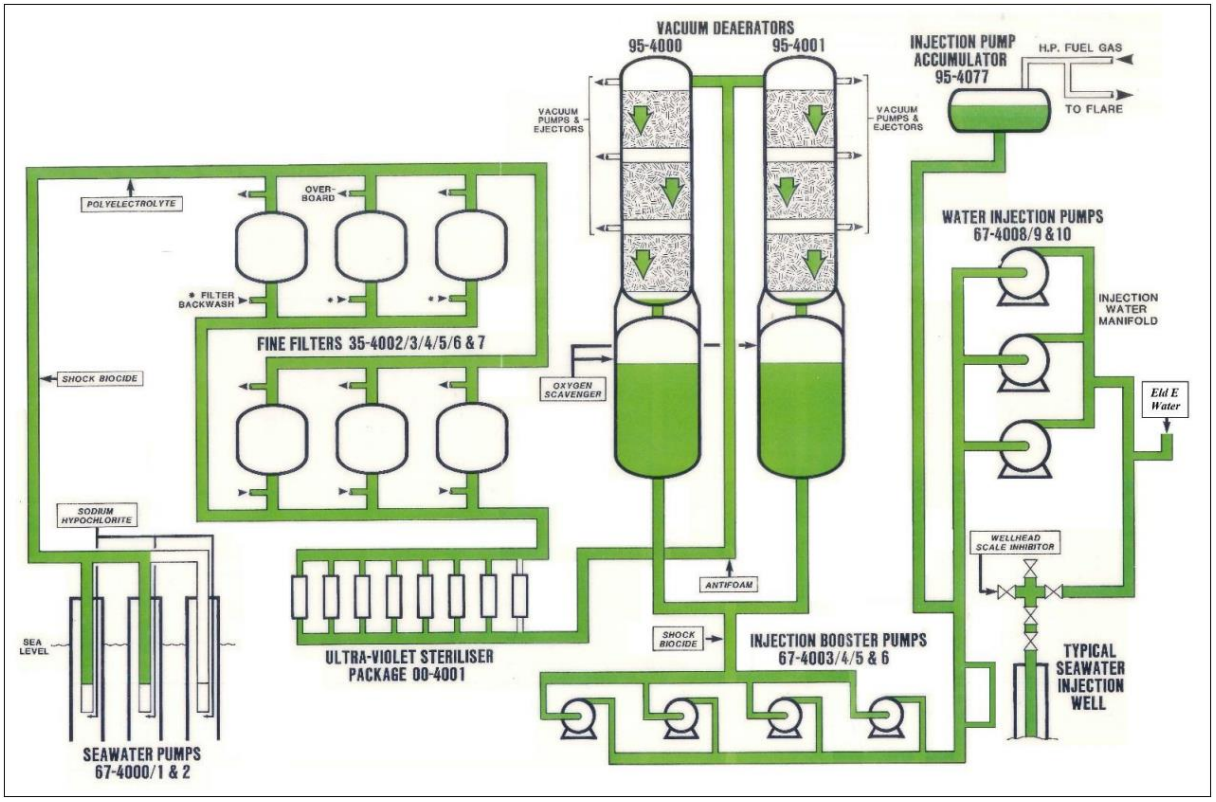

Figure 3.2: Simplified flow diagram of the Ekofisk 2/4K water injection treatment system (ConocoPhillips, 2017).

Ekofisk 2/4K treats 1/3 of the total injection water and distributes the water to Ekofisk 2/4K and Ekofisk 2/4VA. Eldfisk 2/7E treats 2/3 of the total injection water and distributes the water to Eldfisk 2/7A, Eldfisk 2/7B, Eldfisk 2/7S, Ekofisk 2/4VA, Ekofisk 2/4VB and Ekofisk 2/4K. Eldfisk 2/7A, Eldfisk 2/7B and Eldfisk 2/7S share the same distribution pipeline from Eldfisk 2/7E. The pipeline from Eldfisk 2/7E to Eldfisk 2/7B is 6.2 km long. Ekofisk 2/4K and Ekofisk 2/4VB share the same distribution pipeline until a junction 24.6 km downstream Eldfisk 2/7E. The tie-in from the junction to Ekofisk 2/4VB is 5 km long. Both Ekofisk 2/4VA and Ekofisk 2/4VB are subsea injection manifolds and are connected with Ekofisk 2/4M through an umbilical. Pigging helps to remove particles and biofilms from pipelines and is routinely performed between Eldfisk 2/7E and Ekofisk 2/4K and between Eldfisk 2/7E and Eldfisk 2/7B (ConocoPhillips, 2018). An illustration of the distribution of injection water in the Greater Ekofisk Area is presented in figure 3.3.

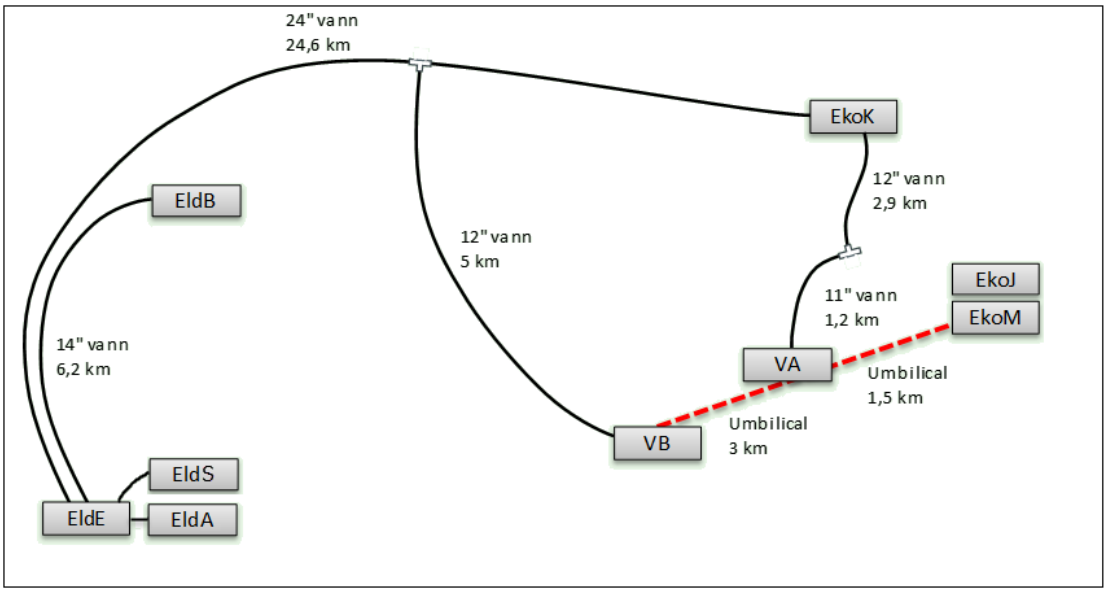

Figure 3.3: Map of injection water distribution in the Greater Ekofisk Area (ConocoPhillips, 2018).

3.4 Produced water

Formation water occurs in the reservoir and is termed produced water when brought to the surface along with oil and gas. In addition, injected water can reach the production wells and further contribute to the produced water flow (Veil et al., 2004). Produced water is a waste product in the petroleum industry, and contains several organic and inorganic compounds, making discharge problematic in terms of pollution. Both mechanical and biochemical treatment of produced water is necessary to minimize its polluting effects, by removal of suspended and dissolved compounds (Ahmadun et al., 2009). Produced water is anaerobic and rich in nutrients, thus supporting SRB growth (Nihalani et al., 2010).

3.5 Sulphate reducing microorganisms

Sulphate-reducing microorganisms (SRM)/SRB comprise all unicellular microorganisms that efficiently reduce sulphate to sulphide. SRB are a group of obligate anaerobes that obtain energy by oxidizing organic matter by using sulphate as the external electron acceptor and drive their metabolism by respiring sulphate and producing sulphide. In lack of sulphate, some strains can operate as fermenters and use pyruvate to produce acetate, hydrogen and carbon dioxide. SRB have similarities to denitrifying bacteria, but they are all strict anaerobes (Jhobalia et al., 2005) and they have been found in every anaerobic environment studied (Ollivier and Magot, 2005).

Sulphate, including thiosulphate, sulphur and sulphite are used as terminal electron acceptors, whereas, hydrogen or organic compounds serve as electron donors. This reaction is called dissimilatory sulphate reduction (Ollivier and Magot, 2005):

$4AH_2 + SO_4^{2-} + H^+ \rightarrow 4A + HS^- + 4H_2O$

Dissimilatory sulphate reduction is an important step in the global sulphur cycle, which evolved approximately 3.47 billion years ago, and is facilitated by SRP, where SRB are central (Barton et al., 2014). The Dissimilatory sulphite reductase (Dsr) enzyme is present in all SRP and the genes encoding this enzyme can be detected as functional groups. When metabolic pathways are shared by microorganisms in a specific system, they are defined as a functional group. In this case, the functional group studied have the ability to reduce sulphate to hydrogen sulphide (Whitby and Skovhus, 2009).

The morphology of SRB is diverse and have shapes which can include spheres, rods and vibrio. There are two main metabolic groups of SRB. The first group, the complete oxidizers, involves complete oxidation of its substrates to CO_2. The second group, the incomplete oxidizers, involves incomplete oxidation of its substrates to CO_2 and acetate. The complete oxidizers oxidize fatty acids and aromatic compounds and the incomplete oxidizers rarely oxidize fatty acids. In the last step of sulphate reduction to sulphide, there is a 6-electron transfer to sulphite. The electron transfer process is mediated by bisulphite reductase, also called (Dsr). There are several types of Dsr enzymes in SRB, such as desulfoviridin, desulfofuscidin, desulfoforubidin and P582 (Ollivier and Magot, 2005). The central Dsr enzyme of SRB is encoded by the dsrAB gene, which encodes both the α and β subunit of dsr and is highly conserved in SRB (Zhu et al, 2005). The functional dsrAB gene can be used to identify SRB by using dsrAB-specific primers (Ben-Dov et al., 2007). The number of dsr genes found in an experiment correlates to the number of SRB, since the dsr gene is found in one copy per SRB (Whitby and Skovhus, 2009). *Desulfovibrio* is the most extensively studied genus of SRB, as it is the most easily cultivated sulphate reducer (Barton et al., 2014).

SRB can be found naturally in oil reservoirs or can be introduced during operations through secondary recovery. Produced sulphide by SRB can remain in the reservoir and cause oil souring and plugging, in addition, top-side facilities such as water tanks and pipelines may also be affected (Gieg et al., 2011). Uncontrolled growth of SRB can lead to toxicity and deterioration of oil and gas (Al-Hashem et al., 1998). In addition to corrosion and plugging, reservoir souring is a major concern in seawater systems and is particularly challenging to prevent. Large amounts of biocides can be injected, but often it is not technically and economically feasible (Patton, 1990).

In order for biological souring to take place, sulphate, carbon and energy sources must be present (Liamleam and Annachhatre, 2007) in addition to trace metals, correct temperature and viable microbes (Kuijvenhoven et al., 2006). Souring can take place close to the water injection well. In this area, the temperature lies between 50-70 °C, due to mixing of cold seawater and hot reservoir fluids, supporting SRB activity (Bødtker et al., 2009; Kaster et al., 2007).

3.6 Microbiologically influenced corrosion

Corrosion is a deterioration of materials such as iron and steel and is considered a world-wide problem. Corrosion affects many industries including shipping, construction, drinking water treatment plants and the petroleum industry (Kip and van Veen, 2015). The corrosion process is characterized by the development of metal pitting and black crusts caused by production of H_2S and cathodic H_2 (Enning et al., 2012).

When solid metals such as Fe dissolve into metal ions (Fe^{2+}) and electrons (oxidation), metal corrosion takes place. Hydrogen (H_2) can be formed in oxygen-free systems when electrons react with free protons (H^+) in the water (reduction). Fe^{2+} can dissolve in water or precipitate as iron sulphide after reacting with sulphide. During electron and metal-loss from electron-conducting metal alloys, an anode ($Fe^0 \rightarrow Fe^{2+}$) and a cathode (e^- loss) will be formed. SRB and methanogens have the ability to utilize electrons in the form of H_2, released from the cathode and cause further corrosion (Skovhus et al., 2012). The process of MIC by SRB is illustrated in figure 3.4.

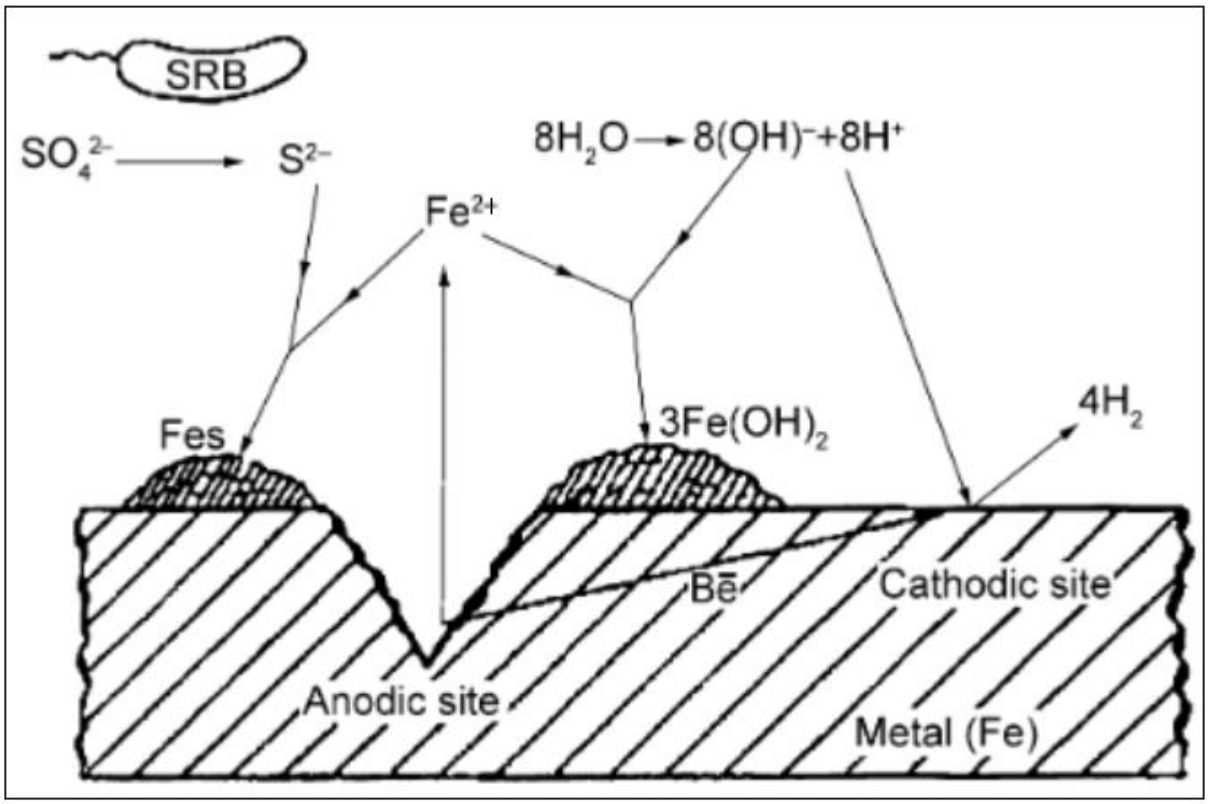

Figure 3.4: Illustration of MIC by SRB (Javaherdashti, 2008).

Regular electrochemical corrosion will not usually occur under anaerobic settings due to the accumulation of hydrogen that causes polarization of the cathode. However, SRB can stimulate electrochemical corrosion by:

(i) Utilizing enzymes to remove the build-up of hydrogen around the cathode.
(ii) Iron sulphide formation which is cathodic to steel.
(iii) Formation of elemental sulphur when sulphides are reoxidized.
(iv) Iron phosphide formation by SRB.

Where (i) and (ii) are the most frequently occurring (Al-Hashem et al., 1998).

MIC may be defined as electrochemical corrosion which includes microbes initiating, enabling or accelerating the corrosion reaction. Iron, copper and ferrous alloys are subject to MIC (Jhobalia et al., 2005). Corrosion caused by SRB is often characterized by pitting attack and these pits are generally filled with iron sulphides, which is a typical corrosion product (Videla et al., 2005). MIC can adversely affect pipelines in the petroleum industry, and it is not as easily observed as rusting of iron in air but occurs in areas that are more hidden, such as the interior of pipes (Enning et al., 2012). The combination of dissolved iron concentrations, nutrient restrictions and fluid

dynamics together constitute the effect SRB have on MIC (Jhobalia et al., 2005). In addition, MIC can cause explosions, hazardous chemical waste and environmental damage (Duncan et al., 2009). MIC as a degradation process has been known since 1934 (von Wolzogen Kuhr and van der Vlught, 1934), but was not recognized fully until the 1980s (Pope et al., 1988). There are several microorganisms that can contribute to MIC, including hydrogen-utilizing methanogens, iron-reducing bacteria, syntrophic bacteria, peptide-fermenting bacteria, sulphur-reducing bacteria (Zuo, 2007), nitrate-reducing bacteria (Xu and Gu., 2014) and as mentioned, SRB (Zuo, 2007). It has been established that SRB is the main contributor to MIC (Enning et al., 2012), however, not all the specific microorganisms causing MIC have been categorized. There is no consensus on the dynamic function of these microorganisms and thereby there are difficulties associated in monitoring and treating MIC (Duncan et al., 2009).

3.7 Corrosion prevention and Biocides

Present-day corrosion prevention deals with inhibition of microbial growth and metabolism. Corrosion prevention includes physical cleaning (pigging), coatings and electrochemical restriction, however, biofilms tend to be resistant to established treatments (Kip and van Veen, 2015). It is necessary to monitor and detect microbial activity to ensure safety and longevity of equipment (Hurst et al., 2007).

3.7.1 Biocides

According to the Council of the European Union (1998), a biocide is defined as a chemical or biological substance that is applied with the intention to destroy or control unwanted organisms. To achieve the most efficient control of microbial activity, mechanical cleaning can be used in conjunction with biocides. The criteria for an effective biocide treatment include targeting specific bacteria in the system, ensuring appropriate conditions and that biocides do not change the characteristics of reservoir fluids, and lastly the biocide must be economically feasible and have low toxicity levels towards higher organisms (Ollivier and Magot, 2005).

Oxidizing biocides include chlorine, chlorine dioxide, hypochlorite, ozone, bromine and hypobromide. Nonoxidizing biocides include aldehydes (such as acrolein, glutaraldehyde and formaldehyde), quaternary amines (alkyl and benzyl derivatives), tetrakishydroxymethyl phosphonium sulphate (THPS), 2,2-dibromo-3-nitrilopropionamide and bronopol (Ollivier and Magot, 2005).

Nitrate treatment is a relatively new method that can be used to reduce the sulphide concentration produced by SRB and enhances the activity of heterotrophic and sulphide-oxidizing nitrate-reducing bacteria (hNRB and soNRB, respectively) (Voordouw et al., 2009). Nitrate has promising features and can replace biocides in limiting SRB activity and reservoir souring. Nitrate prevents sulphates conversion to sulphide or it can react with sulphide and reverse it to sulphate by the help of microbes. Olliver and Magot (2005) revealed that nitrate may not effectively control biofouling which may lead to plugging. In fact, Voordouw et al. (2002) and Dunsmore et al. (2004) discovered that nitrate treatment might support MIC, accordingly, the adverse effects are to be taken into consideration.

Biocides operate by chemical attack, including precipitation of proteins, solubilisation of lipids and several attacks on the bacterial cell. If resistance to a biocide is to occur, the bacterium needs to have a considerable number of mutations to change the structure of its proteins. Such a high mutation rate is unlikely to occur in industrial settings. When biocides no longer seem to be as effective, this is most likely due to a change in the dosing routine, system parameters (such as pH and temperature), change of the manufacturer of the biocide, the biocide treatment may never have been optimised or an increase in biological activity which increases the need for additional biocide (Al-Hashem et al., 2004). Batch and low-level treatments may both contribute to resistant bacteria and suitable monitoring must be established (Al-Hashem et al., 1998). It is important to know whether the bacteria of interest are mesophilic, thermophilic or hypothermophilic. The bacteria in these groups may be related and have comparable metabolic pathways, but they have distinct enzymes that protect them against the denaturing effects of too high or too low temperatures. Biocides have a temperature optimum, and therefore temperature is an important parameter to take into account (Al-Hashem et al., 2004).

Large amounts of seawater undergo biocide treatment and is deoxygenated prior to water injection to avoid bacterial growth (Voordouw et al., 2009). On a standard sized platform up to 12,000 m^3/day of seawater can be treated. Lack of microbial growth control may have a negative effect on the asset integrity (Skovhus et al., 2012). Advances within MMM help to find biocides which target specific microbes (Whitby and Skovhus, 2009).

3.7.2 ConocoPhillips biocide treatment

At Ekofisk 2/4K and Eldfisk 2/7E biocide is injected into the injection water treatment system at two locations, upstream the fine filters (500 ppm) and downstream the deaerator towers (1,000 ppm). The biocide injection lasts for one hour and is applied 3 times a week at Ekofisk 2/4K and 5 times a week at Eldfisk 2/7E. Glutaraldehyde is the primary biocide currently in use (ConocoPhillips, 2018).

3.8 Biofilms

When surfaces are present, bacteria will often adhere and a three-dimensional biofilm-structure will develop (Bridier et al., 2011). Biofilms consist of microbes, polysaccharides, water, nutrients, and metabolic waste, that together can form several distinct microenvironments (Branda et al., 2005). Biofilms can grow under varying environmental conditions with respect to temperature, pH, nutrient availability, water activity, toxicity and pressure (Ollivier and Magot, 2005). Biofilms are comprised of microcolonies, which include one or several types of species and even within these microcolonies the extracelluar polymeric substance (EPS) differs, creating unique microcolonies (Costerton, 1999). Multispecies biofilms bring about the most damaging corrosion and the complex interactions between species may stimulate biochemical reactions in both anoxic and oxic sections of the biofilm, which intensifies the corrosion process (Kip and van Veen, 2015).

Biofilms can be problematic with regards to operations, maintenance and lifespan of oil fields. Issues caused by biofilms include plugging of reservoir rock, filters and reduction in flow capacity, leading to MIC (Ollivier and Magot, 2005). Biofilms can be controlled to a certain extent with biocides, commonly chlorine, but the biofilm matrix helps to protect against biocides (De Beer, 1994). Biofilms are shielded against biocide treatment and will only be affected when higher biocide concentrations are used (Brown et al., 1993). Within the biofilm, lateral gene transfer aids in the adaption process (Bridier et al., 2011). The biofilm population (sessile) is diverse compared to that of a planktonic population, due to higher rates of mutation and selection (Bridier et al., 2011). To reduce resistance to biocide treatment, two different biocides can be used alternatively to achieve synergistic effects (Hurst et al., 2007). The biocide must penetrate the biofilm to reach the bacteria (including SRB) and this requires optimised dose rate and contact time (Ollivier and Magot, 2005). The activity of SRB is increased within biofilms and they thrive at the seawater/steel interface (Videla et al., 2005). In addition, GAB can aid in biofilm development (Alkindi et al., 2007). Figure 3.5 shows biofilms in pipes.

Figure 3.5: Biofilms in pipes (Hoffmann and Spark, 2012).

3.9 Detection and quantification of bacteria

3.9.1 PCR

Polymerase chain reaction (PCR) is a widely used method for amplifying a specific DNA sequence. PCR consists of three stages which are repeated 30-35 times. The first stage is a denaturation, where the temperature is raised to 95°C, creating single stranded DNA (ssDNA). The second stage is annealing, where the temperature is lowered to approximately 55°C, allowing primers to attach. The annealing temperature (T_a) depends on primer length and composition and must be optimised prior to the PCR run. Finally, elongation takes place, the temperature is raised to 72°C and DNA polymerase copies ssDNA from the attached primers and produces double-stranded DNA (dsDNA). Once the elongation is completed, a new cycle begins and the recently copied DNA, working as starting material, makes the reaction exponential (Whitby and Skovhus, 2009). Exponential growth is achieved in the early cycles, but cannot be maintained throughout, especially when ng/µl amounts are present (Edwards et al., 2004). PCR increases the concentration to $>10^9$ copies, a detectable amount (Skovhus et al., 2009). Post PCR, the PCR products are run on an agarose gel and visualised under UV light, thereby making it a semi-quantitative, end-point method (Whitby and Skovhus, 2009). Due to PCR bias and limitations, end-point and initial DNA concentration is not proportional, and therefore conventional PCR is not recommended for quantitative analysis (Kim et al., 2013). Figure 3.6 shows the different stages of a PCR cycle.

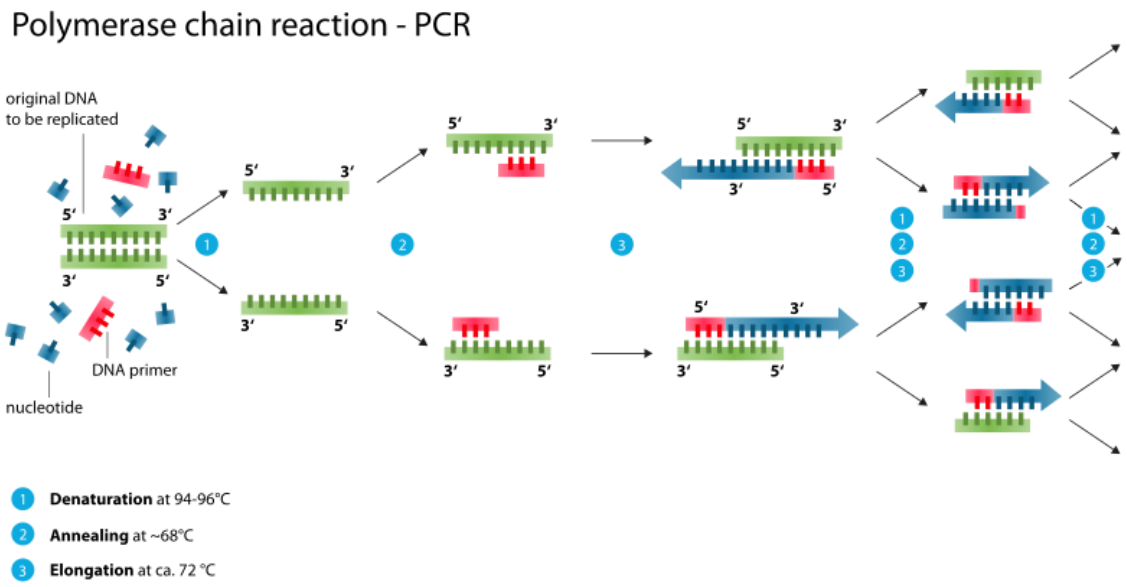

Figure 3.6: Overview of the different stages of PCR (Society for Mucosal Immunology, 2014).

3.9.2 qPCR

qPCR is a highly sensitive method applied in a wide range of disciplines. It is known for its speed and specificity in quantifying nucleic acids in *real-time* (Bustin et al., 2009). qPCR is considered an effective tool for quantifying bacteria in environmental samples and can detect down to genus and species level, both relative and absolute quantities. Such detailed information is difficult to acquire from conventional culture-dependent methods, such as MPN (Whitby and Skovhus, 2009). By using qPCR, PCR amplification and detection are narrowed down to a single step, eliminating the need for time-consuming gel electrophoresis (Thermo Fisher Scientific, 2016). Further, qPCR is not able to distinguish between live and dead cells and it can therefore be problematic to conclude bacterial activity from the cell numbers (Whitby and Skovhus, 2009). On the other hand, reverse transcriptase qPCR (RT-qPCR) can quantify mRNA for the estimation of microbial activity (Bustin, 2008). Sequence specific primers are also required and therefore qPCR cannot detect uncharacterized sequences (Kim et al., 2013).

qPCR utilises fluorescent dyes to label PCR products. The qPCR instrument measures the accumulation of these fluorescent dyes during the exponential phase of the cycle and provides a quantitative analysis of the PCR products. Labelling of the PCR products with fluorescent dyes can be done using either TaqMan™ fluorogenic probes or SYBR® Green I dye. The former is a target-specific oligonucleotide that will produce a fluorescent signal only when the target DNA is amplified during detection (Thermo Fisher Scientific, 2016), and the latter will bind to the minor groove of dsDNA and will fluoresce only when bound (Life Technologies™, 2012). When

attached to dsDNA, the SYBR® Green I dye absorbs and emits light at 440 nm and 520 nm, respectively (Valasek and Repa, 2005). For both SYBR® Green I and TaqMan™, the fluorescent signal is proportional to the amount of target DNA**.** In qPCR reactions, primers and DNA polymerase are used in excess, thereby making the target sample the limiting factor (Thermo Fisher Scientific, 2016). The SYBR® Green I assay is widely used in the industry and research to identify and quantify microorganisms (Zhu et al., 2005). A drawback of using SYBR® Green I assay is its lower specificity compared to the TaqMan® probe, because it cannot distinguish between target and non-target DNA (Life Technologies™, 2012). Figure 3.7 illustrates SYBR® Green I detection chemistry.

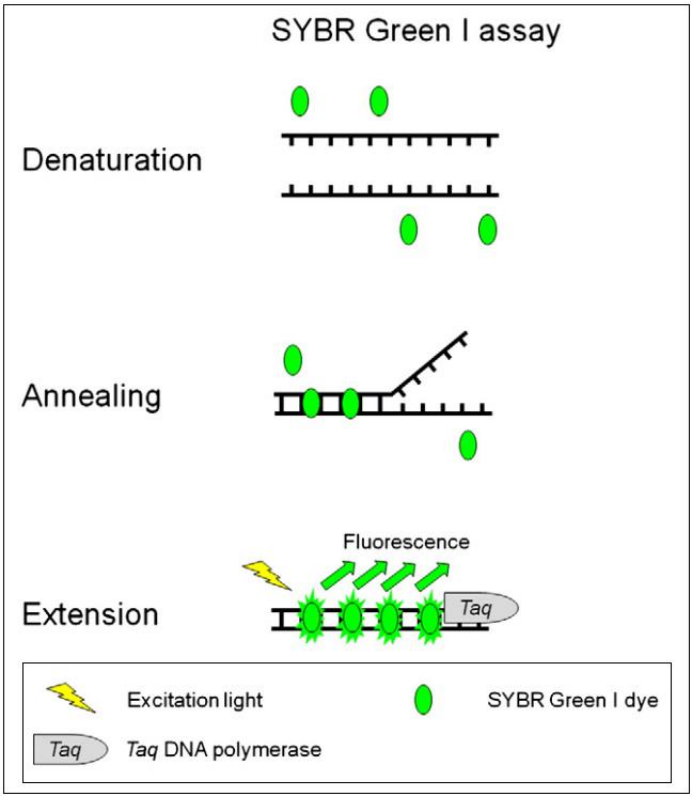

Figure 3.7: SYBR Green I assay detection chemistry (Kim et al., 2013).

qPCR results can be expressed either in an absolute or relative manner. Absolute quantification is widely used within microbiology and requires that an external standard is used, and that amplification efficiency remains the same in all samples and standards. Absolute quantification targets a single sequence and results in an *absolute* value, also called copy number. In relative quantification, mRNA variation between samples can be expressed by comparison to internal controls (Whitby and Skovhus, 2009). According to Dhanasekaran et al. (2010) absolute quantification is a more reliable and informative method for comparison.

Standard curve

A high quality standard curve is essential when performing absolute quantification. Standard curves can be constructed using PCR-amplified target sequences, target sequences inserted into plasmids or commercially available DNA (Dhanasekaran et al., 2010). The standards should always expand throughout the range estimated in the experiment with a minimum of four points and the maximum increment between the points should be $\log_{10}$. Secondary structures should not be present in the standards, as the occurrence of secondary structures may impede the DNA polymerase and result in reduced amplification efficiencies (Life Technologies™, 2012).

The optimal procedure would include a standard curve for each run to obtain the highest quantitative information. However, a standard curve that is run periodically to detect any drift, may be satisfactory. Product threshold levels in qPCR is achieved by plotting the fluorescence against the cycle number (Edwards et al., 2004). To achieve high efficiency, the quantification cycle (Cq) values should be <40 (Bustin et al., 2009). By plotting $\log_{10}$ of template starting quantity against Cq values, a standard curve is made by linear regression (Taylor et al., 2010). The standard curve is then used to quantify unknown samples by interpolation (Life Technologies™, 2012). The R^2 (coefficient of determination) value from the standard curve indicates data linearity (Taylor et al., 2010) and reproducibility (Life Technologies™, 2012). The desired R^2 value is >0.95 (Kim et al., 2013). Linearity denotes variability between replicates and in which degree the efficiency is similar between the different starting sample concentrations (Taylor et al., 2010).

qPCR efficiency shows to which extent the reagents have been converted to amplicon, where 100% efficiency is achieved by a 2-fold increase of amplicon per cycle (Taylor et al., 2010). Low efficiency (<90%) can result in PCR artefacts, and can be caused by Taq inhibitors, inaccurate T_a, sub-optimal concentrations of reagents, secondary structures or incorrectly designed primers. High efficiency (>110%) can be caused by non-specific amplicons or primer-dimers. T_a is critical and should be optimised to prevent primer-dimers and non-specific annealing (Life Technologies™, 2012; Taylor et al., 2010). Both pipetting technique and pipette calibration are critical to avoid both high and low efficiency (Taylor et al., 2010).

Efficiency is given by (Kim et al., 2013):

$$E = 10^{\frac{-1}{slope}} - 1 \qquad \text{Eq. 1}$$

Where E is the efficiency and the slope value should lie between -3.58 and -3.10, corresponding to an efficiency between 90 and 110% (Life Technologies™, 2012).

Initially, there is less fluorescent signal detection, and it increases as the reaction continues. The exponential phase of the amplification starts as the reaction passes the threshold level. This threshold level gives the Cq value of each reaction. Cq values and starting DNA template are inversely proportional. The theoretical limit of detection (LOD) is indicated by the y-intercept value. In theory, qPCR should be able to detect a single copy, but a copy number between 2-10 is more frequently reported as the lowest detectable number. Therefore, the use of y-intercept as a means of detection is limited. The sensitivity of the standard curve is determined by the most diluted sample that can be amplified and is the practical approach of determining LOD (Life Technologies™, 2012).

Melt curve analysis

Melt curve analysis is a method for validating the qPCR reaction by checking for primer-dimers and to confirm specificity. The melt curve is a result of the decrease in fluorescence when the melting point is reached, that occurs when dsDNA together with its dye molecule detaches and ssDNA is formed. A plot between fluorescence and temperature is constructed, and finally the $\Delta F/\Delta T$ and temperature is plotted (Life Technologies™, 2012).

Melt curves are especially important when non-specific probes such as SYBR® Green I are used (Whitby and Skovhus, 2009). A single peak in the melt curve indicates high specificity (Taylor et al., 2010). To ensure that all melt curves are associated with a specific gene, DNA sequencing is necessary (Whitby and Skovhus, 2009). Flat curves or a total absence of an amplicon product may indicate the presence of inhibitors (Edwards et al., 2004). The time-consuming step of gel electrophoresis can be replaced by melt curve analysis. The ideal melt curve peak should consist of a single, narrow and symmetrical peak. Lower melt peaks may indicate primer-dimers and these may result in poor qPCR efficiency and complicate data analysis. No-template-controls (NTCs) should also undergo melt curve analysis to detect primer-dimers, and if detected, there is a possibility of primer-dimer formation in template samples as well. If so, one should consider redesigning the primers. Melt curve analysis for NTCs helps to distinguish random contamination and primer-dimers (Life Technologies™, 2012).

3.9.3 MPN

The most probable number (MPN) method involves diluting a bacterial sample in specific media to extinction (Whitby and Skovhus, 2009). A 1:10 dilution series is used until, in theory, no bacteria are left (NACE TM0194, 2014). The media containing nutrients to support bacterial growth, along with the sample are incubated at a temperature equivalent to conditions in the bacteria's natural habitat, for a given amount of time. Results are drawn from colour change, turbidity or microscopic counting (Whitby and Skovhus, 2009).

There are several disadvantages related to the MPN method, including that considerable amounts of replicates are needed, and there might be biases associated with media selection, where only the fastest growing bacteria can be detected, or the most abundant. As previously stated, a very small fraction of bacteria is culturable, providing an incomplete overview of the bacterial diversity. The method takes several hours to perform by laboratory personnel and if errors are made (such as using the same syringe between serial dilutions) the results will be erroneous. Finally, the bacteria may take up to 30 days to grow (Whitby and Skovhus, 2009). Today there are several MMMs that provide more information than culture-dependent methods, both quantitative and qualitative. However, culture-dependent methods are still widely used in the oil and gas industry, due to its simplicity and well-established routines (Eckert and Skovhus, 2016).

As mentioned earlier, during sulphate reduction, SRB can utilize H_2 and organic acids, in particular lactate, as electron donor (Plugge et al., 2011) and carbon source (Oyekola et al., 2010). Thus, lactate is present in the media termed *Modified Postgate's B* (MPB). MPB contains the required nutrients to support the growth of oil field SRB. Further, the media is given a sufficient redox potential to facilitate sulphate reduction. Iron species present in the media will react with produced sulphide, and will result in iron sulphide precipitation, indicated with a change of colour from white to black (Biotechnology Solutions, 2017).

Phenol Red Dextrose Broth (PDB) is used to determine dextrose fermentation in bacteria where acid and gas will be produced and visualised in Durham's tubes, thereby differentiating bacterial species. PDB contains peptone and beef extract that serve as nitrogen sources, whereas phenol red functions as a pH indicator (a colour shift from red to yellow indicates acidic pH). Finally, osmotic equilibrium is maintained by NaCl (Sigma-Aldrich, 1999).

4. Materials and Methods

This chapter will present sampling locations, sample preparation, qPCR optimization and standard curve construction.

4.1 Sampling locations

Injection water samples were taken from Eldfisk 2/7E downstream UV (DS UV), downstream deaerator (DS DA) and upstream fine filters (US FF), Eldfisk 2/7B wellhead (WH) and Ekofisk 2/4VB WH (through an umbilical connected to Ekofisk 2/4M) and produced water samples were taken from Ekofisk 2/4J both upstream and downstream the high pressure (HP) and low pressure (LP) separators. Figure 4.1 shows a map of the Greater Ekofisk Area with sampling locations highlighted (ConocoPhillips, 2018).

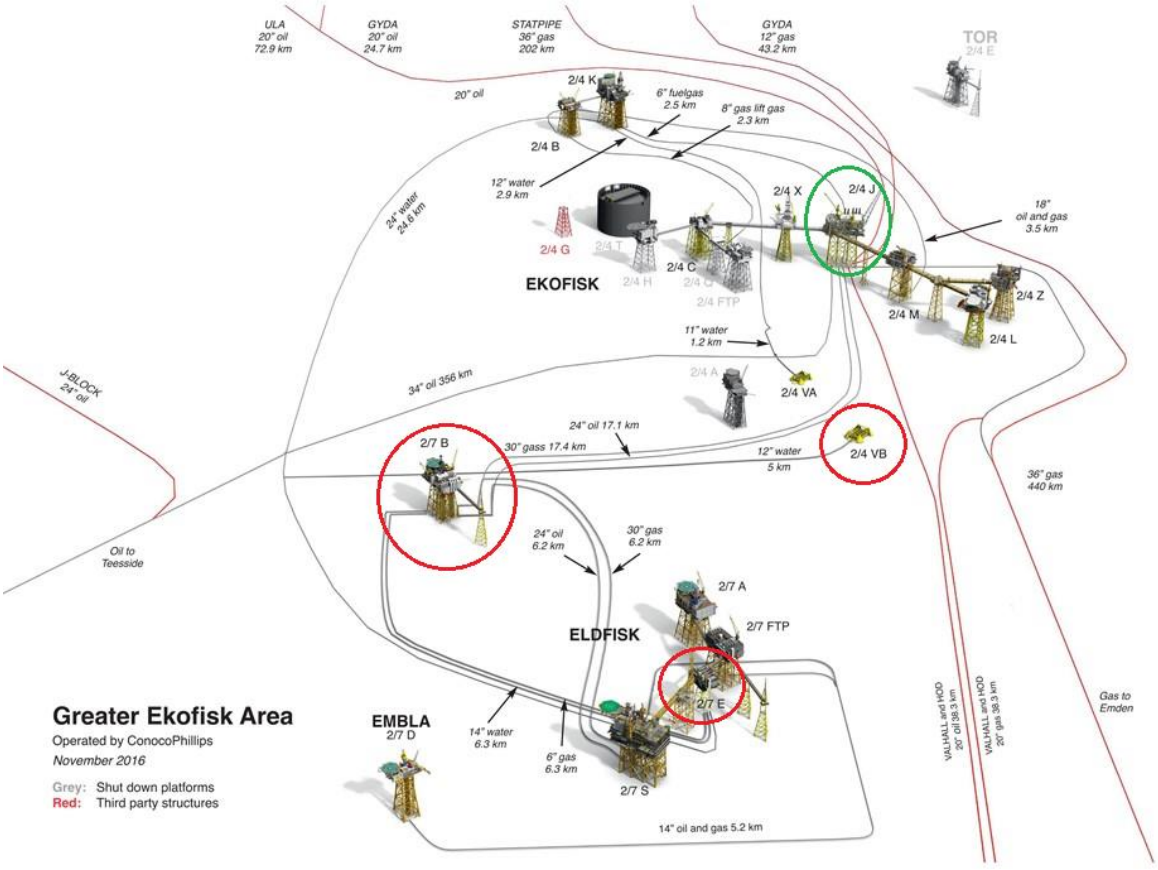

Figure 4.1: Map of the Greater Ekofisk Area. Injection water samples were taken from installations highlighted in red (Eldfisk 2/7B, Eldfisk 2/7E and Ekofisk 2/4VB) and produced water samples were taken from the installation highlighted in green (Ekofisk 2/4J) (ConocoPhillips, 2018).

4.2 Sample preparation

Injection water samples (in 1.0 l sterile neoprene bottles) and produced water samples (in 1.0 l sterile glass bottles or sterile neoprene bottles) were received from Ekofisk, and sample preparation was performed within 24 hours of the samples being taken. The samples were sent on ice to prevent microbial growth during transport.

MPB media

To detect planktonic SRB, MPB media test kits from Intertek™, made in accordance with NACE TM0194 (2014), were used.

PDB media

To detect planktonic GAB, PDB media was made based on NACE TM0194 (2014). 15.0 g Phenol Red Broth, 20.0 g NaCl and 5.0 g Dextrose was dissolved in 1,000 ml MilliQ® water and pH was adjusted to 7.0 ±0.2. The media was transferred to test tubes containing Durham tubes, and autoclaved at 121°C for 15 min.

Inoculation of SRB

To detect SRB, samples were inoculated into MPB media using 22-gauge needles under sterile conditions. 1.0 ml sample was injected into MPB medium and serial dilutions (1:10) in triplicates was performed. The samples were further incubated at one of the following temperatures for 30 days: 30°C, 50°C and/or 70°C.

Inoculation of GAB

To detect GAB, samples were inoculated into PDB medium under sterile conditions. 1.0 ml sample was pipetted into PDB medium and serial dilutions (1:10) in triplicates were performed. The samples were further incubated at one of the following temperatures for 30 days: 30°C, 50°C and/or 70°C.

4.2.1 Injection water samples

The sampling temperature of injection water was approximately 30°C and therefore samples were incubated at 30°C for 30 days. For SRB detection, the samples were diluted in the range of 10^{-1} to 10^{-5}, except for samples from March 2018 that were diluted from 10^{-1} to 10^{-3}. For GAB detection, samples were diluted in the range of 10^{-1} to 10^{-6}. The month and location of the samples are shown in table 4.1.

Table 4.1: Overview of injection water sampling locations.

Month	Sampling location
Sept. 2017	Eldfisk 2/7E DS UV
Oct. 2017	Eldfisk 2/7E US FF
Oct. 2017	Eldfisk 2/7E DS DA
Oct. 2017	Eldfisk 2/7B WH
Nov. 2017	Ekofisk 2/4 VB
Dec. 2017	Ekofisk 2/4 VB
Jan. 2018	Ekofisk 2/4 VB
Mar. 2018	Ekofisk 2/4 VB

4.2.2 Produced water samples

The sampling temperature of the produced water samples ranged between 65.4°C and 87.2°C. Samples were incubated at both 50°C and 70°C for 30 days. At Ekofisk 2/4J a 3-phase separation of the production flow is carried out. Oil, gas and water is separated in HP and LP separators (ConocoPhillips, 2018). Produced water sample 1 was taken from upstream high pressure separator (USHPSP), sample 2 was taken from upstream low pressure separator (USLPSP), sample 3 was taken from downstream high pressure separator (DSHPSP) and sample 4 was taken from downstream low pressure separator (DSLPSP). Figure 4.2 shows produced water sampling points.

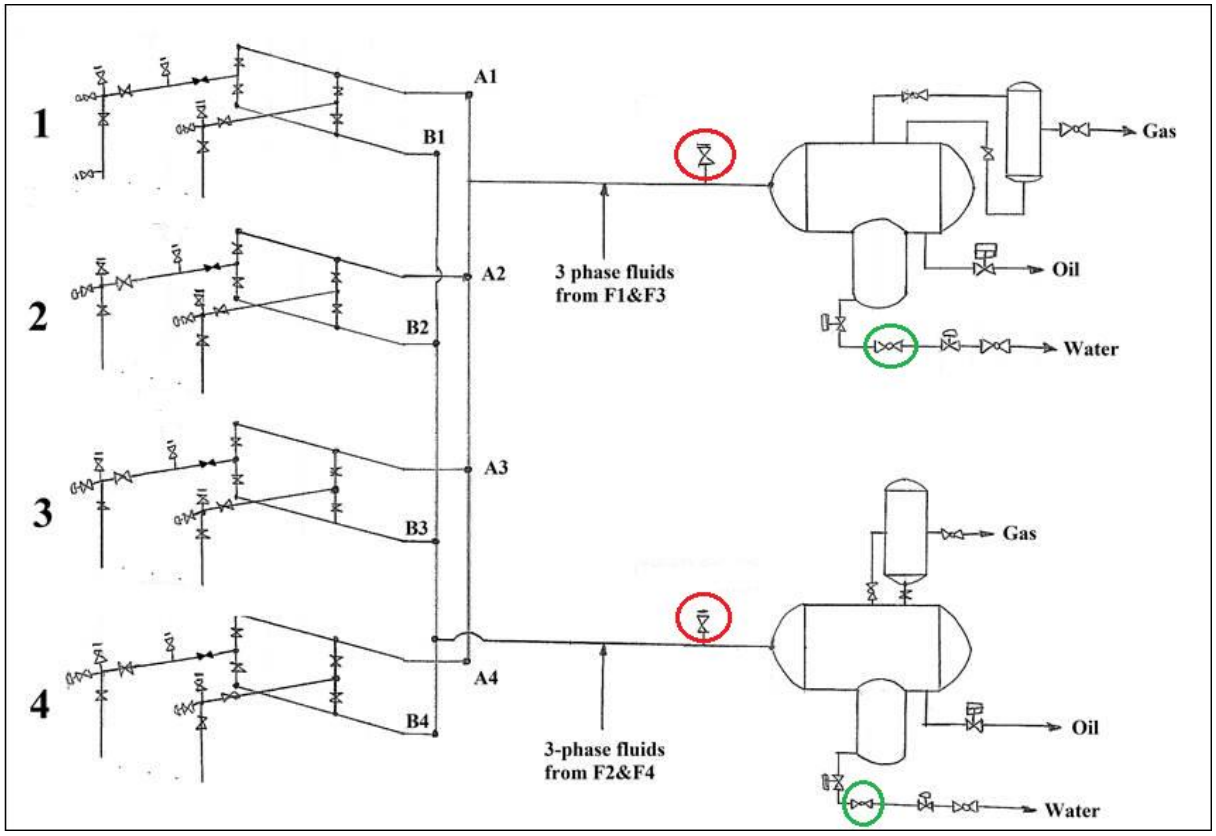

Figure 4.2: Simplified flow-chart of HP (top) and LP (bottom) production separators at Ekofisk 2/4J. Upstream sampling points are highlighted in red and downstream sampling points in green (ConocoPhillips, 2018).

Samples from November 2017

Samples from November were incubated at 70°C. For SRB detection, samples were diluted from 10^{-1} to 10^{-5}. For GAB detection, samples were diluted from 10^{-1} to 10^{-6}.

Samples from December 2017

Both sample 1 and 2 from December were incubated at 50°C and 70°C for SRB detection (dilution range of 10^{-1} to 10^{-3}) and GAB detection (dilution range of 10^{-1} to 10^{-6}). Both sample 3 and 4 were incubated at 50°C for SRB detection (dilution range of 10^{-1} to 10^{-3}) and 70°C for GAB detection (dilution range of 10^{-1} to 10^{-6}).

Samples from January 2018

Samples from January were incubated at 70°C. For SRB detection, samples were diluted from 10^{-1} to 10^{-3} and for GAB detection samples were diluted from 10^{-1} to 10^{-6}.

The sampling temperature and SRB/GAB dilution range with regards to the produced water samples can be seen in table 4.2.

Table 4.2: Sampling location, temperature and dilution range for MPNs of produced water.

Month	Sampling location	Sampling temp. (°C)	SRB dilution	GAB dilution
Nov. 2017	Ekofisk 2/4J - 1	74.1	10^{-1} to 10^{-5}	10^{-1} to 10^{-6}
	Ekofisk 2/4J - 2	87.2	10^{-1} to 10^{-5}	10^{-1} to 10^{-6}
	Ekofisk 2/4J - 3	83.1	10^{-1} to 10^{-5}	10^{-1} to 10^{-6}
	Ekofisk 2/4J – 4	69.4	10^{-1} to 10^{-5}	10^{-1} to 10^{-6}
Dec. 2017	Ekofisk 2/4J – 1	71.2	10^{-1} to 10^{-3}	10^{-1} to 10^{-6}
	Ekofisk 2/4J – 2	65.4	10^{-1} to 10^{-3}	10^{-1} to 10^{-6}
	Ekofisk 2/4J – 3	77.4	10^{-1} to 10^{-3}	10^{-1} to 10^{-6}
	Ekofisk 2/4J – 4	68.6	10^{-1} to 10^{-3}	10^{-1} to 10^{-6}
Jan. 2018	Ekofisk 2/4J – 1	72.4	10^{-1} to 10^{-3}	10^{-1} to 10^{-6}
	Ekofisk 2/4J – 2	79.1	10^{-1} to 10^{-3}	10^{-1} to 10^{-6}
	Ekofisk 2/4J – 3	81.0	10^{-1} to 10^{-3}	10^{-1} to 10^{-6}
	Ekofisk 2/4J - 4	68.3	10^{-1} to 10^{-3}	10^{-1} to 10^{-6}

4.2.3 DNA Sample preparation

3 l of injection water and 300 ml of produced water was vacuum filtered using MF-Millipore™ Mixed Cellulose Membrane Filters (0.22 µm). Post filtration, the filters were stored in PowerSoil® Bead tubes (PowerSoil® DNA Isolation Kit by Qiagen) at -20°C until the DNA extraction was performed.

4.2.4 DNA extraction and Gel electrophoresis

DNA was extracted using the PowerSoil® DNA Isolation Kit (Qiagen). The extraction was performed according to the instructions from the manufacturer Qiagen (2017) with the following adjustments: Step 5 was replaced by homogenizing the sample with the FastPrep®-24 (MP medical) instrument (*Bead beating)* for 60 s and all steps involving 30 s of centrifugation was increased to 60 s. In step 18, the samples were centrifuged for 2 min and finally in step 20, 50.0 µl of solution C6 was added.

DNA samples were run at 100 V for 60 min on a 1.0 % agarose gel containing 5.0 µl GelGreen™. Finally, the gel was visualized using the BioRad GelDOC XR Imagery system to verify the presence of DNA.

4.3 Optimizing qPCR and standard curve construction

A literature survey was conducted to find potential primers for qPCR optimization. 3 primer sets were found from Kondo et al. (2008), Liu et al. (2016) and Dahllof et al. (2000), for the functional genes dsrA, dsrB and the RNA polymerase subunit (rpoB) taxonomic gene, respectively. The three primer sets targeting the dsrA, dsrB and rpoB genes, corresponding sequences and product size are shown in table 4.3.

Table 4.3: Three primer sets targeting the dsrA, dsrB and rpoB genes, corresponding sequences and product size.

Primer	Gene	Sequence	Product size	Reference
Dsr-1F	dsrA	5′-ACSCACTGGAAGCACGCCGG-3′	221 bp	Kondo et al., 2008
Dsr-R	dsrA	5′-GTGGMRCCGTGCAKRTTGG-3′		
Dsr2060F	dsrB	5′-CAACATCGTYCACCAGGG-3′	350 bp	Liu et al., 2016
Dsr4R	dsrB	5′-GTGTAGCAGTTACCGCA-3′		
rpoB1698F	rpoB	5′-AACATCGGTTTGATCAAC-3′	500 bp	Dahllof et al., 2000
rpoB2041R	rpoB	5′-CGTTGCATGTTGGTACCCAT-3′		

PCR

Prior to qPCR, PCR was used in an attempt to optimize T_a of the three primer sets. See table 4.4 for primer sets and tested T_a. The DNA used to optimize the reactions was produced water from Eldfisk 2/7S. Each sample volume consisted of 5.0 µl 10x Key Buffer (Mg^{2+} free, VWR), 1.0 µl (25 mM) dNTP (VWR), 1.0 µl (1.0 µM) forward primer (Invitrogen), 1.0 µl (1.0 µM) reverse primer (Invitrogen), 3.0 µl $MgCl_2$ (25 µM, Sigma-Aldrich), 0.3 µl Taq polymerase (5 U/µl, VWR), 2.0 µl template DNA and 36.7 µl of molecular grade water, giving a final reaction volume of 50.0 µl. For further optimization of PCR, primer concentrations, DNA and $MgCl_2$ volumes were varied. Samples were run on a Applied Biosystems 2720 Thermal Cycler. To verify results, the PCR products were run at 100 V for 60 min on a 1.5 % agarose gel containing 5.0 µl GelGreen™ and visualized by the BioRad GelDOC XR Imagery system.

Table 4.4: Primer sets and tested PCR annealing temperatures (T_a).

Primer set	**T_a**
Dsr-1F/Dsr-R	57-60ºC
Dsr2060F/Dsr4R	48-55ºC
rpoB1698F/rpoB2041R	48-52ºC

Primer set Dsr-1F/Dsr-R

The initial denaturing step was set at 95°C for 10 min, followed by 40 cycles of denaturing at 95°C for 15 s, annealing (tested 57-60°C) for 30 s, and elongation was at 72°C for 30 s. A final elongation was set at 72°C for 7 min and samples were then cooled at 4°C.

Primer set Dsr2060F/Dsr4R

The initial denaturing step was set at 94°C for 5 minutes, followed by 35 cycles of denaturing at 94°C for 45 s, annealing (tested 48-55°C) for 45 s and elongation was set at 72°C for 60 s. A final elongation was set at 72°C for 7 min and samples were then cooled at 4°C.

Primer set rpoB1698F/rpoB2041R

The initial denaturing step was set at 95°C for 10 min, followed by 35 cycles of denaturing at 95°C for 30 s, annealing (tested 48-52°C) for 60 s, and the elongation was set at 72°C for 30 s. A final elongation was set at 72°C for 7 min and samples were then cooled at 4°C.

qPCR

For qPCR optimization, the same thermocycling conditions as applied for the primer sets as described above were used. Varying concentrations of primers, DNA volumes and T_a were tested (see table 4.5). SsoAdvanced™ Universal SYBR® Green Supermix (Bio-Rad, 2013) was held constant at 10.0 µl. Molecular grade water was used to bring the reaction volume up to 20.0 µl. All qPCR reactions were carried out in triplicates using the CFX96™ Real-Time System with a C1000 Touch™ Thermal Cycler (Bio-Rad Laboratories, Inc.). Melt curves (and later on standard curves) were made by the CFX Manager™ Software. All reaction reagents were briefly vortexed to ensure homogeneous solutions. Samples were run on a BioRad HardShell® 96 microplate and a

sealing roller was used to apply the Microseal® B Adhesive Sealer. For all reactions, a melt curve was run from 65 to 95°C with a slope of 0.5°C. The microplate containing the samples was centrifuged for 1 min at 3700 rpm prior to each run.

Table 4.5: Primer sets with varying concentration (µM), volume (µl), DNA volume (µl) and T_a (°C) used for qPCR optimization.

Primer set	Primer conc. (µM)	Primer vol. (µl)	DNA vol. (µl)	T_a (ºC)
Dsr-1F/Dsr-R	0.25	0.5	1.0	60
	0.25	0.5	1.0	59
Dsr2060F/Dsr4R	0.5	1.0	1.0	55
	0.5	1.0	2.0	55
	0.25	0.5	1.0	55
	0.25	0.5	2.0	55
	0.125	0.25	1.0	55
rpoB1698F/rpoB2041R	0.25	0.5	0.25	47
	0.25	0.5	0.5	47
	0.25	0.5	1.0	47
	0.25	0.5	1.0	48
	0.25	0.5	1.0	49
	0.25	0.5	1.0	50
	0.25	0.5	1.0	51
	0.25	0.5	0.5 (1:10)	47
	0.25	0.5	1.0 (1:10)	47

4.3.1 Bacterial strain from pure culture

To construct the standard curve for qPCR, a bacterial strain of *Desulfovibrio vulgaris*, DSM 644, from DSMZ was used. The bacterial culture was obtained from a premade biobank at the *International Research Institute of Stavanger* (IRIS). The bacterial strain was placed in MPB liquid culture and on Postgate medium B agar plates under anaerobic conditions and kept at 38°C for 7 days.

4.3.2 gBlocks® Gene Fragment

A *gBlocks® Gene Fragment* was to be used for standard curve construction. Primer set Dsr2060F/Dsr4R (Liu et al., 2016), was used in a *Basic Local Alignment Search Tool* (BLASTn)

on the *National Center for Biotechnology Information* (NCBI) webpage, with respect to Desulfovibrionales (taxid: 213115). Dsr2060F (5′-CAACATCGTYCACCAGGG-3′) was set as query sequence, where "Y" was replaced by "C". Sequence AB061536.1 (*Desulfovibrio burkinensis*) was selected due to the presence of both dsrA and dsrB gene fragments. For Dsr4R, (5′-GTGTAGCAGTTACCGCA-3′), an identical search was performed, resulting in an alignment with the same sequence. A *gBlocks® Gene Fragment* was ordered from IDT® to serve as standard DNA for the qPCR reaction. The gene fragment, hereby referred to as *GF1*, contained the dsrAB gene.

A new forward primer (5′-CAACATCGTYCAYACCCAGGG-3′) was found by a literature survey (Geets et al., 2006), and was specific for the dsrB gene. The new forward primer, *DSRp2060F* (Geets et al., 2006), was used in a BLASTn search with respect to Desulfovibrionales (taxid:213115). DSRp2060F was set as query sequence, where both "Ys" were replaced by "T", to check sequence alignment with sequence AB061536.1. The new primer set consisted of DSRp2060F and Dsr4R. See table 4.6 for primer details.

Table 4.6: Primer set DSRp2060F/Dsr4R targeting the dsrB gene and corresponding sequences and product size.

Primer	Gene	Sequence	Product size	Reference
DSRp2060F	dsrB	5′-CAACATCGTYCAYACCCAGGG-3′	350 bp	Geets et al., 2006
Dsr4R	dsrB	5′-GTGTAGCAGTTACCGCA-3′		

A second gBlocks® Gene Fragment was ordered from IDT® to serve as standard DNA for the qPCR reaction. This gene fragment, hereby referred to as *GF2*, contained only the dsrB gene. Before ordering GF2 a new BLASTn search was performed. DSRp2060F was used as query sequence with respect to Desulfovibrionales (taxid:213115), and both "Ys" were replaced by "T". Sequence AE017285.1 (*Desulfovibrio vulgaris*) was selected due to the presence of the dsrB gene. Dsr4R was used in an identical search, resulting in an alignment with the same sequence as DSRp2060F.

Upon arrival, GF1 and GF2 were prepared according to the manufacturer's instructions (IDT®, 2017). The gene fragments were centrifuged at 10,000 rpm for 5 s and molecular grade water was added to reach a final concentration of 10 ng/µl. The gene fragments were further incubated at 50°C for 20 min, vortexed and centrifuged at 10,000 rpm for 5 s, and stored at – 20°C. Properties of the gene fragments are presented in table 4.7.

Table 4.7: Properties of GF1 and GF2.

Properties	**GF1**	**GF2**
Length (base pairs)	1941	600
Amount (ng)	1000	500
GC content (%)	62.75	63
Molecular weight (g/mol)	1199461.3	370692.2
fmoles/ng	0.83	2.70
µg/OD_{260}	50	50

4.3.3 PCR and Gel clean-up for gBlocks® Gene Fragments

GF1 and primer set Dsr2060F/Dsr4R

According to the manufacturer, GF1 might have had secondary structures and therefore purification by means of gel clean-up was carried out to minimize the effects. 5 PCR samples were prepared for GF1 with primer set Dsr2060F/Dsr4R (Liu et al., 2016). See chapter 4.3 for PCR reaction details regarding this primer set. The PCR products were run at 100 V for 60 min on a 1.5 % agarose gel with 10.0 µl GelGreen™. The QIAquick Gel Extraction Kit by Qiagen (gel clean-up) was then used according to manufacturer's instructions with one exception; 50.0 µl of EB Buffer was added to samples 1,2 and 3, whereas 30.0 µl was added to samples 4 and 5. The gel extracted products were then run at 100 V for 60 min on a 1.5 % agarose gel with 10.0 µl GelGreen™ to verify the gel clean-up.

GF1 and primer set DSRp2060F/Dsr4R

3 PCR samples with GF1 and primer set DSRp2060F/Dsr4R (Geets et al., 2006) were prepared as described above, except that only 30.0 µl of EB Buffer was added to all samples. The PCR thermocycling conditions were the same as applied for Dsr2060F/Dsr4R.

GF2 and primer set DSRp2060F/Dsr4R

GF2 with primer set DSRp2060F/Dsr4R was used without gel clean-up.

4.3.4 Copy number calculations

The DNA concentration of the gel extracted samples were measured using a Thermo Scientific™ Nanodrop™ One Microvolume UV-Vis Spectrophotometer. Samples with highest and most stable DNA concentration were chosen for calculation of copy number (see Appendix 3 and 4 for DNA concentrations and purity).

The copy numbers were calculated using the following formula:

$$\frac{Xng * 6.0221 * 10^{23} \frac{molecules}{mole}}{\left(N * 660 \frac{g}{mole}\right) * 1 * 10^{9} \frac{ng}{g}} = \frac{number\ of\ copies}{\mu l} \qquad \text{Eq.2}$$

Where X is amount of amplicon (ng), N is the length of dsDNA amplicon, 660 g/mole is the mass of 1 bp dsDNA on average (IDT®, 2018).

For the gel extracted samples, calculation of copy numbers was based on average DNA concentration. Since GF2 with primer set DSRp2060F/Dsr4R was used without gel clean-up, the copy number was calculated based on properties as listed in table 4.7.

4.3.5 Standard curve optimization with GF1 and GF2

All samples were diluted (1:10) in the range of 10^8 to 10^1 in molecular grade water to serve as standards in the qPCR reaction. For optimization of the standard curve, different combinations of gene fragments and primers were tested. Optimization involved testing of various dilution series, primer concentrations and DNA volumes. New standards were made prior to each run. Table 4.8 shows the combination of various reagents and parameters during standard curve optimization.

Table 4.8: Combination of gene fragments and primer sets for the optimization of the standard curve.

Gene fragment	Primer set	Dilution series	Primer conc. (µM)	DNA vol. (µl)
GF1	Dsr2060F/Dsr4R	10^8-10^1	0.25	1.0
		10^7-10^1	0.25	1.0
		10^7-10^2	0.25	1.0
		10^7-10^3	0.5	1.0
		10^7-10^3	0.25	2.0
GF1	DSRp2060F/Dsr4R	10^7-10^3	0.25	1.0
GF2	DSRp2060F/Dsr4R	10^7-10^3	0.5	1.0
		10^7-10^3	0.5	2.0

4.4 TOPO® TA Cloning®

The cloning procedure was carried out in accordance with the TOPO® TA Cloning® Kit by Invitrogen (Thermo Fisher Scientific, 2014).

PCR products were made with different DNA template sources and primer sets. DNA sources consisted of produced water from Eldfisk 2/7S and gBlocks® gene fragments (GF1 and GF2). Samples were prepared for a PCR run with the same composition and reaction conditions as described in chapter 4.3. See table 4.9 for different combinations of DNA sources and primer sets in PCR samples.

Table 4.9: Combination of DNA sources and primer sets in PCR samples.

Sample No.	DNA source	Primer set
1	Produced water	Dsr2060F/Dsr4R
2	Produced water	DSRp2060F/Dsr4R
3	GF1	Dsr2060F/Dsr4R
4	GF1	DSRp2060F/Dsr4R
5	GF2	Dsr2060F/Dsr4R
6	GF2	DSRp2060F/Dsr4R

Gel clean-up was performed for the PCR products prior to the TOPO® TA Cloning® reaction.

4.4.1 TOPO® TA Cloning® reaction

The TOPO® TA Cloning® reaction consisted of the gel purified PCR products, salt solution and the TOPO® vector as shown in table 4.10.

Table 4.10: Reagents for TOPO cloning (Thermo Fisher Scientific, 2014).

Reagent	**Chemically Competent *E.coli* (DH5α)**
Gel purified PCR product	4.0 µl
Salt solution	1.0 µl
TOPO® vector	1.0 µl
Final volume	6.0 µl

The reaction mixture was incubated for 5 min at room temperature and kept on ice for further application.

Transformation

2.0 µl of the TOPO cloning reaction mixture was added into a vial of One Shot® Chemically Competent *E.coli* (DH5α), gently mixed and incubated on ice for 10 min. The cells were then heat-shocked at 42°C for 30 s and kept on ice before 250 µl of S.O.C. medium was added. The tubes were then shaken horizontally at 200 rpm at 37°C for 1 hour. Afterwards, 50.0 µl of each transformation together with 20.0 µl S.O.C. medium was spread on prewarmed agar plates containing kanamycin (50 µg/ml), and the plates were incubated overnight at 37°C. The following day, positive colonies were chosen and cultured overnight in Falcon tubes containing 5.0 ml LB medium with kanamycin (50 µg/ml).

Plasmid purification

The day after, plasmid purification was carried out using PureLink™ Quick Plasmid Miniprep Kit (Thermo Fisher Scientific, 2011).

PCR of purified plasmid using M13 primers

The purified plasmids were further used in a PCR reaction with M13 forward primer (5´-GTAAAACGACGGCCAG-3´) and reverse primer (5´-CAGGAAACAGCTATGAC-3´). Samples were prepared with the same composition as described in chapter 4.3. The initial denaturing step was set at 95°C for 10 min, followed by 35 cycles of denaturing at 94°C for 40 s, T_a was 50°C for 40 s, and the elongation was set at 72°C for 90 s. A final elongation was set at 72°C for 10 min and samples were then cooled at 4°C.

Further, a gel clean-up was performed. Finally, samples were quantified using Thermo Scientific™ Nanodrop™ One Microvolume UV-Vis Spectrophotometer.

Linearising the plasmid

The ScaI digestion protocol from Thermo Fisher Scientific (2012) was used. The restriction enzyme ScaI cuts at the AGT|ACT site at 37°C as shown in figure 4.3.

Figure 4.3: ScaI cutting site (Thermo Fisher Scientific, 2012).

Different reaction mixture compositions and incubation times were tested in an attempt to linearize the plasmid as shown in table 4.11.

Table 4.11: ScaI digestion reaction mixture composition and incubation times at 37°C.

Reagent	**Volume (3 h inc.)**	**Volume (1.5 h inc.)**	**Volume (3 h inc.)**
Molecular grade water	16 µl	15 µl	12 µl
10x Buffer ScaI	2.0 µl	2.0 µl	2.0 µl
DNA	1.0 µl	2.0 µl	5.0 µl
ScaI	2.0 µl	2.0 µl	2.0 µl

Digested products were run at 100 V for 60 min on a 1.5 % agarose gel with 10.0 µl GelGreen™ to verify the presence of linearized plasmids.

4.4.2 Standard curve optimization of cloned plasmid DNA with PCR insert

The copy number was calculated using eq.2. The chosen sample was diluted (1:10) in the range of 10^8-10^3 in molecular grade water to serve as standard in the qPCR reaction. Primer concentration of 0.5 µM (1.0 µl) was tested with 35 and 38 cycles. New standards were made prior to each run.

5. Results

In this chapter results from MPN, qPCR optimization and final qPCR results with quantified samples will be presented.

5.1 MPN results

The interpretation of MPN results was done according to table 2 as presented by Oblinger and Koburger (1975).

5.1.1 Injection water

No colour change was observed in the MPB media, indicating <1 bacteria/ml with respect to SRB.

GAB growth was detected by a colour change in PDB media (from red to yellow) without gas production, indicating carbohydrate fermentation with acid production. Colour change was not observed for samples from September (Eldfisk 2/7E DS UV) and October (Eldfisk 2/7E US FF, Eldfisk 2/7E DS DA and Eldfisk 2/7B WH), indicating <1 bacteria/ml. Samples from November, December, January and March, indicated 9300 (1500-38,000), 4300 (700-21,000), 23 (4-120) and 93 (15-380) bacteria/ml, respectively (bacterial number and 95% confidence interval, respectively). The MPN results for injection water are shown in table 5.1.

Table 5.1: MPN results for injection water.

Month	Sampling Point	GAB Bacteria/ml	95% Confidence interval
Nov. 2017	Ekofisk 2/4VB	9300	1500-38,000
Dec. 2017	Ekofisk 2/4VB	4300	700-21,000
Jan. 2018	Ekofisk 2/4VB	23	4-120
Mar. 2018	Ekofisk 2/4VB	93	15-380

5.1.2 Produced water

No colour change was observed in MPB media, indicating <1 bacteria/ml with respect to SRB.

Due to unforeseen circumstances, it was not possible to detect GAB in samples incubated at 70°C from November and December. No GAB growth was detected in samples incubated at 50°C in December, indicating <1 bacteria/ml. Based on these results it was decided to incubate samples from January at 70°C. GAB growth was detected in samples from January by a colour change in PDB media (from red to yellow) without gas production, indicating carbohydrate fermentation

with acid production. Sample 1-4 from January indicated 9300 (1500-38,000), 2100 (350-4700), 4600 (710-24,000) and 2100 (350-4700) bacteria/ml, respectively (bacterial number and 95% confidence interval, respectively). The MPN results for produced water are shown in table 5.2.

Table 5.2: MPN results for produced water from Ekofisk 2/4J.

Month	Sample Point	GAB Bacteria/ml	95% Confidence interval
Jan. 2018	Ekofisk 2/4J - 1	9300	1500-38,000
	Ekofisk 2/4J - 2	2100	350-4700
	Ekofisk 2/4J - 3	4600	710-24,000
	Ekofisk 2/4J - 4	2100	350-4700

5.2 qPCR optimization

qPCR optimization involved a considerable amount of testing with different gene fragments and primer sets. In the following sections T_a optimization by PCR, qPCR primer optimization, BLAST results, primer sets, cloning results, and the process of standard curve optimization will be shown. Finally, the optimized qPCR protocol with quantified samples will be presented.

5.2.1 DNA extraction and gel electrophoresis

DNA extraction and gel electrophoresis verified the presence of DNA in injection water samples from Ekofisk 2/4VB and produced water samples from Ekofisk 2/4J. DNA could not be detected in samples from Eldfisk 2/7B and Eldfisk 2/7E. See table 5.3 for detection of DNA in injection water samples and table 5.4 for produced water samples. Gel electrophoresis images of DNA extraction can be found in Appendix 1.

Table 5.3: Detection of DNA in injection water samples.

Month	Sampling point	DNA
Sept. 2017	Eldfisk 2/7E DS UV	-
Oct. 2017	Eldfisk 2/7E US FF	-
Oct. 2017	Eldfisk 2/7E DS DA	-
Oct. 2017	Eldfisk 2/7B WH	-
Nov. 2017	Ekofisk 2/4VB	+
Dec. 2017	Ekofisk 2/4VB	+
Jan. 2018	Ekofisk 2/4VB	+
Mar. 2018	Ekofisk 2/4VB	+

Table 5.4: Detection of DNA in produced water samples.

Month	Sampling point	DNA
Nov. 2017	Ekofisk 2/4J - 1	+
Nov. 2017	Ekofisk 2/4J - 2	+
Nov. 2017	Ekofisk 2/4J - 3	+
Nov. 2017	Ekofisk 2/4J - 4	+
Dec. 2017	Ekofisk 2/4J - 1	+
Dec. 2017	Ekofisk 2/4J - 2	+
Dec. 2017	Ekofisk 2/4J - 3	+
Dec. 2017	Ekofisk 2/4J - 4	+
Jan. 2018	Ekofisk 2/4J - 1	+
Jan. 2018	Ekofisk 2/4J - 2	+
Jan. 2018	Ekofisk 2/4J - 3	+
Jan. 2018	Ekofisk 2/4J - 4	+

5.2.2 PCR

PCR was used prior to qPCR to optimize T_a for the different primer sets. Optimized T_a for primer set Dsr2060F/Dsr4R (Liu et al., 2016) was found to be 55 ºC and 48ºC for primer set rpoB1698F/rpoB2041R (Dahllof et al., 2000). Optimized T_a for primer set Dsr-1F/Dsr-R (Kondo et al., 2008) could not be attained. Results are shown in table 5.5. Gel electrophoresis images of primer set Dsr2060F/Dsr4R and rpoB1698F/rpoB2041R can be found in Appendix 2.

Table 5.5: Optimized annealing temperature (T_a), primer concentrations, DNA volumes and $MgCl_2$ volumes for primer sets by qPCR.

Primer set	Optimized T_a (ºC)	Primer conc. (µM)	Primer vol. (µl)	DNA vol. (µl)	$MgCl_2$ vol. (µl)
Dsr-1F/Dsr-R	-	-	-	-	-
Dsr2060F/Dsr4R	55ºC	1.0	1.0	2.0	3.0
rpoB1698F/rpoB2041R	48ºC	1.0	1.0	2.0	2.0

5.2.3 qPCR optimization

All three primer sets were tested with qPCR. It was not possible to optimize primer set Dsr-1F/Dsr-R due to consequent amplification of NTCs and lack of amplified samples. Primer set Dsr2060F/Dsr4R was optimized with a primer concentration of 0.25 µM, 1.0 µl template DNA, Cq standard deviation of 1.09 and T_a at 55°C. Primer set rpoB1698F/rpoB2041R was optimized with a primer concentration of 0.25 µM, 1.0 µl template DNA, Cq standard deviation of 2.26 and T_a at 48°C. See table 5.6 for results from qPCR optimization.

Table 5.6: Optimized primer concentration (µM), DNA volume (µl), T_a (°C) and Cq standard deviation.

Primer set	T_a (ºC)	Primer conc. (µM)	Primer vol. (µl)	DNA vol. (µl)	Cq Std. Dev
Dsr-1F/Dsr-R	-	-	-	-	-
Dsr2060F/Dsr4R	55	0.25	0.5	1.0	1.09
rpoB1698F/rpoB2041R	48	0.25	0.5	1.0	2.26

Dsr2060F/Dsr4R was selected for standard curve construction based on lower Cq standard deviation and its specificity towards the dsrB gene.

5.2.4 Standard curve construction

The bacterial strain of *Desulfovibrio vulgaris*, DSM 644, from IRIS did not grow in liquid media, nor on agar plates with MPB. This was indicated by no colour change from clear to black. Due to no indication of bacterial growth, it was decided to order a *gBlocks® Gene Fragment* from IDT® to serve as standard DNA. Results from BLASTn search showed that primer set Dsr2060F/Dsr4R had no irregular nucleotides with respect to sequence AB061536.1 (*Desulfovibrio burkinensis*). The new forward primer, DSRp2060F (Geets et al., 2006), had 2 irregular nucleotides with

respect to the same sequence. Further, DSRp2060F had 1 irregular nucleotide with respect to sequence AE017285.1 (*Desulfovibrio vulgaris*).

5.2.5 Copy numbers and DNA concentrations

Copy numbers based on average DNA concentration (ng/µl) for GF1 with Dsr2060F/Dsr4R and DSRp2060F/Dsr4R were $2.4x10^{10}$ and $7.12x10^{10}$ dsrB copies/µl, respectively. The copy number of GF2 with DSRp2060F/Dsr4R was $7.60x10^{10}$ dsrB copies/µl. See table 5.7 for average DNA concentration and copy numbers.

Table 5.7: gBlocks® Gene Fragments with respective primer sets and calculated copy numbers.

Gene Fragment	Primer set	Sample	Avg. DNA conc. (ng/µl)	Copy number (copies/ µl)
GF1	Dsr2060F/Dsr4R	5	10.13	$2.4x10^{10}$
GF1	DSRp2060F/Dsr4R	3	30.3	$7.12x10^{10}$
GF2	DSRp2060F/Dsr4R	1	-	$7.60x10^{10}$

5.2.6 Cloning results

Sample 1 (produced water with Dsr2060F/Dsr4R) did not display any visible bands after PCR and was therefore not further used. In addition, sample 3 (GF1 with Dsr2060F/Dsr4R), 4 (GF1 with DSRp2060F/Dsr4R), 5 (GF2 with Dsr2060F/Dsr4R) and 6 (GF2 with DSRp2060F/Dsr4R) were not tested in qPCR standard curve construction.

Sample 2 (produced water with DSRp2060F/Dsr4R) was selected for standard curve optimization. For sample 2, the measurement of 7.1 ng/µl was considered an outlier, giving an average of 9.2 ng/µl (Appendix 5). The interval between the M13 forward primer (448 bp) and M13 reverse primer (205 bp) was found to be 243 bp from the pCR™ II-TOPO® map (Thermo Fisher Scientific, 2014) and was further used to calculate the copy number. The length of dsDNA amplicon was found by adding the PCR product (350 bp) to the interval (243 bp), which equals 593 bp. The length of dsDNA and the average DNA concentration was used to calculate the copy number, giving $1.42x10^{10}$ dsrB gene copies/µl.

Linearization of the cloned plasmids was not attainable and therefore supercoiled plasmids were used.

5.2.7 Standard curve optimization using GF1 with primer set Dsr2060F/Dsr4R

Dsr2060F/Dsr4R had previously been optimized by qPCR with primer concentration at 0.25 µM, DNA volume of 1.0 µl and T_a at 55°C with 35 cycles. Therefore, these parameters were mainly used for standard curve optimization in this section. In the following section, a selection of the qPCR runs is presented. Table 5.8 shows the main parameters that were adjusted during testing (primer concentration and DNA volume) and standard curve variables.

Table 5.8: Optimizing standard curve with GF1 and Dsr2060F/Dsr4R.

Test No.	Primer conc. (µM)	DNA vol. (µl)	Efficiency	R^2	Slope	y-int	No. of N/A
2	0.25	1.0	94.4%	0.596	-3.464	43.416	12
4	0.25	1.0	99.4%	0.996	-3.336	42.360	7
9	0.25	1.0	85.6%	0.998	-3.723	43.003	1
14	0.5	1.0	86.5%	0.998	-3.693	44.124	0
24	0.25	2.0	86.0%	0.994	-3.711	44.551	0

Initially, the linear range was from 10^8 to 10^1. Test 2 had an efficiency >90%, R^2-value <0.95 and 12 N/As were observed. None of the standards were aligned with the curve. Melt curve analysis for test 2 showed one main peak with minor peaks below. 10^2-10^1 dilutions were not amplified, giving flat melt curves. The minor peaks consisted mainly of dilutions in the range of 10^4-10^3 and no melt peaks were observed for the NTCs. Standard curve and melt curve for test 2 are shown in figure 5.1.

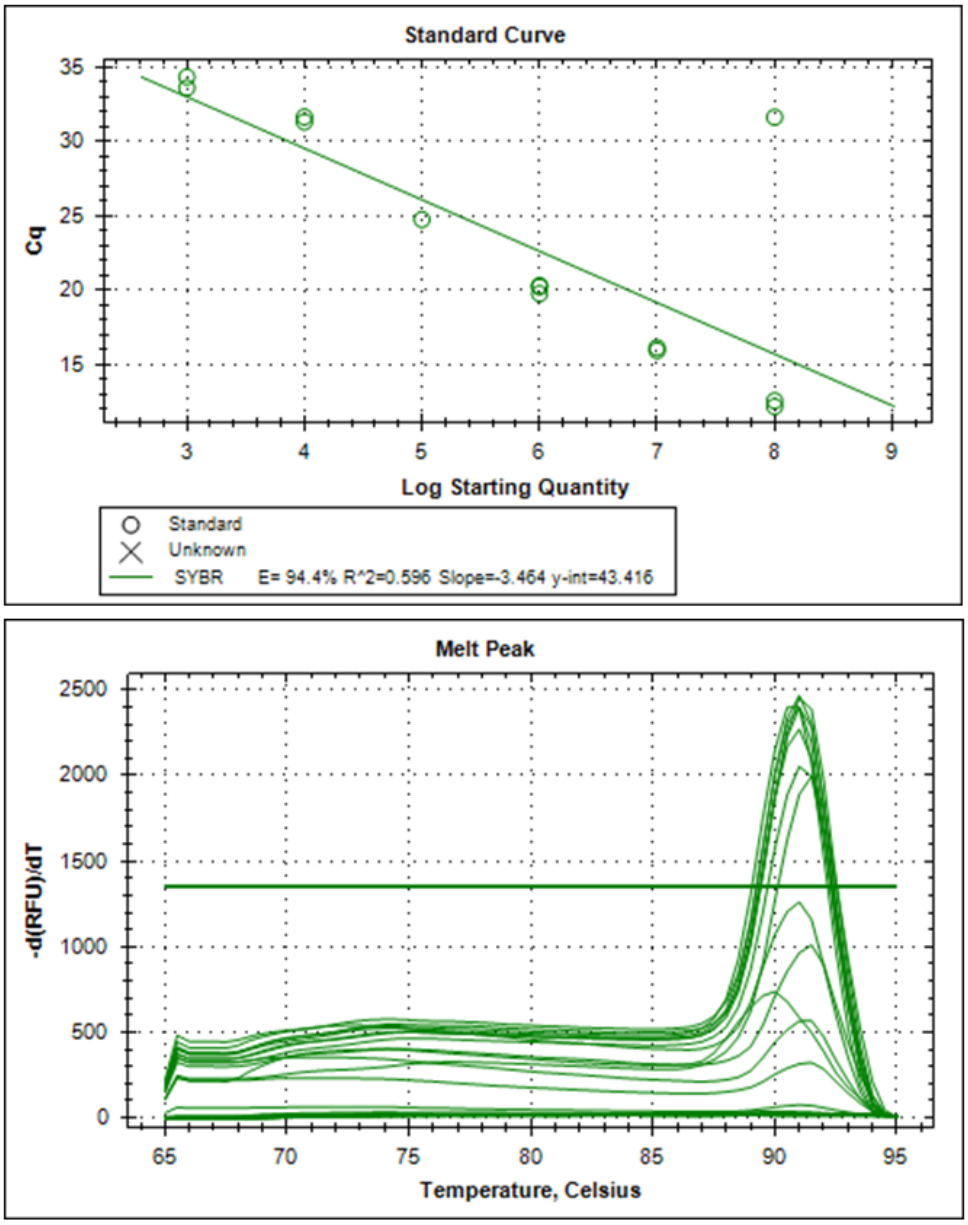

Figure 5.1: Standard curve and melt curve for test 2, GF1 and Dsr2060F/Dsr4R.

To increase the specificity and reduce the number of N/As, 10^8 was excluded from the dilution range. Test 4 had an efficiency >90%, R^2-value >0.95 and 7 N/As were detected. Most of the standards were aligned with the curve. Melt curve analysis for test 4 showed one main peak with two significant minor peaks below. 10^1 dilutions were not amplified, giving flat melt curves. The minor peaks consisted mainly of dilutions in the range of 10^3-10^2 and no melt peaks were observed for NTCs. Standard curve and melt curve for test 4 are shown in figure 5.2.

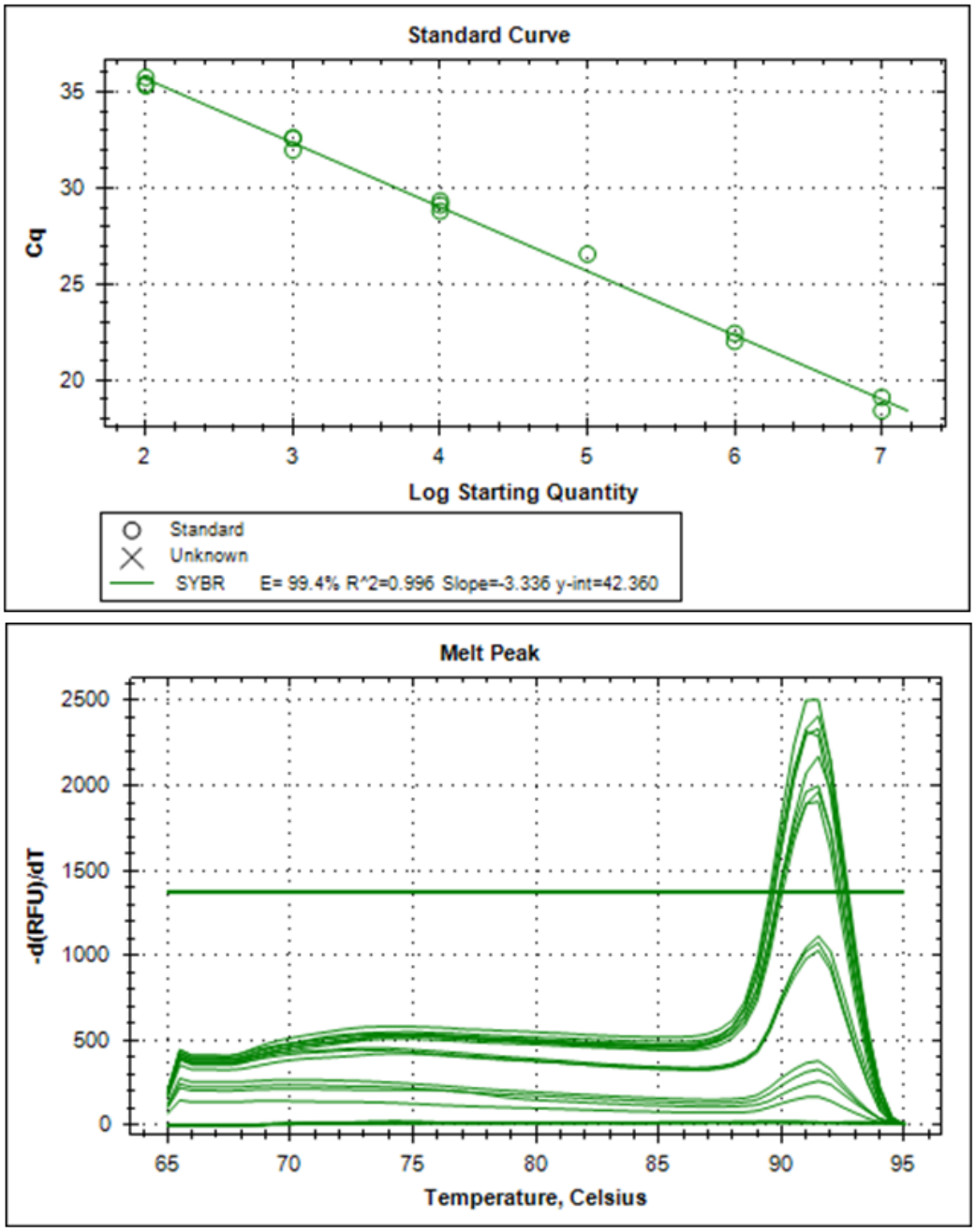

Figure 5.2: Standard curve and melt curve for test 4, GF1 and Dsr2060F/Dsr4R.

To further increase specificity and reduce the number of N/As, 10^1 was excluded from the dilution range. Test 9 had an efficiency <90%, R^2-value >0.95 and 1 N/A was observed. Most of the standards were aligned with the curve. Melt curve analysis for test 9 showed one main peak with two significant minor peaks below. The minor peaks consisted mainly of dilutions in the range of 10^3-10^2 and no melt peaks were observed for NTCs. Standard curve and melt curve for test 9 are shown in figure 5.3.

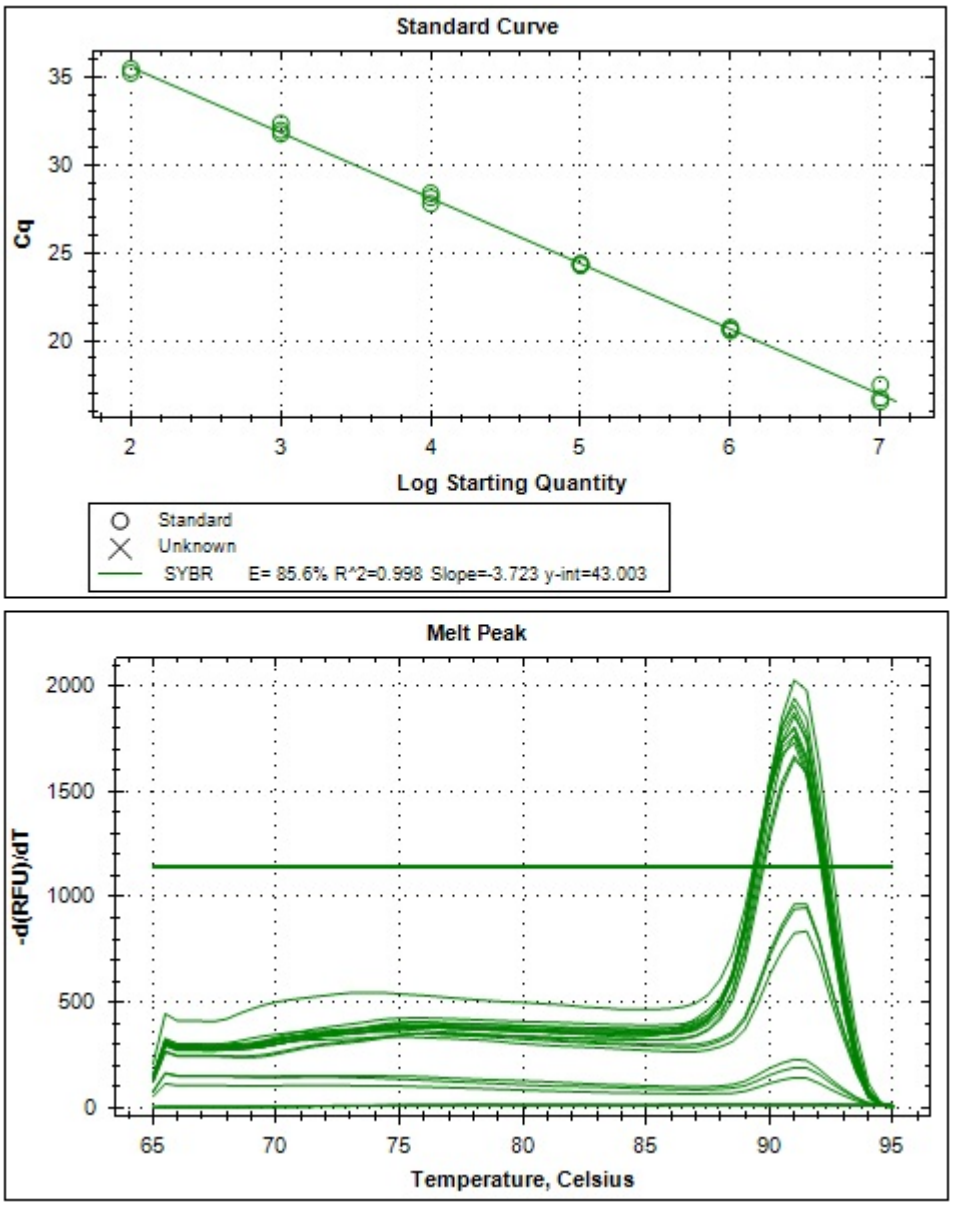

Figure 5.3: Standard curve and melt curve for test 9, GF1 and Dsr2060F/Dsr4R.

From test 14 to test 23 it was decided to increase the primer concentration from 0.25 to 0.5 µM (0.5 to 1.0 µl). 10^2 was excluded from the dilution range. Test 14 had an efficiency <90%, R^2-value >0.95 and no N/A was observed. Most of the standards were aligned with the curve. Melt curve analysis for test 14 showed one main peak with one significant minor peak below. The minor peaks consisted of 10^3 dilutions and no melt peaks were observed for NTCs. The standard curve and melt curve for test 14 are shown in figure 5.4.

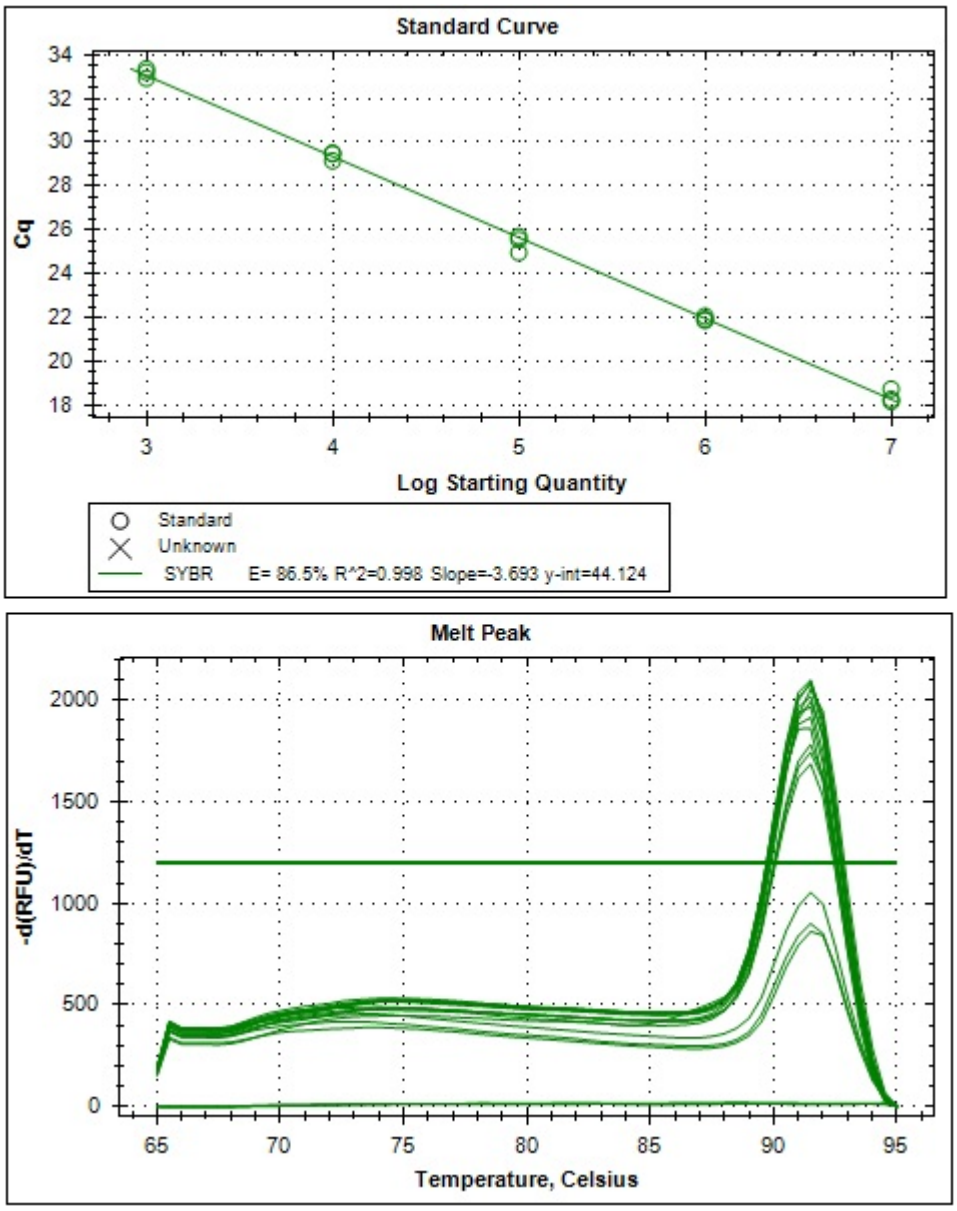

Figure 5.4: Standard curve and melt curve for test 14, GF1 and Dsr2060F/Dsr4R.

For test 24 it was decided to reduce the primer concentration from 0.5 to 0.25 µM and increase the DNA volume from 1.0 to 2.0 µl. Test 24 had an efficiency <90%, R^2-value >0.95 and no N/A was observed. Most of the standards were aligned with the curve. Melt curve analysis for test 24 showed one main peak with minor peaks below. The minor peaks consisted of 10^3 dilutions and no melt peaks were observed for NTCs. Standard curve and melt curve for test 24 are shown in figure 5.5.

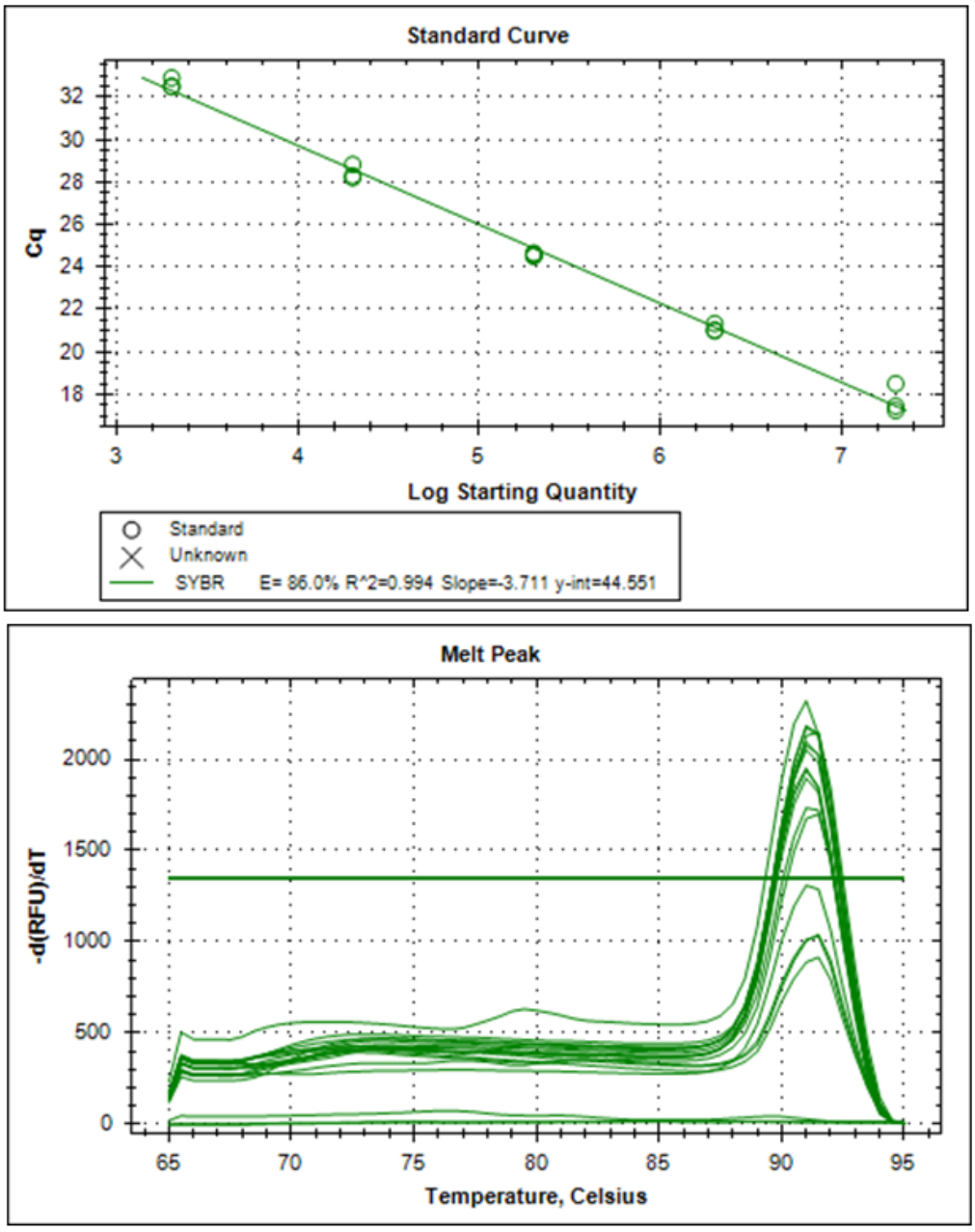

Figure 5.5: Standard curve and melt curve for test 24, GF1 and Dsr2060F/Dsr4R.

See Appendix 6 for additional standard curves and melt curves.

5.2.8 Standard curve optimization using GF1 with primer set DSRp2060F/Dsr4R

In the following section, one qPCR run with GF1 and DSRp2060F/Dsr4R is presented. Table 5.9 shows the main parameters during testing (primer concentration and DNA volume) and standard curve variables. Test 2 had a linear range of 10^7-10^3, an efficiency <90%, R^2-value >0.95 and 4 N/As were observed.

Table 5.9: Optimizing standard curve with GF1 and DSRp2060F/Dsr4R.

Test No.	Primer conc. (µM)	DNA vol. (µl)	Efficiency	R^2	Slope	y-int	No. of N/A
2	0.25	1.0	83.6%	0.994	-3.791	43.937	4

Most of the standards were aligned with the curve. Melt curve analysis for test 2 showed one main peak with minor peaks below. The minor peaks consisted of 10^3 dilutions and no melt peaks were observed for NTCs. Standard curve and melt curve for test 2 are shown in figure 5.6.

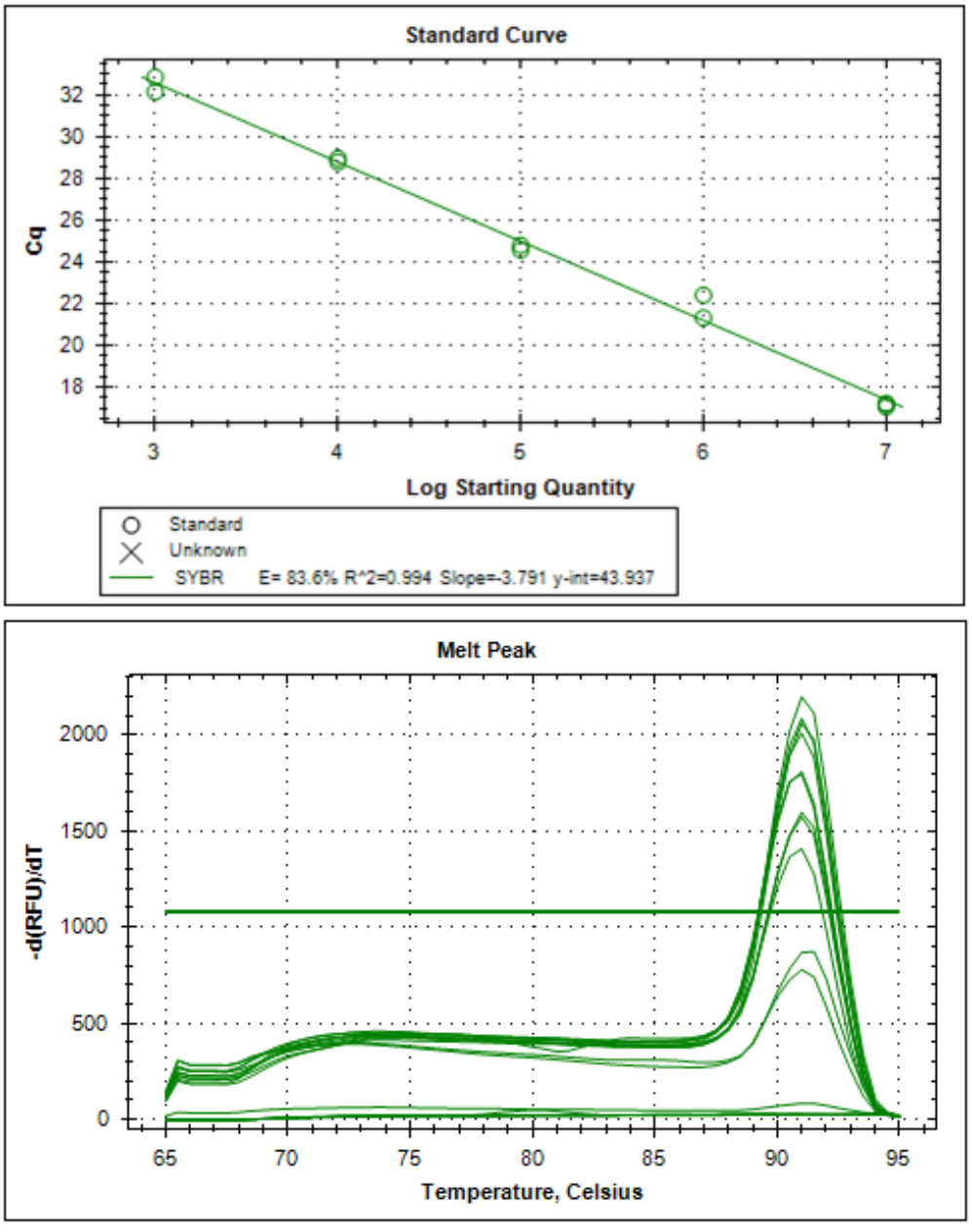

Figure 5.6: Standard curve and melt curve for test 2, GF1 and DSRp2060F/Dsr4R.

See Appendix 7 for additional standard curve and melt curve.

5.2.9 Standard curve optimization using GF2 with DSRp2060F/Dsr4R

In the following section, two qPCR runs with GF2 and DSRp2060F/Dsr4R are presented. Table 5.10 shows the main parameters during testing (primer concentration and DNA volume) and standard curve variables.

Table 5.10: Optimizing standard curve with GF2 and DSRp2060F/Dsr4R.

Test No.	Primer conc. (µM)	DNA vol. (µl)	Efficiency	R^2	Slope	y-int	No. of N/A
1	0.5	1.0	81.8%	0.973	-3.853	42.369	2
2	0.5	2.0	55.1%	0.955	-5.248	53.937	2

Both qPCR runs were tested in the linear range of 10^7-10^3. Test 1 had an efficiency <90%, R^2-value >0.95 and 2 N/As were observed. Some standards were not aligned with the curve. Melt curve analysis for test 1 showed one main peak with minor peaks below. The minor peaks consisted of 10^3 dilutions and no melt peaks were observed for NTCs. Standard curve and melt curve for test 1 are shown in figure 5.7.

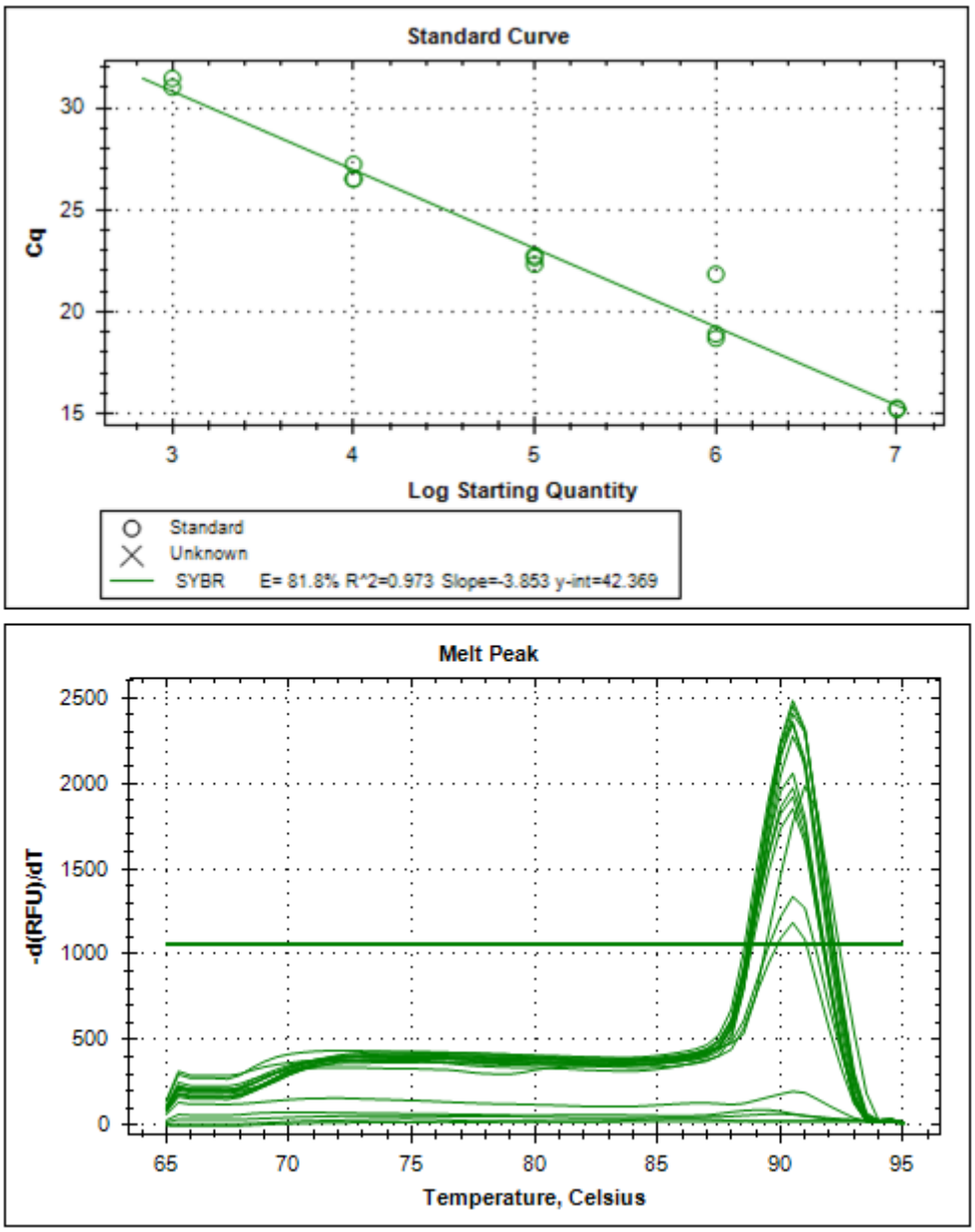

Figure 5.7: Standard curve and melt curve for test 1, GF2 and DSRp2060F/Dsr4R.

For test 2 it was decided to increase the DNA volume from 1.0 to 2.0 µl. Test 2 had an efficiency <90%, R^2-value >0.95 and 2 N/As were observed. Most of the standards were not aligned with the curve. Melt curve analysis for test 2 showed one main peak with minor peaks below. The minor peaks consisted of 10^5- 10^3 dilutions and no melt peaks were observed for NTCs. Standard curve and melt curve for test 2 are shown in figure 5.8.

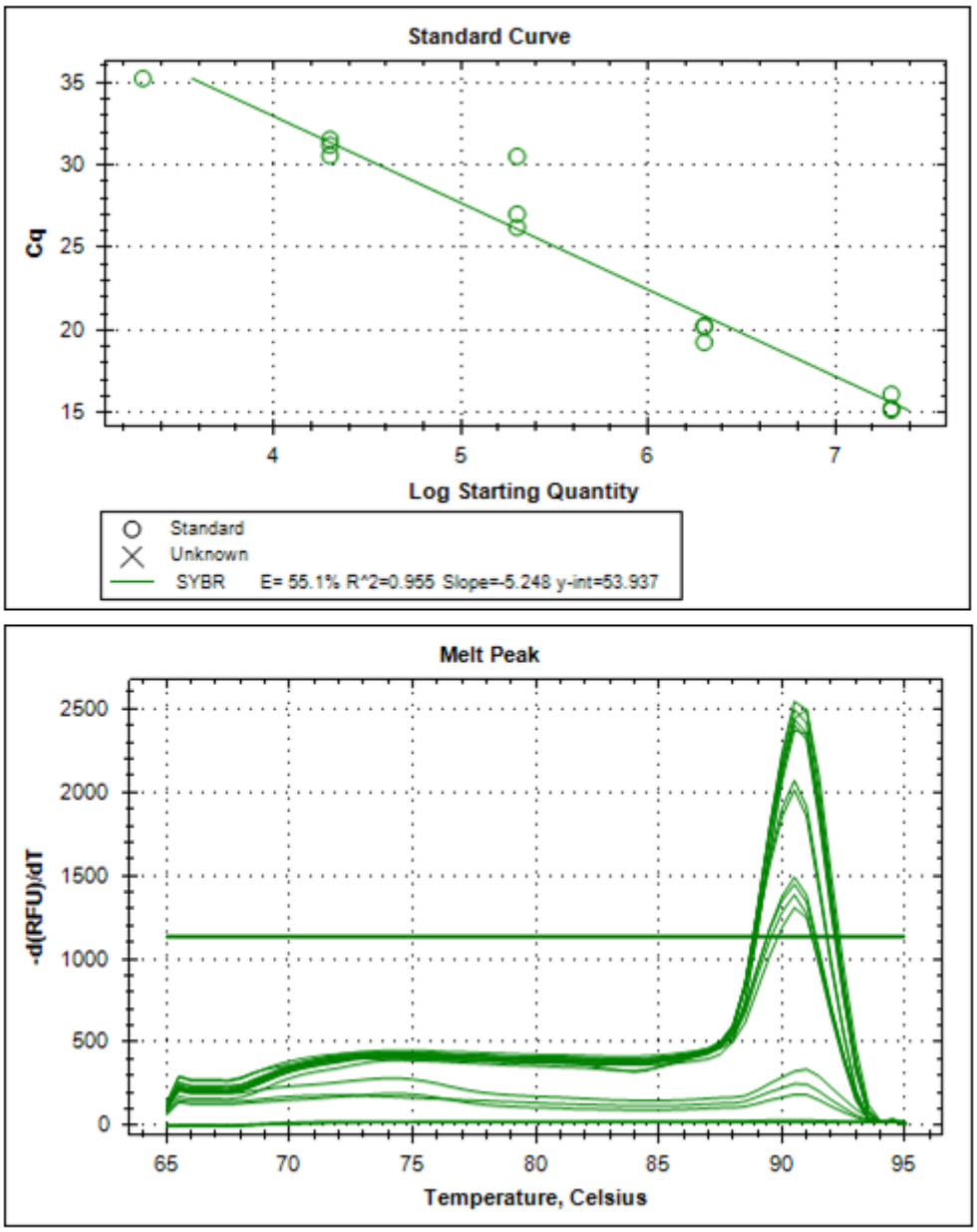

Figure 5.8: Standard curve and melt curve for test 2, GF2 and DSRp2060F/Dsr4R.

See Appendix 8 for additional standard curve and melt curve.

5.2.10 Standard curve optimization post cloning with primer set DSRp2060F/Dsr4R

In the following section, one qPCR run with cloned plasmid DNA with PCR insert (DNA from produced water Eldfisk 2/7S, *sample 2*) and DSRp2060F/Dsr4R is presented. Table 5.11 shows the main parameters during testing (primer concentration and DNA volume) and standard curve variables. The qPCR run for test 5 consisted of 38 cycles instead of the established 35. Test 5 had a linear range of 10^7-10^3, an efficiency <90%, R^2-value >0.95 and no N/As were observed. However, all NTCs were amplified.

Table 5.11: Optimizing standard curve by using cloned plasmid DNA PCR insert (from Eldfisk 2/7S, summer 2017) with DSRp2060F/Dsr4R.

Test No.	Primer conc. (µM)	DNA vol. (µl)	Efficiency	R^2	Slope	y-int	No. of N/A
5	0.5	1.0	88.8%	0.992	-3.625	45.735	0

Standards were mostly aligned with the curve. Melt curve analysis for test 5 showed one main peak with minor peaks below. The minor peaks consisted of 10^3 dilutions and melt peaks were observed for NTCs. In addition, 10^7-10^6 had extra peaks to the right. Standard curve and melt curve for test 5 are shown in figure 5.9.

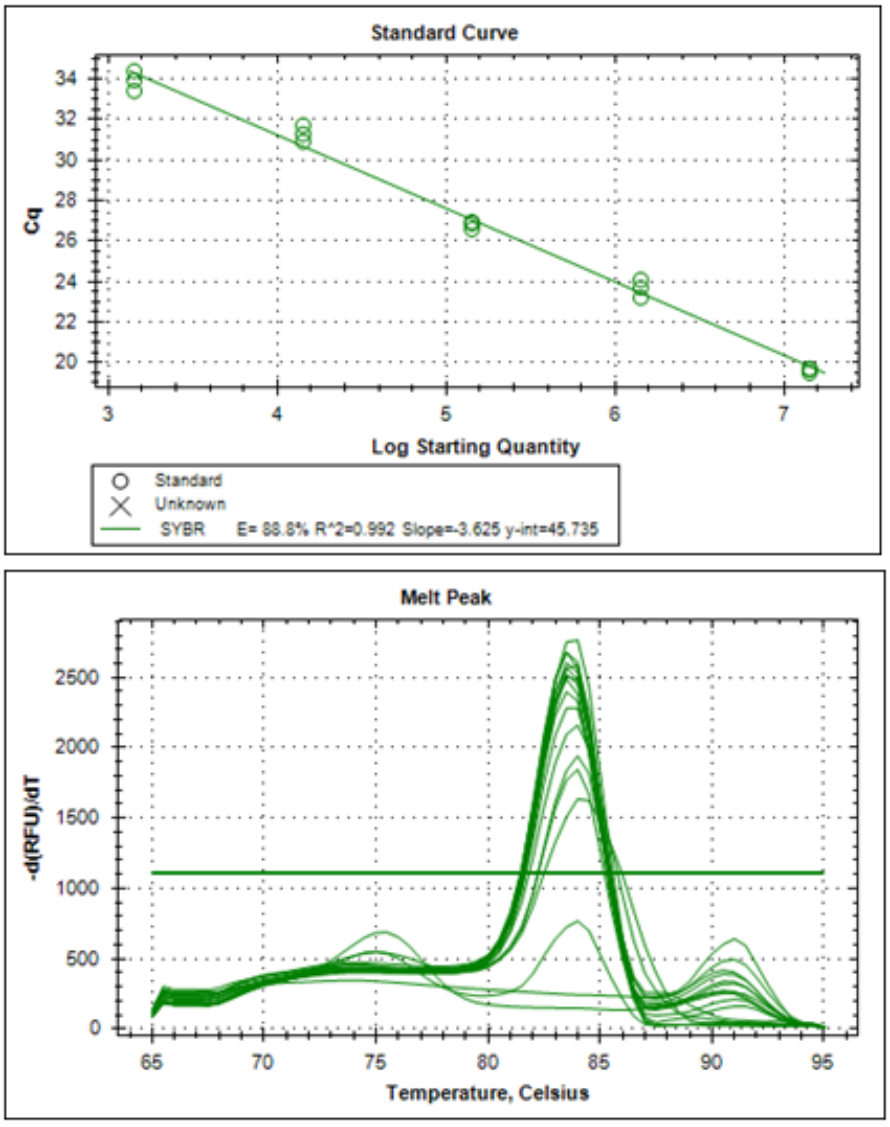

Figure 5.9: Standard curve and melt curve for test 5, post cloning with DSRp2060F/Dsr4R.

See Appendix 9 for additional standard curves and melt curves.

5.2.11 Standard curve optimization post cloning with primer set DSRp2060F/Dsr4R and samples

In the following section, two qPCR runs with cloned plasmid DNA with PCR insert (DNA from produced water Eldfisk 2/7S) with primer set DSRp2060F/Dsr4R and quantified samples are presented. Table 5.12 shows the main parameters during testing (primer concentration and DNA volume) and standard curve variables.

Table 5.12: Optimizing standard curve by using cloned plasmid DNA with PCR insert (using DSRp2060F/Dsr4R) and quantified samples.

Test No.	Primer conc. (µM)	DNA vol. (µl)	Efficiency	R^2	Slope	y-int	No. of N/A
1	0.5	1.0	113%	0.910	-3.045	43.600	8
2	0.5	1.0	98.8%	0.881	-3.352	45.479	7

The standard curve for test 1 had a linear range of 10^7-10^3, an efficiency >110%, R^2-value <0.95 and 8 N/As were observed. Standards were not aligned with the curve. Standard curve for test 1 is shown in figure 5.10.

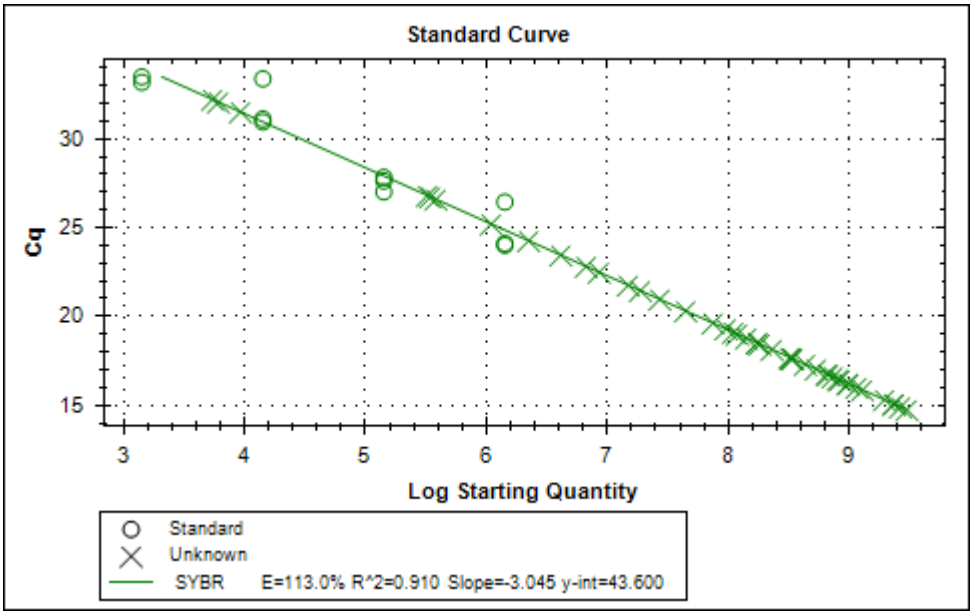

Figure 5.10: Standard curve for test 1, post cloning with DSRp2060F/Dsr4R and quantified samples.

The melt curve for test 1 showed multiple melt peaks and is shown in figure 5.11. Produced water samples from Ekofisk 2/4J gave the highest peaks (highlighted in black). Injection water samples from Ekofisk 2/4VB gave minor peaks with development of shoulders (highlighted in orange) and standard DNA gave intermediate peaks (highlighted in red). NTCs gave flat curves.

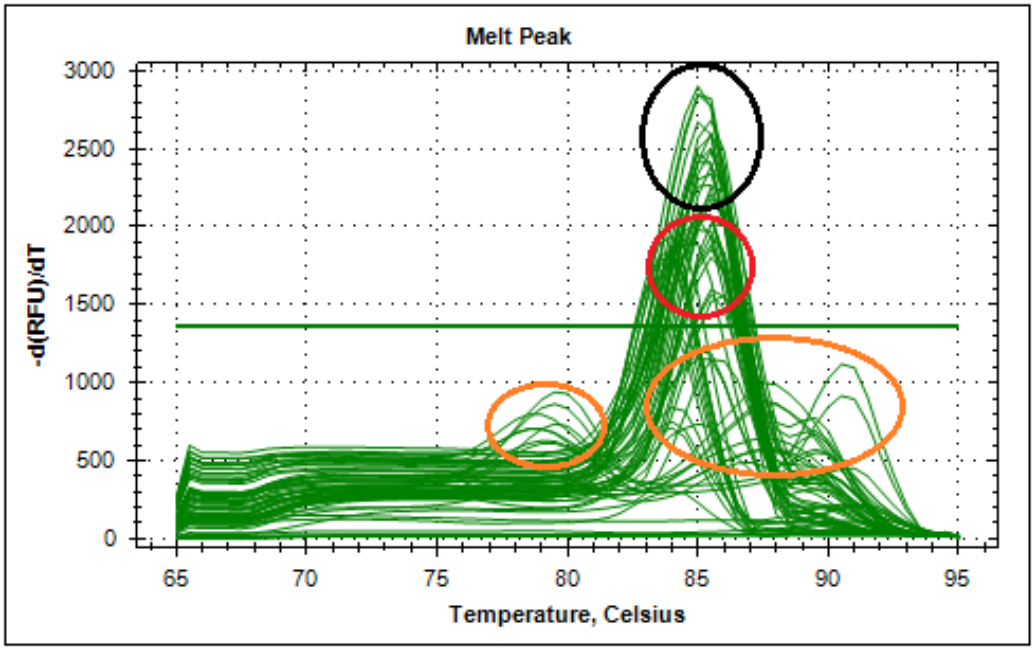

Figure 5.11: Melt curve for test 1, post cloning with DSRp2060F/Dsr4R and quantified samples. Standard DNA highlighted in red, produced water samples highlighted in black and injection water samples highlighted in orange.

The standard curve for test 2 had a linear range of 10^8-10^3, an efficiency >90%, R^2-value <0.95 and 7 N/As were observed. Standards were not aligned with the curve. Standard curve for test 2 is shown in figure 5.12.

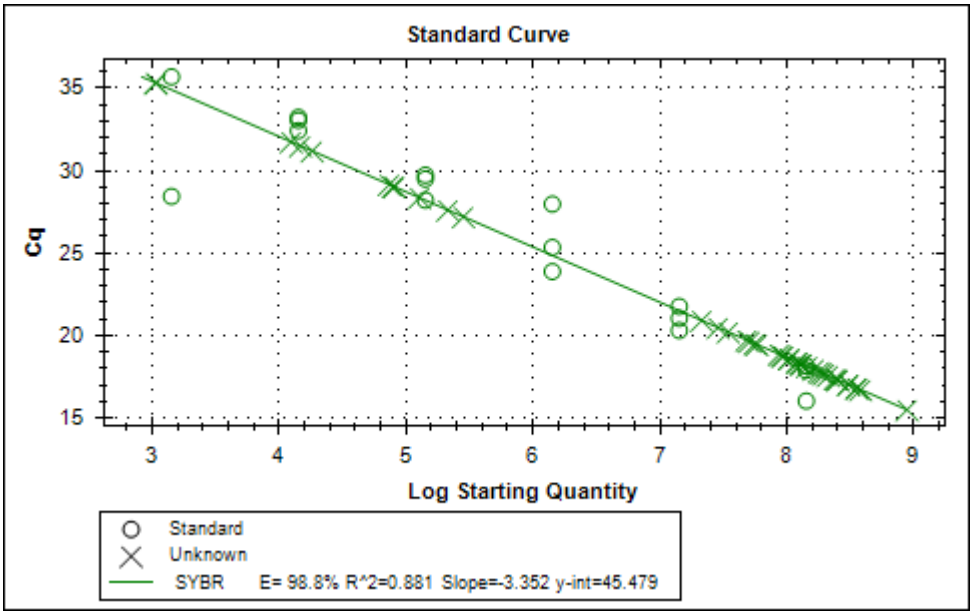

Figure 5.12: Standard curve for test 2, post cloning with DSRp2060F/Dsr4R and quantified samples.

The melt curve for test 2 showed multiple melt peaks and is shown in figure 5.13. Produced water samples from Ekofisk 2/4J gave the highest peaks (highlighted in black) with some shoulder development. Injection water samples from Ekofisk 2/4VB gave minor peaks with shoulders

(highlighted in orange). The left peak in the melt curve consists of standard DNA from 10^8 to 10^5 (highlighted in red), whereas 10^4-10^3 melt peaks were spread in multiple peaks below. NTCs gave flat curves.

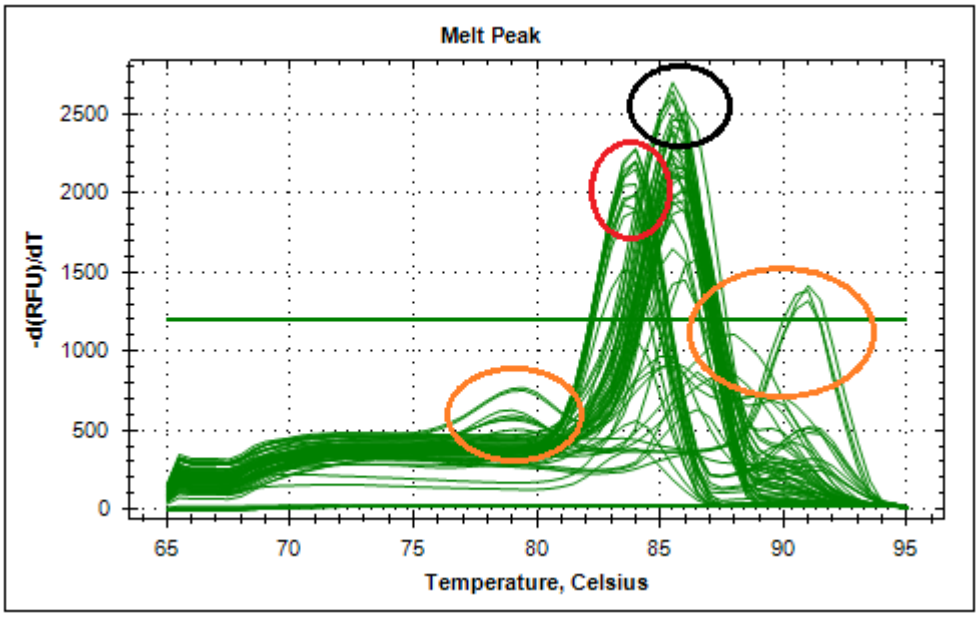

Figure 5.13: Melt curve for test 2, post cloning with DSRp2060F/Dsr4R and quantified samples. Standard DNA 10^8-10^5 highlighted in red, produced water samples highlighted in black and injection water samples highlighted in orange.

See Appendix 10 for additional standard curve and melt curve.

5.3 qPCR results

In test 7, the final qPCR results were achieved by the standard curve that was constructed using cloned plasmid DNA with the PCR insert (DNA from produced water Eldfisk 2/7S, *sample 2*) and DSRp2060F/Dsr4R. For test 7 all reagents, except template DNA, were combined prior to pipetting into plate wells. The optimized reagent mix is presented in table 5.13.

Table 5.13: Optimized reagent mix for qPCR.

Reagent	Volume
SYBR® Green Supermix	10 µl
Forward primer (DSRp2060F)	1.0 µl*
Reverse primer (Dsr4R)	1.0 µl*
Template DNA	1.0 µl
Molecular grade water	7.0 µl
Total reaction volume	20 µl

*0.5 µM

The standard curve had a linear range from $1.42x10^8$ to $1.42x10^3$, making the LOD 10^3 dsrB copies/µl. A 95.2% efficiency was achieved with no N/As, and a R^2-value of 0.988. Table 5.14 shows the main parameters (primer concentration and DNA volume) and standard curve variables.

Table 5.14: qPCR results.

Test No.	Primer conc. (µM)	DNA vol. (µl)	Efficiency	R^2	Slope	y-int	No. of N/A
7	0.5	1.0	95.2%	0.988	-3.442	46.129	0

The standards are partially aligned with the curve, while the unknown samples are concentrated in the middle (10^5 copies/µl) and the lower end of the curve (10^7-10^8 copies/µl). Standard curve for the final qPCR run is shown in figure 5.14.

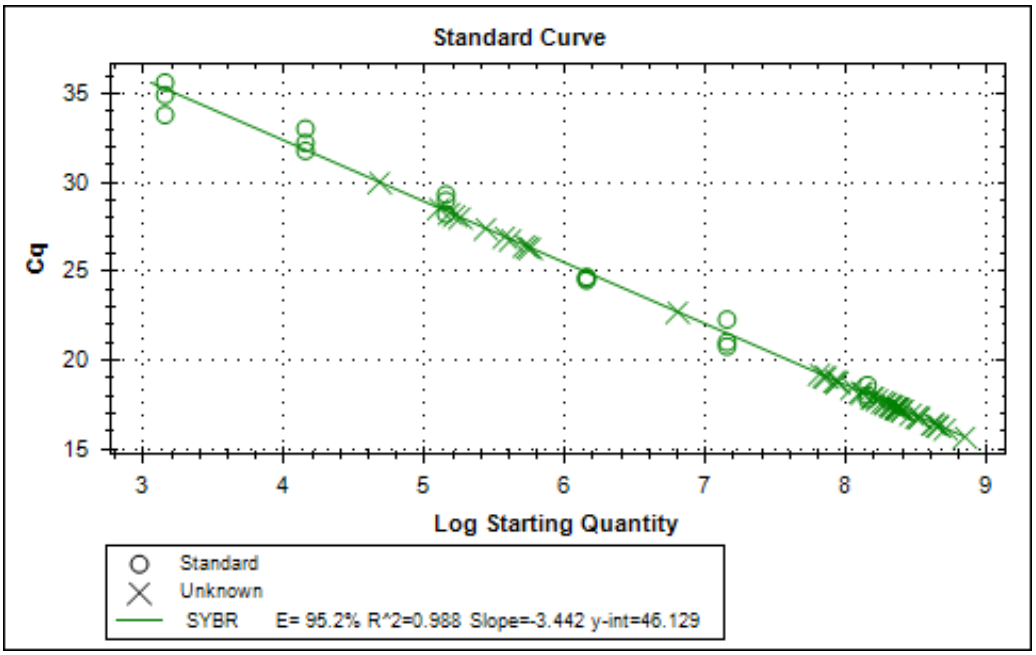

Figure 5.14: Optimized standard curve with quantified samples.

The melt curve showed multiple melt peaks and is presented in figure 5.15. The left peak in the melt curve consists of standard DNA from 10^8 to 10^5 (highlighted in red), where 10^8-10^6 had shoulder development. Standard 10^4-10^3 melt peaks were spread in multiple peaks below. The highest peak consists mainly of produced water samples from Ekofisk 2/4J (highlighted in black), while the lower peaks on both sides, consist of injection water samples from Ekofisk 2/4VB (highlighted in orange). All injection water samples had significant shoulders. Two NTCs had minor peaks (highlighted in blue), but no amplification was detected. For raw melt data, see Appendix 11.

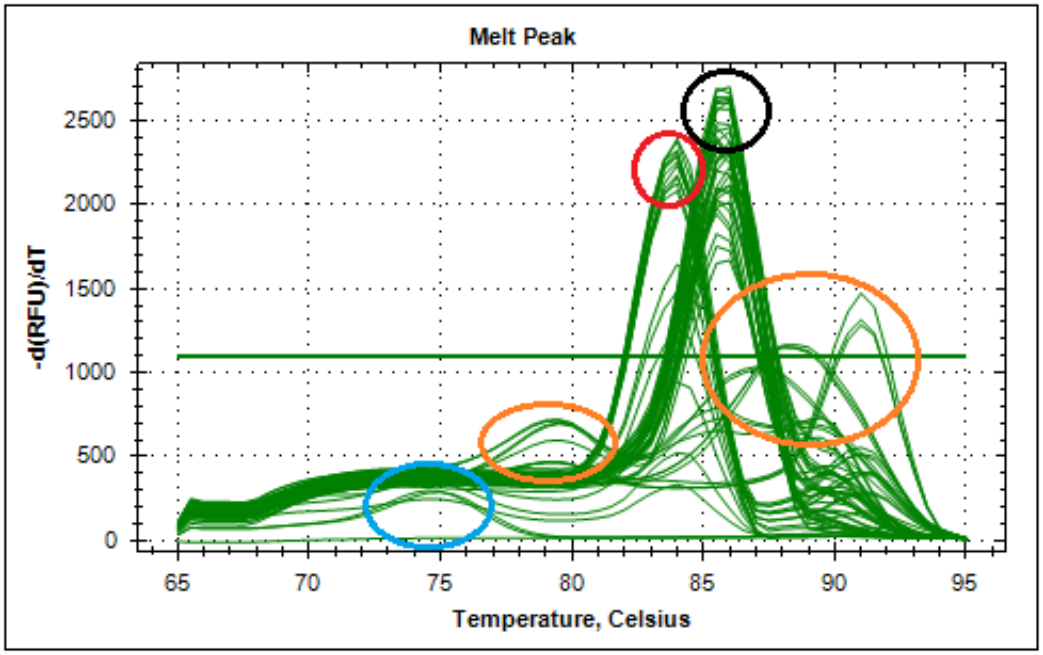

Figure 5.15: Final melt curve for qPCR with quantified samples. Standard DNA 10^8-10^5 highlighted in red, produced water samples highlighted in black, injection water samples highlighted in orange and NTCs highlighted in blue.

The amplification plot shows that most of the samples have Cq values between 16 and 20 (see figure 5.16).

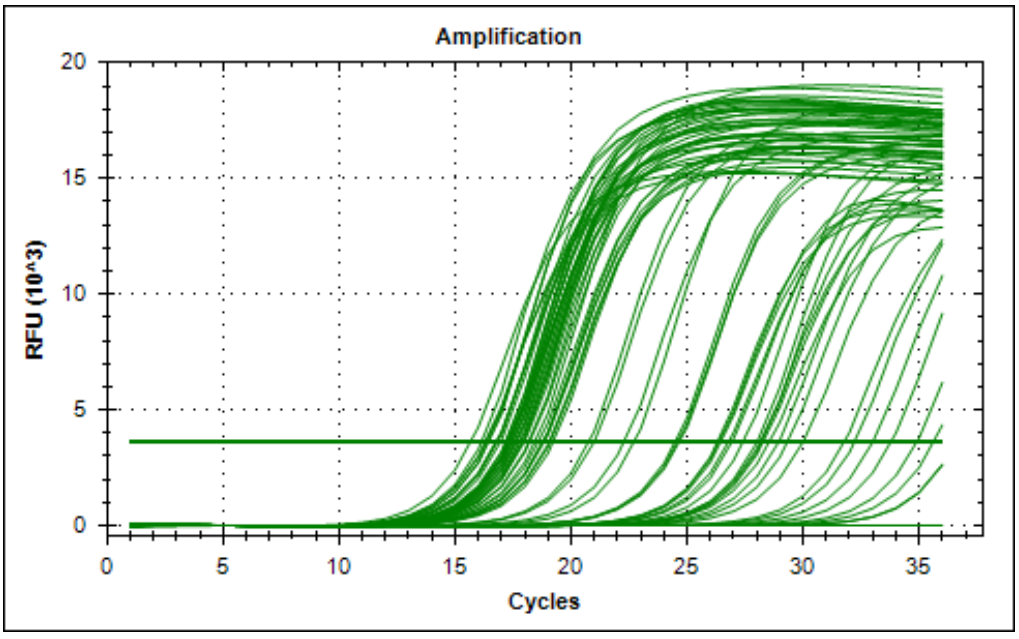

Figure 5.16: Amplification plot of optimized standard curve with quantified samples.

The amplification alignment of the triplicates is indicated by the standard deviation of Cq values (see table 5.15). The standard deviation between the average Cq values for standards varies between 0.1 and 0.92.

Table 5.15: Cq average and standard deviation for optimized standard curve.

Content	Cq average	Cq Std. Dev.
$1.42x10^8$	18.13	0.41
$1.42x10^7$	21.35	0.81
$1.42x10^6$	24.59	0.1
$1.42x10^5$	28.84	0.57
$1.42x10^4$	32.34	0.63
$1.42x10^3$	34.78	0.92

Injection and produced water samples were quantified using the standard curve generated. The average dsrB copy number at Ekofisk 2/4VB varies from 10^5 to 10^6, while the average dsrB copy number at Ekofisk 2/4J varies from 10^7 to 10^8. Samples for Ekofisk 2/4VB in November, December and January have the highest standard deviations with respect to average Cq and varies from 0.98 to 2.91. Results are presented in table 5.16. For raw data, see Appendix 11.

Table 5.16: Cq average, Cq standard deviation and average quantity for samples.

Month	Sampling point	Cq average	Cq Std. Dev.	Average copies/µl
	Ekofisk 2/4J - 1	16.59	0.38	$3.91x10^8$
	Ekofisk 2/4J - 2	17.43	0.17	$2.18x10^8$
Nov. 2017	Ekofisk 2/4J - 3	16.62	0.32	$3.78x10^8$
	Ekofisk 2/4J - 4	17.67	0.48	$1.91x10^8$
	Ekofisk 2/4VB	28.91	0.98	$1.14x10^5$
	Ekofisk 2/4J - 1	17.15	0.32	$2.65x10^8$
	Ekofisk 2/4J - 2	18.91	0.17	$8.07x10^7$
Dec. 2017	Ekofisk 2/4J - 3	16.10	0.37	$5.38x10^8$
	Ekofisk 2/4J - 4	18.10	0.39	$1.42x10^8$
	Ekofisk 2/4VB	26.06	2.91	$2.26x10^6$
	Ekofisk 2/4J - 1	17.23	0.08	$2.48x10^8$
	Ekofisk 2/4J - 2	17.89	0.07	$1.60x10^8$
Jan. 2018	Ekofisk 2/4J - 3	19.03	0.22	$7.50x10^7$
	Ekofisk 2/4J - 4	17.47	0.14	$2.12x10^8$
	Ekofisk 2/4VB	27.15	1.01	$3.70x10^5$
Mar. 2018	Ekofisk 2/4VB	26.58	0.33	$4.87x10^5$

The average dsrB copy number in injection water from *Ekofisk 2/4VB* was increased from November to December (10^5 to 10^6), and a decrease was observed from December to January (10^6 to 10^5). Further, a slight increase was observed from January to March. The average dsrB copy number in produced water samples did not show any particular trend, except for a reduction in sampling location *Ekofisk 2/4J-2* from November to December (10^8 to 10^7). In addition, sampling location *Ekofisk 2/4J-3* was reduced from December to January (10^8 to 10^7).

The average dsrB copy numbers for all samples are presented in figure 5.17.

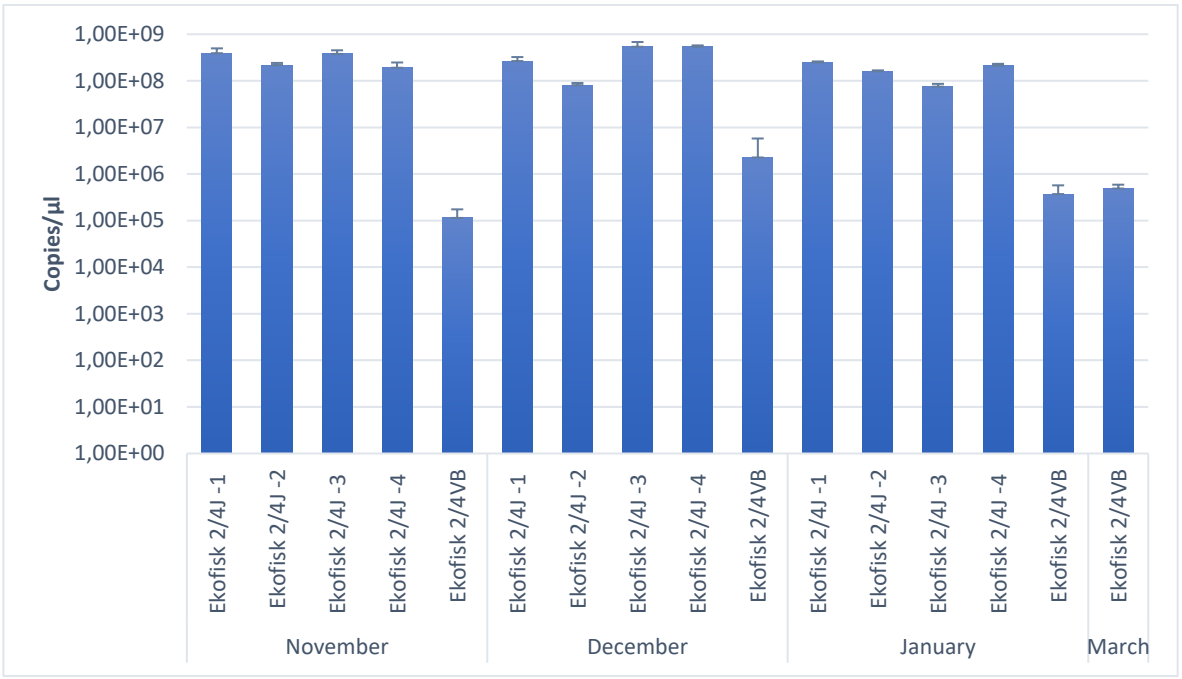

Figure 5.17: Average dsrB gene copy number (copies/µl) in injection and produced water samples, with error bars.

6. Discussion

In this chapter, optimization of the qPCR protocol including standard curve optimization will be discussed. Further, a comparison between the MPN and qPCR methodologies will be made. In addition, the qPCR data will be compared to MPN results obtained from this thesis and reports from ConocoPhillips.

6.1 Optimizing qPCR protocol

The use of PCR prior to qPCR was useful to optimize primer T_a, by narrowing the T_a range that needed to be tested. The *dsrA* specific primer set Dsr-1F/Dsr-R (Kondo et al., 2008) could not be optimized by PCR. Nevertheless, Dsr-1F/Dsr-R was tested by qPCR but could still not be optimized due to amplification of NTCs, multiple N/As and high Cq standard deviation. Primer set rpoB1698F/rpoB2041R (Dahllof et al.,2000) which targeted the RNA polymerase beta subunit (rpoB) was optimized at 48°C (T_a) by PCR and qPCR. Results from the optimization with Dsr-1F/Dsr-R was in accordance with Zhu et al. (2005), reporting that optimized reagent and reaction conditions in PCR may not necessarily be optimal when applied in qPCR. Meanwhile, the primer set Dsr2060F/Dsr4R (Liu et al., 2016) and rpoB1698F/rpoB2041R had the same T_a in both PCR and qPCR. Due to a two-fold higher Cq standard deviation for rpoB1698F/rpoB2041R compared to the *dsrB* specific Dsr2060F/Dsr4R, indicating slightly lower assay specificity, it was decided to proceed standard curve construction with Dsr2060F/Dsr4R.

6.1.1 Standard curve optimization using GF1 with primer set Dsr2060F/Dsr4R

GF1 could not be optimized in this study due to issues related to low efficiencies or high number of N/A, which may be caused by the secondary structures present in the gene fragment. Secondary structures might reduce the amplification efficiency and the specificity of the qPCR assay (Life Technologies™, 2012). The manufacturer of GF1 recommended either gel purification or cloning to reduce the secondary structure effects. Gel purification was carried out but did not seem to have a significant impact on amplification efficiency and reproducibility.

During the optimization of the standard curve, a linear range of 10^8-10^1 gave a low R^2-value and many N/As (test 2). To improve results, 10^8 was excluded from the standard curve, resulting in increased efficiency, R^2-value and a significant reduction of N/As (test 4). To reduce the number of N/As, 10^1 was excluded, resulting in reduced efficiency, slightly increased R^2-value and

significant reductions of N/As (test 9). Due to a low degree of amplification of 10^2 dilutions, these were excluded, and the primer concentration was increased from 0.25 to 0.5 µM (0.5 µl to 1.0 µl) (test 14). This adjustment gave a slight increase of amplification efficiency and N/As were eliminated. Increased pipetting volume of primers might have contributed to the slight increased amplification efficiency and elimination of N/As. At this point, a dilution range of 10^7-10^3 was established. According to Taylor et al. (2010), the exclusion of high and low dilution series may be necessary steps to attain amplification efficiency and R^2-values within the valid range. This practical approach was applied in this study with improved results.

Overall, adjustments made to this point, gave a reduced linear range resulting in elimination of N/As, however, the amplification efficiency was negatively affected. Increased DNA volume (2.0 µl) combined with reduced primer concentration (0.25 µM) gave minor changes in parameters (test 24). In between tests that are presented, this study tested the reproducibility of the assays. Melt curve analysis for all qPCR runs showed that the lower melt peaks consisted of dilutions in the range of 10^3-10^1, indicating lower specificity for these dilutions. According to Taylor et al. (2010) inaccurately calibrated pipettes and inadequate pipetting skills may lead to amplification efficiencies outside the valid range of 90-110%. After numerous adjustments and trials, the combination of GF1 and Dsr2060F/Dsr4R did not meet the assay criteria and a new forward primer, DSRp2060F (5′-CAACATCGTYCAYACCCAGGG-3′) (Geets et al., 2006) was tested.

6.1.2 Standard curve optimization using GF1 with primer set DSRp2060F/Dsr4R

The primer set DSRp2060F/Dsr4R was used to increase the specificity i.e. the amplification efficiency but this was not achieved, which may be due to 2 irregular nucleotides between primer and target sequence. However, Lomans et al. (2016) state that a few irregular nucleotides between primer and target sequence can be successfully applied for qPCR reactions. Melt curve analysis showed lower melt peaks for the lowest dilutions, similar to GF1 with primer set Dsr2060F/Dsr4R.

6.1.3 Standard curve optimization using GF2 with primer set DSRp2060F/Dsr4R

Since GF1 could not be optimized with neither Dsr2060F/Dsr4R nor DSRp2060F/Dsr4R, a new gene fragment (GF2) was used. However, DSRp2060F/Dsr4R in combination with GF2 did in fact *reduce* the amplification efficiency, despite GF2 being one third of the length of GF1. By increasing the DNA volume from 1.0 to 2.0 µl (from test 1 to test 2), the amplification efficiency

dropped from 81.8% to 55.1%, however, in test 2, the R^2-value met the criteria and 2 N/As were detected. Based on these results the use of 1.0 µl DNA and a primer concentration of 0.5 µM was established. Despite only one irregular nucleotide between GF2 and DSRp2060F/Dsr4R, compared to the previous set (GF1 with DSRp2060F/Dsr4R), the amplification efficiency was negatively affected.

According to the user manual from IDT®, the gene fragments were ready for use after initial treatment (IDT®, 2017). However, both GF1 and GF2 needed further purification before they could be applied for standard curve construction. GF2 together with DSRp2060F/Dsr4R did not undergo any purification such as gel clean-up. This might have contributed to the inconsistent results obtained. Erroneous data could have been avoided by amplifying short target sequences and ideally target sequences should be between 60 and 200 bp. If long, slightly degraded sequences are used, for instance over 1200 bp such as GF1 (1941 bp), primer annealing might be affected (Life Technologies™, 2012). Whitby and Skovhus (2009) recommend target sequences in the range of 75-250 bp and that sequences longer than 250 bp may lower the assay sensitivity. Despite the application of GF2 (350 bp), insufficient amplification efficiencies were still an issue. An observation for most of the tests with gene fragments (GF1 and GF2) was that the lower dilutions (10^3-10^1) were often not amplified, indicating reduced specificity for these dilutions. Since the gene fragments together with Dsr2060F/Dsr4R and DSRp2060F/Dsr4R could not be optimized, a cloning procedure had to be initiated.

6.1.4 Standard curve optimization post cloning with primer set DSRp2060F/Dsr4R

The qPCR run for test 5 consisted of 38 cycles instead of the optimized 35. This adjustment was made because 10^3 dilutions were not amplified in previous tests. The result was elimination of N/As but amplification of all NTCs, which was apparent in melt curve analysis in the form of minor melt peaks. Based on these results the use of 35 cycles was resumed and used for all future tests. An interesting observation was the development of new lower melt peaks beside the main melt peak and shoulder development post cloning. This might indicate primer-dimers and/or inhibitors. The presence of inhibitors can reduce the amplification efficiency (Opel et al., 2010; Life Technologies™, 2012), however, cloning the gene seems to have contributed to an overall increase in the amplification efficiency.

6.1.5 Standard curve optimization post cloning with primer set DSRp2060F/Dsr4R and samples

After the introduction of samples, the amplification efficiency increased, the R^2-value decreased and N/As were detected. The detection of N/As and reduced R^2-value is most likely due to pipetting errors. Melt curve analysis showed several melt peaks where some had significant development of shoulders, especially when using the injection water samples.

6.2 Optimized qPCR

The initial optimized concentration of primer set Dsr2060F/Dsr4R by qPCR was 0.25 µM, however, at test 14 (GF1 and Dsr2060F/Dsr4R) during standard curve construction, the concentration was increased to 0.5 µM for several tests and used in final qPCR results. This shows the continuous optimization of the qPCR protocol. Results with amplification efficiencies outside the interval of 90-110% are not reliable, leading to a lower dynamic range and reduces the practical applicability of qPCR (Life Technologies™, 2012). However, a review by Zhang and Fang (2006) suggested that amplification efficiencies could lie in the interval 80-115%. The final qPCR results obtained had an amplification efficiency of 95.2% and R^2-value of 0.988, which is well within the valid range.

Initial quantification of samples gave multiple N/As (table 5.12). After recommendations from Bio-Rad (2018) the SsoAdvanced™ Universal SYBR® Green Supermix, primers and molecular grade water were mixed prior to pipetting into wells. This simplification increased the pipetting volume and thereby reduced the risk of pipetting errors and eliminated N/As. The linear range in test 1 in standard curve optimization (post cloning with DSRp2060F/Dsr4R and samples) was 10^7-10^3. However, some of the quantified samples were outside the linear range of the standard curve, leading to a reintroduction of 10^8 dilutions to the standard curve. The melt curve obtained had several lower peaks and shoulders. Injection water samples from Ekofisk 2/4VB gave the least specific results due to the combination of lower melt peaks with significant shoulders and highest Cq standard deviation. According to Opel et al. (2010), an alteration of the melt curve may indicate the presence of inhibitors. PCR inhibitors such as Polyaromatic Hydrocarbons (PAH's) and heavy metals present in produced water from Ekofisk 2/4J might contribute to the decreased specificity (Lozano-A et al., 2008). As mentioned, lower melt peaks may indicate primer-dimers and these may result in a poor qPCR efficiency and complicates data analysis (Life Technologies™, 2012). Nonetheless, the amplification efficiency for the final results was within

the acceptable range.

The last step in the cloning procedure involved plasmid linearization, which was not attainable, and thereby the supercoiled plasmid was further used for qPCR optimization. Linearization might have been possible by increasing the DNA volume and/or increasing incubation time. There is no consensus whether a supercoiled plasmid or a linearized plasmid is most suitable for construction of standard curves (Kim et al., 2013). According to Suzuki et al. (2000), amplification efficiency can be negatively affected by the supercoiled structure of plasmids. Whelan et al. (2003) showed no significant difference between supercoiled and linearized plasmids in constructing standard curves. In addition, it was shown that supercoiled plasmids were more suitable for long-term storage (Whelan et al., 2003). Nonetheless, both forms of plasmids are widely applied (Kim et al., 2013).

The three main methods in obtaining DNA for standard curve construction (using PCR-amplified target sequences, target sequences inserted into plasmids or commercially available DNA), as described by Dhanasekaran et al. (2010), were tested in this study. Plasmids containing the target PCR insert seems to have worked with the highest efficiency. DNA quality measured by Nanodrop™ gave low values for A_{260}/A_{230} (Appendix 5). According to Thermo Fisher (2015) the A_{280}/A_{260} absorbance should ideally be ~1.8 for DNA, and A_{260}/A_{230} absorbance should be in the range of 2.0-2.2. Corresponding average values for sample 2 (Plasmid with target PCR insert, DSRp2060F/Dsr4R primer set) which was selected for final standard curve construction, were 1.86 and 0.02. The low values for A_{260}/A_{230} may be due to residuals from the DNA extraction (Thermo Fisher, 2015).

The LOD was 10^3 dsrB copies/µl, however, all the samples were within the range of the standard curve. It was challenging to reproduce standard curves with 10^1-10^2 copy numbers as precision and sensitivity is reduced with the copy number (Bustin et al., 2009). The standard triplicates should ideally be aligned along the curve, but this was only partially achieved. This may be caused by minor errors in sample preparation such as preparing dilutions. Standard deviation for Cq values shows that several samples within triplicates vary with more than one cycle, which could negatively affect the amplification efficiency. In this study, the efficiency does not seem to be affected. SYBR® Green I is limited by its low specificity but it is widely applied because of its simplicity and low cost (Kim et al., 2013). If the probe-based TaqMan assay would have been used, it might have increased the specificity, detection sensitivity and reproducibility of the qPCR results (Thermo Fisher, 2018).

According to Klein et al. (2001) the Dsr enzyme has been identified in all SRP that have been studied. Thus, the additional melt peaks may be caused by amplification of Archaea, in particular, the *Archaeoglobus* species. The dsr gene is also present in sulphite-reducing bacteria (Agrawal and Lal, 2009) which may further contribute to additional melt peaks as observed in this study. Despite several distinct and lower melt peaks obtained in this study, the efficiency and R^2-value were satisfactory. According to Dhanasekaran et al. (2010) standard curve construction requires considerable amount of work and the reproducibility is of vital importance, especially when comparing multiple samples over time. Bustin et al. (2010) discussed that repeatability of the qPCR assay should be documented. It would have been useful to repeat the final qPCR run to verify the linearity, specificity and quantification of unknown samples, but remaining amounts of standard DNA and samples were limiting factors. The secondary objective in this thesis was to develop a qPCR protocol for use in bacteriological monitoring. Due to the extensive testing, this objective required most of the workload during the thesis work. As a consequence, there was less time for analysis of a broader range of samples.

6.3 Comparing qPCR and MPN

SRB growth was not detected in any of the injection nor produced water samples by means of MPN. The highest difference between sampling temperatures for produced water samples was 21.8 °C, which made it challenging to select a suitable incubation temperature for the MPNs and might have been a contributing factor for the observation of no SRB growth. SRB were detected in both injection and produced water by qPCR using dsrB specific primers. qPCR results for both injection and produced water have few variations, but not enough to reveal any trend. Water injection samples obtained from September and October 2017, could not be utilized in qPCR due to lack of DNA. Thus, leading to a limited selection of samples. Lee et al. (2015) suggest a broad range of sampling locations and sample points to establish the presence of any trends. Only based on *these* results, can the bacteriological monitoring programs be evaluated and adjusted. Furthermore, Lomans et al. (2016) state that establishing a trend of bacterial numbers has more value than single measurements. The breakdown of algae and zooplankton functions as a source of carbon in injection water systems (Alkindi et al., 2007). In the North Sea, algae and zooplankton growth is most prevalent in the end of spring and in the fall (Spark and Mutch, 2002), but these variations could not be studied in this thesis due to time restrictions for sampling. SRB detection by qPCR in produced water were quantified near the upper level of the standard curve (10^7-10^8) and SRBs in injection water were quantified from 10^5 to 10^6. Since sessile

microorganism quantification by MPN and qPCR was not included in this thesis, the SRB numbers in the system might be higher than detected. qPCR lacks the ability to distinguish between live and dead cells and therefore one should take into consideration that the copy number might overestimate the actual microbiological population. Bae and Wuertz (2009) suggest that qPCR can be combined with intercalating DNA-binding chemicals to reduce the detection of dead cells. In addition, RT-qPCR can be used to detect bacterial activity but is not commonly applied in oilfields due to RNA instability (Johnson and Crane, 2017).

In MPB media as used in this study, lactate is used as the electron donor and carbon source for sulphate reduction. However, if the MPB media contained another electron donor source, such as formate, acetate or ethanol, detection might have been possible (Liamleam and Annachhatre, 2007). Since the MPB media was premade by Intertek, it could not be further optimized. For future studies, different media compositions for SRB cultivation could be tested, such as reported by Ghazy et al. (2011). Hamouda (1991) tested different carbon sources for SRB in injection water at Ekofisk 2/4K, such as acetate, butyric acid, propionic acid and benzoic acid. In addition, Postgate C, Postgate G and BTZ media were tested. From these experiments it was concluded that SRB from Ekofisk 2/4K indeed were lactate utilizers, and MPB media was further used. Hamouda (1991) also conducted MPN for detection of GAB and SRB in the injection water treatment system at Ekofisk 2/4K and was able to detect both GAB and SRB downstream the deaerator and booster pumps. No detection of GAB and SRB downstream the UV sterilizer unit was achieved. In this study there was no detection of bacterial DNA in any of the injection water sample locations, except from Ekofisk 2/4VB.

Robinson et al. (2010) conducted a study at the South Arne field (North Sea, Denmark). They reported GAB and SRB detection by MPN in the water injection system, with identical incubation temperatures as in this thesis. Downstream the deaerator (*pre-biocide*), both GAB and SRB detection was 95 bacteria/ml. Whereas downstream the deaerator (*post biocide*) the GAB and SRB detection was 45 bacteria/ml and 4.5 bacteria/ml, respectively. Samant and Anto (1993) were able to detect both SRB and GAB by MPN in produced water from production separators at the Bombay High Field and the detection range of GAB was 15-47,000 bacteria/ml. Jensen et al. (2013) conducted a study of the produced water system at the South Arne field (North Sea, Denmark) comparing the MPN and qPCR methods for detection of SRB. Out of 74 MPN measurements, only 3 measurements gave bacterial numbers >10 cells/ml. The qPCR detected up to 1,000 cells/ml SRB. Based on these findings, qPCR was added to the regular biomonitoring and risk assessment program. These results further demonstrate a drawback of relying entirely on

MPN data. Jensen et al. (2013) concluded that the application of qPCR for monitoring SRB in oilfields provide a more realistic overview of the microbial status versus the culture-dependent MPN method.

6.4 ConocoPhillips routines and reports

The first step in the MPN method for SRB detection used at the Ekofisk lab, involves filtering 10 l of sample directly from the sampling point, by using 0.45 µm filters. Each filtration step is carried out with 1/10 of the previous filtration volume, directly from the sampling point. In other words, 10 l, 1.0 l and 0.1 l. 1.0 ml is sampled only if SRB have been detected in all three previous dilution steps. This methodical difference in SRB sampling might contribute to the different detection results between this study and ConocoPhillips reports. Due to limitations with regards to logistics and practicality at the University lab, the sample volume had to be reduced to 3.0 l for injection water and 1.0 l for produced water. For GAB detection, the lab at Ekofisk uses the same method as in this thesis (Clariant, 2018). Microbiological measurements should be below the key performance indicators (KPI) as applied by ConocoPhillips, as shown in table 6.1 (ConocoPhillips, 2017). ConocoPhillips performs routine MPN analysis of injection water at several locations, however, only samples received from Eldfisk 2/7E, Eldfisk 2/7B and Ekofisk 2/4VB will be discussed in the following sections. Data comparison will be limited to planktonic bacteria, unless stated otherwise. Due to lack of comparative data, the MPN results from Ekofisk 2/4J produced water will not be discussed.

Table 6.1: Key performance indicators (KPI) applied by ConocoPhillips for bacterial counts (ConocoPhillips, 2017).

Bacteria	KPI
GAB Planktonic	<1000 bacteria/ml
GAB Sessile	<2000 bacteria/cm^2
SRB Planktonic	<1/11.1 L
SRB Sessile	<0.3 bacteria/cm^2

6.4.1 MPN results September 2017

Routine testing of injection water quality is performed at Eldfisk 2/7E US FF, US UV, DS UV and DS Booster pumps. ConocoPhillips (2017) reported detection of GAB <KPI in September 2017 at DS UV. However, MPN results obtained in this thesis at DS UV indicated no GAB growth. In addition, DNA could not be obtained from DS UV water samples. Neither ConocoPhillips nor this thesis detected SRB growth in September 2017.

6.4.2 MPN results October 2017

In October 2017, no GAB or SRB was detected at Eldfisk 2/7E US FF, by filtration of 10 l injection water (ConocoPhillips, 2017), and the same MPN results were obtained in this thesis. In addition, this study tested injection water samples from Eldfisk 2/7E DS DA and Eldfisk 2/7B WH, with no detection of GAB and SRB.

Since DNA could not be obtained from September and October injection water samples, qPCR could not be performed for these samples. In the following sections MPN and qPCR results from Ekofisk 2/4VB obtained in this study will be compared with MPN results from ConocoPhillips.

6.4.3 MPN and qPCR results - Ekofisk 2/4VB

Results obtained in this study and ConocoPhillips MPN reports related to planktonic bacteria at Ekofisk 2/4VB are presented in table 6.2 (ConocoPhillips, 2018). Note that SRB results for March 2018 from ConocoPhillips were not published during the thesis work. ConocoPhillips (2017) reported SRB growth >KPI (1/11.1 L) in November 2017 but SRB could not be detected by MPN in this thesis in the same period. This difference in detection might be due to different filtration volumes (10 l vs. 3 l). However, in this thesis SRB was detected by qPCR with an average of $1.14x10^5$ dsrB copies/µl in November 2017, demonstrating the superior detection capability of qPCR compared to that of MPN. In January 2018, ConocoPhillips reported SRB detection <KPI. In comparison, qPCR results reported $3.70x10^5$ dsrB copies/µl. This demonstrates the importance of collecting and analyzing as much relevant data as possible, by combining different methodologies, to effectively assess the microbial flora.

GAB detection results in this thesis were in accordance with ConocoPhillips reports with regards to KPI during all sampling months, except for December 2017. ConocoPhillips (2018) reported GAB detection <KPI, whereas this thesis detected GAB >KPI (4300 bacteria/ml). This difference in detection might be related to subjective observations and possible errors in assessment of the MPNs. In addition, bacterial growth during transportation could occur, despite samples being kept on ice. This observation further demonstrates some of the limitations of culture-dependent methods.

Table 6.2:Comparison of MPN and qPCR results with respect to planktonic bacteria (ConocoPhillips, 2018).

	MPN		qPCR
	SRB (bacteria/ml)	GAB (bacteria/ml)	SRB (DsrB copies/µl)
November 2017			
ConocoPhillips	>KPI	>KPI	-
Thesis	-	9300	$1.14x10^5$
December 2017			
ConocoPhillips	>KPI	<KPI	-
Thesis	-	4300	$2.26x10^6$
January 2018			
ConocoPhillips	<KPI	<KPI	-
Thesis	-	23	$3.70x10^5$
March 2018			
ConocoPhillips	-	<KPI	-
Thesis	-	93	$4.87x10^5$

As mentioned earlier, Eldfisk 2/7E distributes injection water to Ekofisk 2/4VB. In November and December 2017, ConocoPhillips (2017) reported GAB <KPI at Eldfisk 2/7E DS Booster pumps, which is the last sampling point prior to further distribution of injection water. In the same period, this study detected GAB in the range of 4300-9300 bacteria/ml at Ekofisk 2/4VB. In addition, ConocoPhillips (2017) reported that on average 92% of the samples (November and December 2017) from Ekofisk 2/4VB had values >KPI, including sessile GAB and SRB. These combined results show that treatment of injection water at Eldfisk 2/7E is satisfactory with regards to KPI. The results from Ekofisk 2/4VB indicate a significant increase in the bacterial flora in the injection water pipeline from Eldfisk 2/7E to Ekofisk 2/4VB.

According to Bennet (2016) injection water systems are ironically ideal places for SRB growth. Insufficient chlorine dosages from partly unreliable electro-chlorination units may reduce sterilisation and further facilitate bacterial growth. In addition, the use of deaerator towers gives remaining SRBs ultimate conditions for growth (Bennet, 2016). But lack of GAB detection from samples from Eldfisk 2/7B and Eldfisk 2/7E in combination with no detectable presence of DNA, indicates a well-functioning injection water treatment at Eldfisk 2/7E. The application of oxidizing (hypochlorite) and non-oxidizing (glutaraldehyde) biocides at Ekofisk seems to achieve synergistic effects by reducing bacterial resistance to biocide treatment. The injection water at Ekofisk 2/4VB has undergone the same treatment as the injection water samples from the other sample points (ConocoPhillips, 2018). According to Bennet (2016) batch biocide treatment will

never accomplish 100% microbiological removal. Thus, at any point in time, some bacterial cells will survive the treatment at Eldfisk 2/7E. The travel distance for injection water to Ekofisk 2/4VB, is 23.4 km longer than the distance to Eldfisk 2/7B, giving a longer residence time for bacteria to grow (see figure 3.3). Previous contamination may accumulate in the pipeline, contribute to biofilm growth and the survival of new bacterial cells. Pigging is performed routinely in the injection water pipeline from Eldfisk 2/7E to Ekofisk 2/4K and Eldfisk 2/7B (ConocoPhillips, 2017). Increased frequency of pigging reduces the time for biofilm to grow and bi-weekly pigging is recommended (Pots et al., 2002). However, pigging is not routinely performed downstream the junction towards Ekofisk 2/4VB (ConocoPhillips, 2017). Thus, this part of the pipeline may accumulate GAB and SRB, hence the detection of GAB by MPN and SRB by qPCR at Ekofisk 2/4VB in this study. It should be noted that contamination can occur in the umbilical connecting Ekofisk 2/4VB and Ekofisk 2/4M, which might have caused the detection of SRB. This aspect should not be over-looked and further investigation might be useful. However, there exist plans to treat the umbilical with biocide (ConocoPhillips, Personal communication, 2018).

According to Larsen et al. (2009) the petroleum industry relies mostly on culture-dependent methods such as MPN. Given that only 0.001-15% of the viable bacteria can be cultured (Larsen et al., 2008), relying entirely on MPN data may lead to erroneous interpretation of the bacterial flora causing MIC. Since determination of MPN results involves interpretation of turbidity and colour change, a somewhat subjective conclusion might be drawn. qPCR on the other hand, compared to MPN, is quantitative, with objective criteria to validate results, as reported by Malorny et al. (2008). Optimization of the qPCR protocol involved extensive testing and when optimized, gave more reliable and precise results compared to the MPN method. Lee et al. (2015) reported that qPCR is beneficial for application offshore due to onsite quantification of bacteria and may help to modify biocide programs. MMM for oilfield application should follow a standardized protocol, including important aspects such as sampling method, transport, storage, sample preparation, sample runs and interpretation of results (Hoffman et al., 2007), as documented during this thesis work.

7. Conclusion

The *primary* objective of this study was to compare the culture-dependent MPN method with the culture-independent qPCR method, for absolute quantification of SRB in injection and produced water from the Greater Ekofisk Area. Results in this study document that qPCR is more suitable and reliable for detection and quantification of bacteria compared to the MPN method. Quantitative results by qPCR can be acquired within a few hours, compared to a 30 days incubation period for MPN.

The *secondary* objective was to develop a qPCR protocol for absolute quantification of SRB. A detailed qPCR protocol specific for the functional dsrB gene in SRB was successfully developed, and it would be beneficial for ConocoPhillips to apply qPCR in detection of bacteria in future biomonitoring. It is imperative that the qPCR protocol is performed by qualified personnel to achieve reliable results.

The results obtained in this thesis are not enough to define any trend, nor recommend adjustments in the water injection treatment program. Results from Ekofisk 2/4VB indicate higher bacterial numbers, and measures should be taken to reduce the microbial flora, to further prevent MIC. Relatively high bacterial numbers in produced water were to be expected, but do not show any significant variation in the sampling period. Except for Ekofisk 2/4VB, other injection water sampling locations did not show any signs of bacterial growth, indicating a highly efficient injection water treatment system.

8. Future research

For future research it is recommended to include more samples from various sampling locations over a longer period to establish a trend. The breakdown of algae and zooplankton might affect the bacterial flora in seawater injection systems, and it would be relevant for future studies. To achieve a broader understanding of the bacterial diversity within the water injection system, it would be beneficial to apply dsrA and rpoB primers in addition to inclusion of sessile SRB and GAB. Optimization of these primers should continue. In addition, including 16S rRNA primers for qPCR would increase the overview of the microbial flora in injection water systems. Further, sequencing of the bacteria would determine which SRB populations are present.

The developed qPCR protocol should be repeated to verify its reproducibility and one should seek to reduce additional melt peaks. To assess the efficiency of the biocide treatment that is to be applied to the umbilical between Ekofisk 2/4VB and Ekofisk 2/4M, qPCR could be a useful tool.

Reference list

Agrawal, A. and Lal, B. (2009). Rapid detection and quantification of bisulfite reductase genes in oil field samples using real-time PCR. FEMS Microbial ecology Vol 69, p.301-312.

Ahmadun, F. R., Pendashteh, A., Abdullah, L. C., Biak, D. R. A., Madaeni, S. S. and Abidin, Z. Z. (2009). Review of technologies for oil and gas produced water treatment. Journal of Hazardous Materials. Vol. 170, p. 530-551.

Al-Hashem, A., Carew, J. and Salman, M. (1998). Control of Microbially Influenced Corrosion in an Effluent Water Injection System in West Kuwait. NACE International, paper No.293.

Al-Hashem, A. and Carew, J. (2004). Screening Test for Six Dual Biocide Regimes against Planktonic and Sessile Populations of Bacteria. NACE International, paper No. 04748.

Alkindi, A., Prince-Wright, R., Moore, W., Walsh, J., Morgenthaler, L. and Kuijvenhiven, C. (2007). Challenges for Waterflooding in a Deepwater Environment. Offshore Technology Conference. OTC 18523.

Bae, S. and Wuertz, S. (2009). Discrimination of Viable and Dead Fecal *Bacteroidales* Bacteria by Quantitative PCR with Propidium Monoazide. Applied and Environmental Microbiology, Vol. 75, No. 9, p.2940-2944.

Barton, L. L., Fardeau, M. L. and Fauque, G. D. (2014). Hydrogen Sulfide: A Toxic Gas Produced by Dissimilatory Sulfate and Sulfur Reduction and Consumed by Microbial Oxidation. Metal ions in life sciences, chapter 10, p. 238-272.

Ben-Dov, E., Brenner, A., Kushmaro, A. (2007). Quantification of Sulfate-reducing Bacteria in Industrial Wastewater, by Real-time Polymerase Chain Reaction (PCR) Using dsrA and apsA Genes. Microbial Ecology, Vol.54, p. 439-451.

Bennet, D. G. (2016). Oilfield Microbiology: Detection Techniques Used in Monitoring Problematic Microorganisms Such as Sulphate-Reducing Bacteria SRB. OTC-26788-MS.

Bio-Rad. (2013). SsoAdvanced™ Universal SYBR® Green Supermix. Instruction manual [Online]. Available: http://www.bio-rad.com/webroot/web/pdf/lsr/literature/10031339.pdf last accessed: 14.04.18.

Bio-Rad. (2018). Personal communication.

Biotechnology Solutions (BTS). (2017). Modified Postgate's B Media (MPB) [Online]. Available: https://biotechnologysolutions.com/modified-postgates-b-media-mpb/# last accessed 07.02.18.

Branda, S.S., Vik, A., Friedman, L. and Kolter, R. (2005). Biofilms: the matrix revisited. Trends in Microbiology, Vol. 13, No.1, p. 20-26.

Bridier, A., Briandet, R., Thomas, V. and Dubois-Brissonnet, F. (2011). Resistance of bacterial biofilms to disinfectants: a review. Biofouling – The Journal of Bioadhesion and Biofilm Research. Vol. 27, No. 9, p. 1017-1032.

Brown, M. R. W. and Gilbert. P. (1993). Sensitivity of biofilms to antimicrobial agents. J. Applied Bacteriological Symp. Suppl. Vol. 74, p. 87-97.

Bustin, S. (2008). Real-time quantitative PCR – opportunities and pitfalls. European Pharmaceutical Review. Issue 4.

Bustin, S. A., Benes, V., Garson, J. A., Hellemans, J., Huggett, J., Kubista, M., Mueller, R., Nolan, T., Pfaffl, M. W., Shipley, G. L., Vandesompele, J. and Wittwer, C. T. (2009). The MIQE Guidelines: Minimum Information for Publication of Quantitative Real-Time PCR Experiments. Clinical Chemistry. 55:4, p. 611-622.

Bustin, S. A., Beaulieu, J. F., Huggett, J., Jaggi, R., Kibenge, F. S. B., Olsvik, P. A., Penning, L. C. and Toegel, S. (2010). MIQE précis: Practical implementation of minimum standard guidelines for fluorescence-based quantitative real-time PCR experiments. BMC Molecular Biology, 11:74.

Bødtker.G., Lysnes. K., Torsvik.T., Bjørnestad. E.Ø. and Sunde, E. (2009). Microbial analysis of backflowed injection water from a nitrate-treated North Sea oil reservoir. Journal Ind Microbiological Biotechnology Vol. 36, p. 439-450.

Clariant Oil Services Scandinavia AS. (2018). Personal communication. Hovd, T.

ConocoPhillips. (2017). 2017 GEA Injection Water Quality Report. Kinn, M.

ConocoPhillips. (2018). Personal communication. Shutemov, D.

Costerton, J. W. Introduction to biofilm. (1999). International Journal of Antimicrobial Agents Vol. 11, p. 217-221.

Council of the European Union, European Parliament. (1998). DIRECTIVE 98/8/EC OF THE EUROPEAN PARLIAMENT AND OF THE COUNCIL [Online]. Available: http://www.reach-

compliance.eu/greek/legislation/docs/launchers/biocides/launch-1998-8-EC.html last accessed: 01.03.18.

Dahllof, I., Baillie, H. and Kjelleberg, S. (2000). rpoB-Based Microbial Community Analysis Avoids Limitations Inherent in 16S rRNA Gene Intraspecies Heterogeneity. Applied and Environmental Microbiology. Vol. 66, No. 8, p. 3376-3380.

De Beer, D., Srinivasan, R. and Stewart, P. S. (1994). Direct Measurement of Chlorine Penetration into Biofilms during Disinfection. Applied and Environmental Microbiology. Vol.60, No.12, p.4339-4344.

Dhanasekaran, S., Doherty, T. M., Kenneth, J., and TB Trials Study Group. (2010). Comparison of different standards for real-time PCR-based absolute quantification. Journal of Immunological Methods 354, p.34-39.

Duncan, K. E., Gieg, L. M., Parisi, V. A., Tanner, R. S., Tringe, S. G., Bristow. J. and Suflita. J. M. (2009). Biocorrosive Thermophilic Microbial Communities in Alaskan North Slope Oil Facilities. Environmental Science Technology. Vol. 43, p.7977-7984.

Dunsmore, B. C., Whitfield, T. B., Lawson, P. A. and Collins, M. D. (2004). Corrosion by sulphate-reducing bacteria that utilize nitrate. NACE 2004. Paper 04763. NACE International, Houston, Texas.

Eckert, R. B. and Skovhus, T. L. (2016). Advances in the application of molecular microbiological methods in the oil and gas industry and links to microbiologically influenced corrosion. International Biodeterioration & Biodegradation.

Edwards, K., Logan, J. and Saunders, N. (2004). Real-time PCR: An Essential Guide. Chapter 6. Horizon Bioscience, Wymondham.

Enning, D., Venzlaff, H., Garrelfs, J., Dinh, H. T., Meyer, V., Mayrhofer, K., Hassel, A. W., Stratmann, M. and Widdel, F. (2012). Marine sulfate-reducing bacteria cause serious corrosion of iron under electroconductive biogenic mineral crust. Environmental Microbiology. Vol. 14, p. 1772-1787.

Geets, J., Borremans, B., Ludo, D., Springael, D., Vangronsveld, J., van der Lelie, D. and Vanbroekhoven, K. (2006). DsrB gene-based DGGE for community and diversity surveys of sulfate-reducing bacteria. Journal of Microbiological Methods. Vol.66, p. 194-205.

Ghazy, E. A., Mahmoud, M. G., Asker, M. S., Mahmoud, M. N., Abo Elsoud, M. M. and Abdel Sami, M. E. (2011). Cultivation and Detection of Sulfate Reducing Bacteria (SRB) in Sea Water. Journal of American Science. Vol. 7.

Gieg. L.M., Jack. T.R. and Foght. J.M. (2011). Biological Souring and Mitigation in Oil Reservoirs. Applied Microbiology Biotechnology, Vol. 92, p.263-282.

Hamouda, A. A. (1991). Water Injection Quality in Ekofisk – UV Sterilization and Monitoring Techniques. SPE 21048.

Hoffmann, H., Devine, C. and Maxwell, S. (2007). Application of Molecular Microbiology Techniques as Tools for Monitoring Oil Field Bacteria. NACE International, paper No. 07508.

Hoffmann, H. and Spark, I. (2012). Injection Seawater versus Produced Water SRB and Archaea Populations in Oilfield Systems. SPE 155101.

Hurst, C., Crawford, R., Garland, J., Lipson, D., Mills, A. and Stetzenbach, L (ed). (2007). Manual of Environmental Microbiology. Chapter 71: Oil Field Microbiology. Third Edition. ASM Press, Washington DC.

Integrated DNA Technologies. (2017). Tips for working with gBlocks Gene Fragments [Online]. Available: https://eu.idtdna.com/pages/education/decoded/article/tips-for-working-with-gblocks-gene-fragments last accessed: 19.12.18.

Integrated DNA Technologies. (2018). Calculations: Converting from nanograms to copy number [Online]. Available: https://eu.idtdna.com/pages/education/decoded/article/calculations-converting-from-nanograms-to-copy-number last accessed: 21.03.18.

Javaherdashti, R. (2008). Microbiologically Influenced Corrosion: An Engineering Insight. London, United Kingdom: Springer London, pp. 49-57.

Jensen, M. L., Lundgaard, T., Jensen, J. and Skovhus, T. L. (2013). Improving Risk Based Inspection with Molecular Microbiological Methods. NACE International. Paper No. 2247.

Jhobalia, C. M., Hu, A., Gu, T. and Nesic, S. (2005). Biochemical Engineering Approaches To MIC. Paper No. 5500. Corrosion 2005.

Johnson, R. J. and Crane, J. (2017). Combining Advanced Biocide Evaluation and Microbial Monitoring to Optimise Microbial Control. SPE-184521-MS.

Kaster, K. M., Grigoriyan, A., Jenneman, G. and Voordouw, G. (2007). Effect of nitrate and nitrite on sulfide production by two thermophilic, sulfate-reducing enrichments from an oil field in the North Sea. Applied Microbiology Biotechnology, Vol.75, p.195-203.

Kim, J., Lim, J. and Lee, C. (2013). Quantitative real-time PCR approaches for microbial community studies in wastewater treatment systems: Applications and considerations. Biotechnology Advances, Vol. 31, p.1358-1373.

Kip, N. and van Veen, J. A. (2015). Mini Review, The Dual role of microbes in corrosion. Department of Microbial Ecology, Netherlands Institute of Ecology. The ISME Journal, Vol.9, p.542-551.

Klein, M., Friedrich, M., Roger, A. J., Hugenholtz, P., Fishbain, S., Abicht, H., Blackall, L. L., Stahl, D. A. and Wagner, M. (2001). Multiple Lateral Transfers of Dissimilatory Sulfite Reductase Genes between Major Lineages of Sulfate-Reducing Prokaryotes. Journal of Bacteriology. P. 6028-6035.

Kondo, R., Shigematsu, K. and Butani, J. (2008). Rapid enumeration of sulphate-reducing bacteria from aquatic environments using real-time PCR. Plankton Benthos Research. Vol. 3, p. 180-183.

Kuijvenhoven, C., Noirot, J., Bostock, A. M., Chappell, D. and Khan, A. (2006). Use of nitrate to mitigate reservoir souring in Bonga deepwater development offshore Nigeria. SPE 92795. Production and Operations.

Larsen, J., Skovhus, T.L., Saunders, A.M., Højris, B. and Agerbæk, M. (2008). Molecular Identification of MIC Bacteria from Scale and Produced Water: Similarities and Differences. NACE Corrosion. Paper No. 08652.

Larsen, L., Sørensen, K., Højris, B. and Skovhus, T. L. (2009). Significance of Troublesome Sulfate-Reducing Prokaryotes (SRP) in Oil Field Systems. NACE International. Paper No. 09389.

Larsen, J., Rasmussen, K., Pedersen, H., Sørensen, K. B., Lundgaard, T., and Skovhus, T. L. (2010). Consortia of MIC Bacteria and Archaea causing Pitting Corrosion in Top Side Oil Production Facilities. Corrosion 2010, Paper No. 10252. Houston, TX:NACE International.

Larsen, J., Sørensen, K. B., Holmkvist, L. and Skovhus, T. L. (2011). Identification and quantification of Microorganisms involved in Downhole MIC in a Dan Oil Producing Well. Corrosion Paper No. 17792. (Houston, TX:NACE International).

Lee, C., Brown, B., Jones, D., Duet, S., Cornell, J., Sharma, N. and Lin, X (2015). Field Applications for On-Site DNA Extraction and qPCR. NACE International, Paper No. 5686.

Liamleam, W. and Annachhatre, A. P. (2007). Electron donors for biological sulfate reduction. Biotechnology Adv Vol. 25, Issue 5, p.452-463.

Life Technologies™. (2012). Real-time PCR handbook [Online]. Available: www.gene-quantification.com/real-time-pcr-handbook-life-technologies-update-flr.pdf last accessed: 05.05.18.

Lin, X., Sharma, N. and Lee, C. (2015). Development and Validation of In-Field qPCR Methods for Water Microbial Analysis at Oil and Gas Facilities. NACE International, Paper No. 5948.

Liu, H., Tan, S. Yu, T. and Liu, Y. (2016). Sulfate reducing bacterial community and in situ activity in mature fine tailings analysed by real time qPCR and microsensor. Journal of Environmental Sciences. Vol. 44, p. 141-147.

Lomans, B. P., de Paula, R., Geissler, B., Kuijvenhoven, C. A. T. and Tsesmetzis, N. (2016). Proposal of Improved Biomonitoring Standard for Purpose of Microbiologically Influenced Corrosion Risk Assessment. SPE-179919-MS.

Lozano-A, L.C., Bautista, M. A., Dussan-G, J. and Vives-Florez, M. J. (2008). DNA Extraction from Heavy Oil Contaminated Microcosms and RpoB Gene PCR Amplification. Actual Biology. Vol 30 (88), p. 7-14.

Malorny, B., Lofstrom, C., Wagner, M., Kramer, N. and Hoorfar, J. (2008). Enumeration of *Salmonella* Bacteria in Food and Feed Samples by Real-Time PCR for Quantitative Microbial Risk Assessment. Applied and Environmental Microbiology, Vol.74, No.5. p.1299-1304.

NACE International. (2014). Standard Test Method. Field Monitoring of Bacterial Growth in Oil and Gas Systems. TM0194-2014.

Nihalani, M. C., Verma, S., Kumar, J., Dubey, H., Bharali, N. K., Mandal, A. K. and Lal, B. (2010). Managing Sulphate Reducing Bacteria (SRB) Problem Associated With Produced Water in One of the Oil Fields of Oil India Limited – A Case Study. SPE 127418.

Oblinger, J. L. and Koburger, J. A. (1975). Understanding and Teaching the Most Probable Number Technique. Journal of Milk Food Technologies. Vol. 38, No. 9, p. 540-545.

Ollivier, B. and Magot, M. (2005). Petroleum Microbiology. ASM Press, Washington, D.C.

Opel, K. L., Chung, D. and McCord, B. R. (2010). A Study of PCR Inhibition Mechanisms Using Real Time PCR. Journal of Forensic Sciences. Vol. 55, No. 1.

Oyekola, O. O., van Hille, R. P., Harrison, S. T. L. (2010). Kinetic analysis of biological sulphate reduction using lactate as carbon source and electron donor: Effect of sulphate concentration. Chemical Engineering Science, Vol. 65, s.4771-4781.

Patton, C. C. (1990). Injection-Water Quality. SPE 21300.

Plugge, C. M., Zhang, W., Scholten, J. C. M. and Stams, A. J. M. (2011). Metabolic flexibility of sulfate-reducing bacteria. Frontiers in Microbiology. Vol. 2, article 81.

Pope, D. H., Dziewulski, D. M., Zintel, T. P. and Siebert, O. (1988). Guide to the investigation of microbial corrosion in gas industry facilities. Gas Research Institute, Chicago.

Pots, B. F. M., John, R. C., Rippon, I. J., Thomas, M. J. J. S., Kapusta, S. D., Girgis, M. M. and Whitham, T. (2002). Improvements On De Waard-Milliams Corrosion Prediction and Applications to Corrosion Management. NACE International. Paper No. 02235.

QIAGEN. 2015. QIAEX® II Handbook – For DNA extraction from agarose and polyacrylamide gels and for desalting and concentrating DNA from solutions [Online]. Available: file:///C:/Users/Eier/Downloads/HB-1167-002-1090250%20HB%20QIAEX%20II%201214%20WW.pdf last accessed: 02.03.18.

QIAGEN. 2017. DNeasy® PowerSoil® Kit Handbook – For the isolation of microbial genomic DNA from all soil types [Online]. Available: file:///C:/Users/Eier/Downloads/HB-2257-001_1104560_HB_DNY_PowerSoil_0517_WW.pdf last accessed: 15.05.18.

Robinson, K., Ginty, W., Samuelsen, E., Lundgaard, T. and Skovhus, T. L. (2010). Reservoir Souring in a Field With Sulphate Removal: A Case Study. SPE 132697.

Rochon, J., Creusot, M.R. and, Rivet.P., Roque, C and Renard, M. (1996). Water Quality for Water Injection Wells. SPE 31122.

Samant, A. K. and Anto, P. F. (1993). Microbial Induced Corrosion and Subsea Pipeline Failure. The International Society of Offshore and Polar Engineers.

Sigma-Aldrich. (1999). Phenol Red Dextrose Broth product information [Online]. Available: https://www.sigmaaldrich.com/content/dam/sigma-aldrich/docs/Sigma/Datasheet/5/p9226dat.pdf last accessed: 27.10.17.

Skovhus, T.L., Holmkvist. L., Andersen. K., Pedersen. H. and Larsen.J. (2012). MIC Risk Assessment of the Halfdan Oil Export Spool. SPE 155080.

Skovhus, T.L., Ramsing.N.B., Holmstrom. C., Kjelleberg. S. and Dahllof,I. (2004). Real-Time Quantitative PCR for Assesment of Abundance of *Psedoalteromonas* Species in Marine Samples. Applied and Environmental Microbiology. Vol. 70, No.4, p.2373-2382.

Society for Mucosal Immunology. (2014). PCR: The Polymerase Chain Reaction [Online]. Available: http://www.socmucimm.org/pcr-polymerase-chain-reaction/ last accessed: 08.05.18.

Spark, I. and Mutch, K. (2002). Microbial Monitoring to Minimise Corrosion and Formation Damage in the Oil Industry. SPE 78572.

Smits, T.H.M., Devenoges, C., Szynalski, K., Maillard, J and Holliger, C. (2004). Development of a real-time PCR method for quantification of the three genera *Dehalobacter*, *Dehalococcoides* and D*esulfitobacterium* in microbial communites. Journal of Microbial Methods Vol.57, p.369-378.

Suzuki, M. T., Taylor, L. T. and Delong, E. F. (2000). Quantitative analysis of small-subunit rRNA genes in mixed microbial populations via 5'-Nuclease assays. Applied Environmental Microbiology. Vol. 66, p.4605-4614.

Taylor, S., Wakem, M., Dijkman, G., Alsarraj, M. and Nguyen, M. (2010). A practical approach to RT-qPCR-Publishing data that conform to the MIQE guidelines. Elsevier. Methods 50, S1-S5.

Thermo Fisher Scientific. (2011). PureLink Quick Plasmid Miniprep Kit [Online]. Available: https://assets.thermofisher.com/TFS-Assets/LSG/manuals/purelink_quick_plasmid_qrc.pdf last accessed: 27.03.18.

Thermo Fisher Scientific. (2012). ScaI product information [Online]. Available: https://assets.thermofisher.com/TFS-Assets/LSG/manuals/MAN0012119_ScaI_10_UuL_1000U_UG.pdf last accessed: 15.04.18.

ThermoFisher Scientific. (2014). TOPO® TA Cloning® Kit [Online]. Available: https://tools.thermofisher.com/content/sfs/manuals/topota_man.pdf last accessed: 15.04.18.

Thermo Fisher Scientific. (2015). Assessment of Nucleic Acid Purity [Online]. Available: https://tools.thermofisher.com/content/sfs/brochures/TN52646-E-0215M-NucleicAcid.pdf last accessed: 15.04.18.

Thermo Fisher Scientific. (2016). Real-time PCR (qPCR) defined [Online]. Available: https://www.thermofisher.com/no/en/home/life-science/pcr/real-time-pcr/qpcr-education.html last accessed: 10.05.18.

Thermo Fisher Scientific. (2018). TaqMan vs. SYBR Chemistry for Real-Time PCR [Online]. Available: http://www.thermofisher.com/no/en/home/life-science/pcr/real-time-pcr/real-time-pcr-learning-center/real-time-pcr-basics/taqman-vs-sybr-chemistry-real-time-pcr.html last accessed: 01.05.18.

Valasek, M. A. and Repa, J. J. (2005). The power of real-time PCR. Advanced Physiological Education. Vol. 29, p. 151-159.

Veil, J. A., Puder, M. G., Elcock, D. and Redweik, R.J. (2004). A White Paper Describing Produced Water from Production of Crude Oil, Natural Gas, and Coal Bed Methane. Prepared for: U.S. Department of Energy. National Energy Technology Laboratory.

Videla, H. A., Herrera, L. K. and Edyvean, R. G. (2005). An updated overview of SRB induced corrosion and protection of carbon steel. Corrosion, Paper No. 05488.

von Wolzogen Kuhr, C. A. H. and van der Vlugt, L. S. (1934). The graphitization of cast iron as an electrochemical process in anaerobic soil. Water 18, p.147-165.

Voordouw, G., Nemati, M. and Jenneman, G. E. (2002). Use of nitrate-reducing, sulfide oxidizing bacteria to reduce souring in oilfields: interactions with SRB and effects on corrosion. Corrosion, paper No. 02034. NACE International, Houston, Texas.

Voordouw, G., Grigoryan, A. A., Lambo, A., Lin, S., Park, H. S., Jack, T. R., Coombe, D., Clay, B., Zhang, F., Ertmoed, R., Miner, K. and Arensdorf, J. J. (2009). Sulfide Remediation by Pulsed Injection of Nitrate into a Low Temperature Canadian Heavy Oil Reservoir. Environmenta.Science.Technology, Vol. 43, p. 9512-9518.

Whelan, J. A., Russel, N. B. and Whelan, M. A. (2003). A method for the absolute quantification of cDNA using real time PCR. Journal Immunol Methods 278, p.261-269.

Whitby, C. and Skovhus, T. L. (2009). Applied Microbiology and Molecular Biology in Oilfield Systems. Springer. London.

Xu, D. and Gu, T. (2014). Carbon source starvation triggered more aggressive corrosion against carbon steel by the *Desulfovibrio vulgaris* biofilm. International Biodeterioration & Biodegradiation 91, p.74-81.

Zhang, T. and Fang, H. H. P. (2006). Applications of real-time polymerase chain reaction for quantification of microorganisms in environmental samples. Applied Microbial Biotechnology, 70, p.281-289.

Zhu, X. Y., Ayala, A., Modi, H and Kilbane II, J. J. (2005). Application of Quantitative, Real-time PCR in Monitoring Microbiologically-Influenced Corrosion (MIC) in Gas Pipelines. Corrosion Paper No. 05493.

Zuo, R. (2007). Biofilms: strategies for metal corrosion inhibition employing microorganisms. Applied Microbiology Biotechnology. 76, p.1245-1253.

Appendix

Appendix 1: DNA extraction and gel electrophoresis results

Appendix 2: Gel electrophoresis results for optimized primer set Dsr2060F/Dsr4R and rpoB1698F/rpoB2041R

Appendix 3: DNA concentration and purity of GF1 with primer set Dsr2060F/Dsr4R

Appendix 4: DNA concentration and purity of GF1 with primer set DSRp2060F/Dsr4R

Appendix 5: DNA concentration and purity of plasmid DNA with PCR insert

Appendix 6: Standard curve optimization, GF1 with primer set Dsr2060F/Dsr4R

Appendix 7: Standard curve optimization, GF1 with primer set DSRp2060F/Dsr4R

Appendix 8: Standard curve optimization, GF 2 with primer set DSRp2060F/Dsr4R

Appendix 9: Standard curve optimization post cloning with primer set DSRp2060F/Dsr4R

Appendix 10: Standard curve optimization post cloning with primer set DSRp2060F/Dsr4R and samples

Appendix 11: Raw data for standard curve, quantified samples and raw melt data

Appendix 1: DNA extraction and gel electrophoresis results

DNA extraction and gel electrophoresis results. Extracted DNA was run a 1.0% agarose gel containing 5.0 µl GelGreen™ at 100 V for 60 minutes.

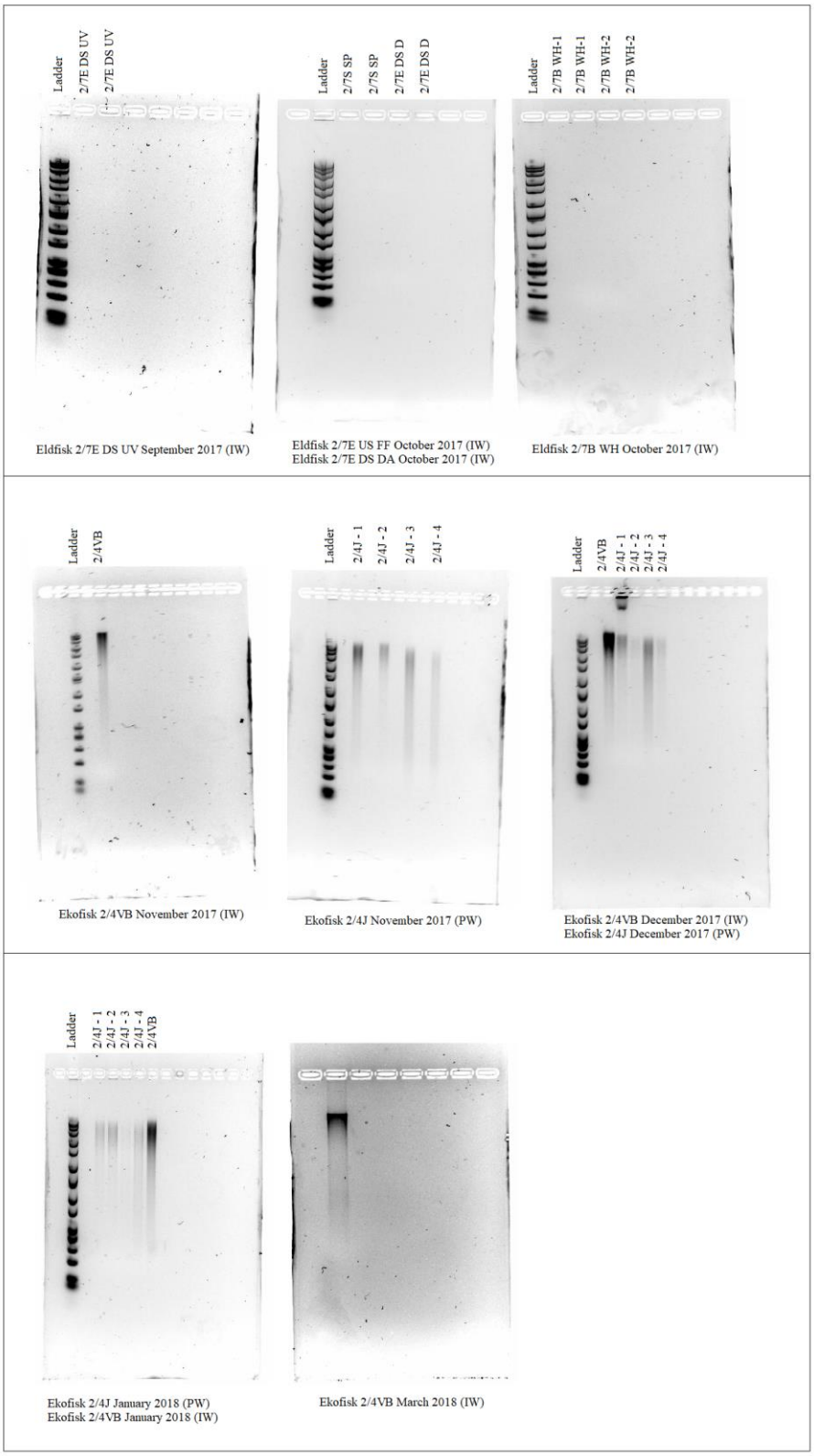

Appendix 2: Gel electrophoresis results for optimized primer set Dsr2060F/Dsr4R and rpoB1698F/rpoB2041R.

Gel electrophoresis results for optimized primer set Dsr2060F/Dsr4R (left, T_a=55°C) and rpoB1698F/rpoB2041R (right, T_a=48°C).

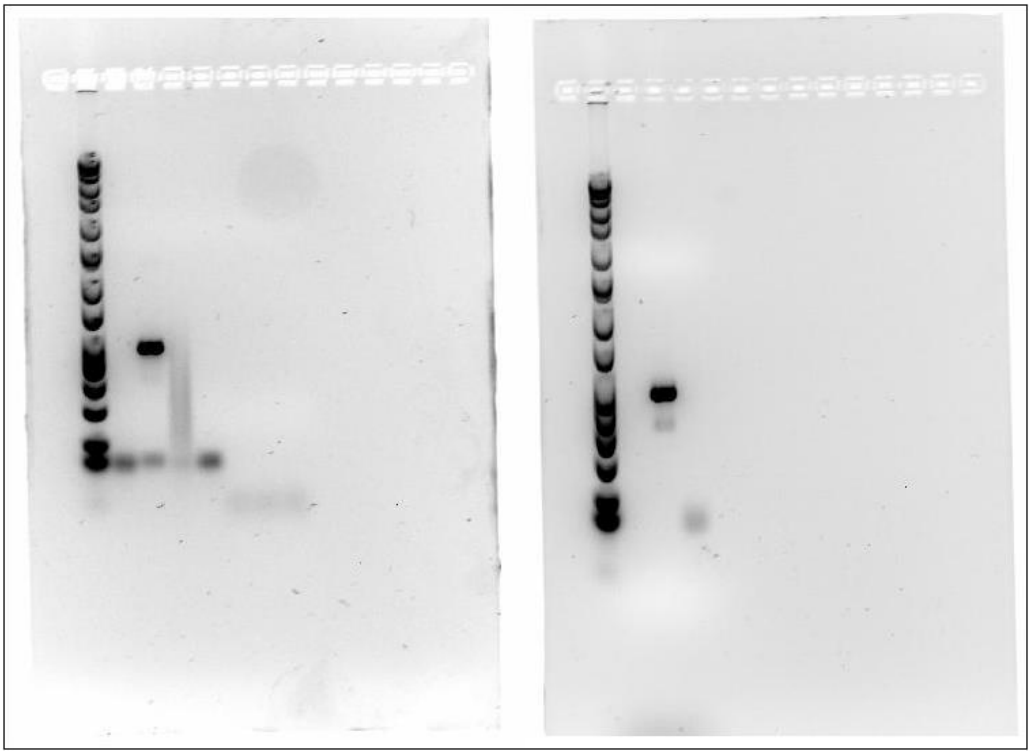

Appendix 3: DNA concentration and purity of GF1 with primer set Dsr2060F/Dsr4R

DNA and purity measured by Thermo Scientific™ Nanodrop™ One Microvolume UV-Vis Spectrophotometer.

	ng/µl	Avg. ng/µl	A_{260}/A_{280}	A_{260}/A_{230}
Sample 1	4.7	4.3	1.92	0.03
	3.8		1.68	0.02
	4.5		1.78	0.02
Sample 2	7.4	4.4	1.78	0.08
	3.3		1.42	0.04
	3.5		1.56	0.04
	3.5		1.74	0.04
Sample 3	8.9	5.4	1.65	0.08
	5.2		1.82	0.05
	3.9		2.07	0.04
	3.5		1.88	0.03
Sample 4	3.5	3.6	2.38	0.02
	3.9		1.83	0.02
	3.5		2.00	0.02
Sample 5	11.3	10.1	1.87	0.02
	9.3		2.02	0.01
	9.8		2.03	0.02

Appendix 4: DNA concentration and purity of GF1 with primer set DSRp2060F/Dsr4R

DNA and purity measured by Thermo Scientific™ Nanodrop™ One Microvolume UV-Vis Spectrophotometer.

	ng/µl	Avg. ng/µl	A_{260}/A_{280}	A_{260}/A_{230}
Sample 1	51.6	40.9	1.75	0.12
	31.8		1.84	0.08
	39.4		1.81	0.09
Sample 2	40.8	33.5	1.84	0.08
	29.3		1.94	0.06
	30.3		2.00	0.06
Sample 3	30.4	30.3	1.97	0.12
	30.0		1.99	0.12
	30.5		1.97	0.12

Appendix 5: DNA concentration and purity of plasmid DNA with PCR insert (primer set DSRp2060F/Dsr4R)

DNA and purity measured by Thermo Scientific™ Nanodrop™ One Microvolume UV-Vis Spectrophotometer.

	ng/µl	Avg. ng/µl	A_{260}/A_{280}	A_{260}/A_{230}
Sample 2	9.3	8.5	1.84	0.02
	9.1		1.87	0.02
	7.1		1.87	0.02
Sample 3	5.7	6.0	2.07	0.01
	7.0		2.43	0.01
	5.4		2.52	0.01
Sample 4	5.8	4.9	1.73	0.01
	4.4		1.90	0.01
	4.4		2.64	0.01
Sample 5	7.5	5.7	2.06	0.01
	5.5		2.49	0.01
	4.1		3.64	0.01
Sample 6	12.5	9.4	1.84	0.02
	7.9		1.97	0.01
	7.7		2.05	0.01

Appendix 6: Standard curve optimization, GF1 with primer set Dsr2060F/Dsr4R

Test 5, dilution series from 10^7 to 10^1 and primer concentration 0.25µM.

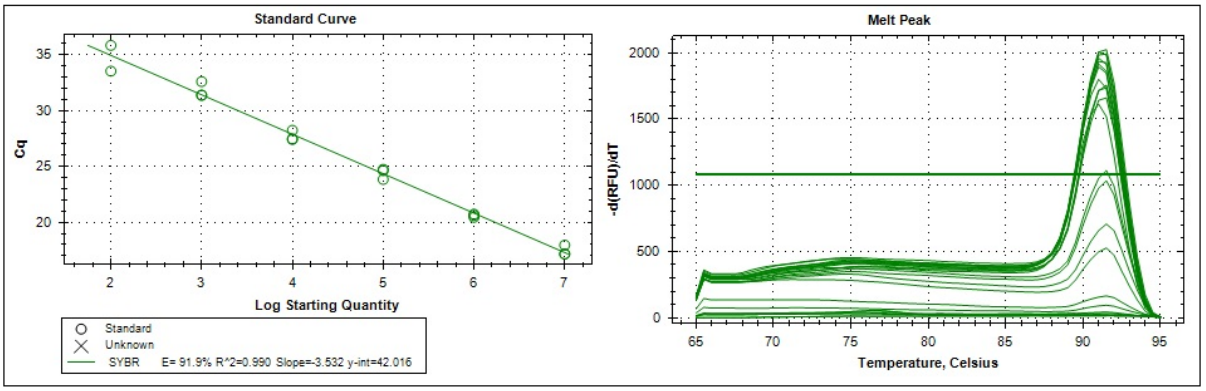

Test 6, dilution series from 10^7 to 10^1 and primer concentration 0.25 µM.

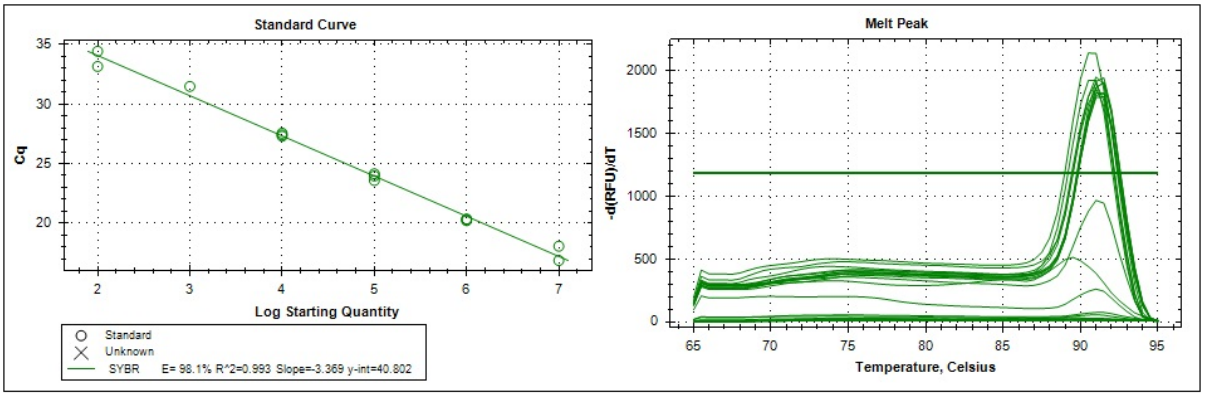

Test 16, Dilution series from 10^7 to 10^3 and primer concentration 0.5 µM.

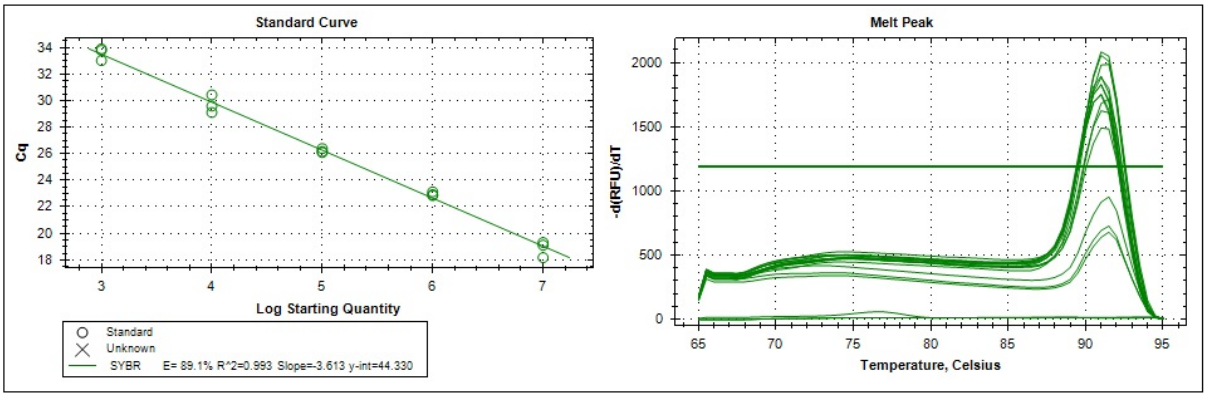

Test 18, dilution series from 10^7 to 10^3 and primer concentration 0.5 µM.

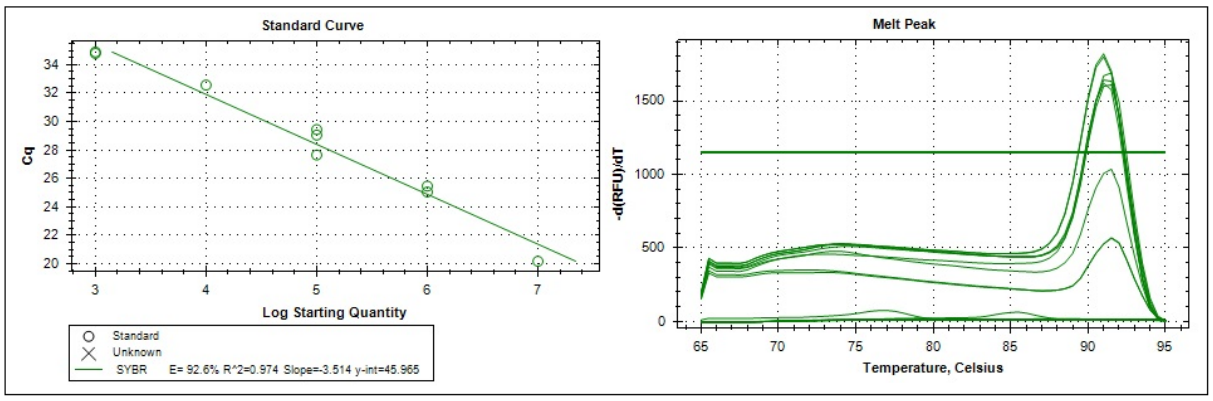

Test 23, Dilution series from 10^7 to 10^3 and primer concentration 0.5 µM.

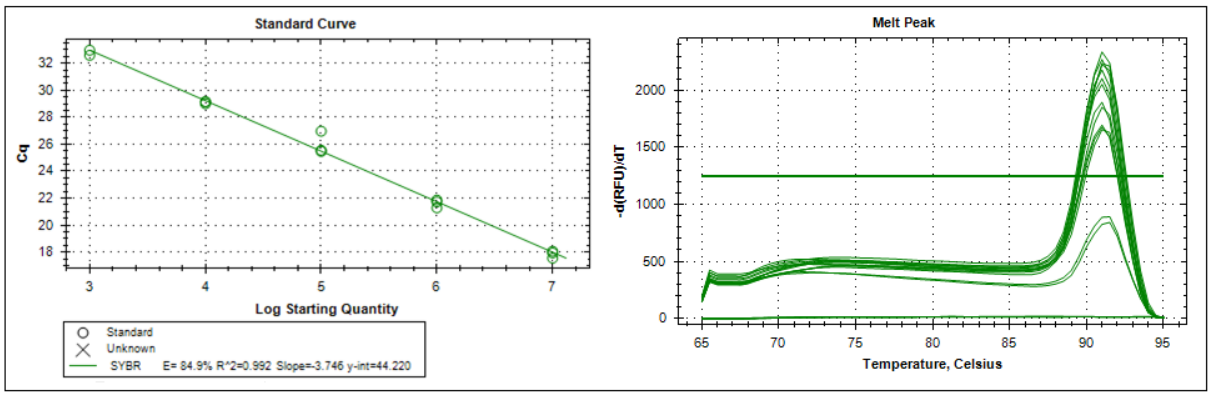

Appendix 7: Standard curve optimization, GF1 with primer set DSRp2060F/Dsr4R

Test 3, dilution series from 10^7 to 10^3 and primer concentration 0.25 µM.

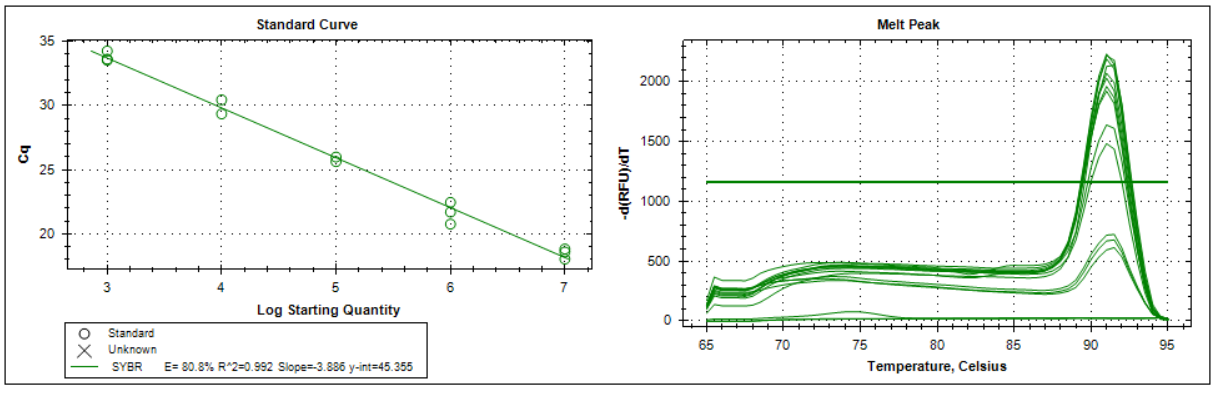

Appendix 8: Standard curve optimization, GF 2 with primer set DSRp2060F/Dsr4R

Test 3, Dilution series from 10^7 to 10^3 and primer concentration 0.5 µM.

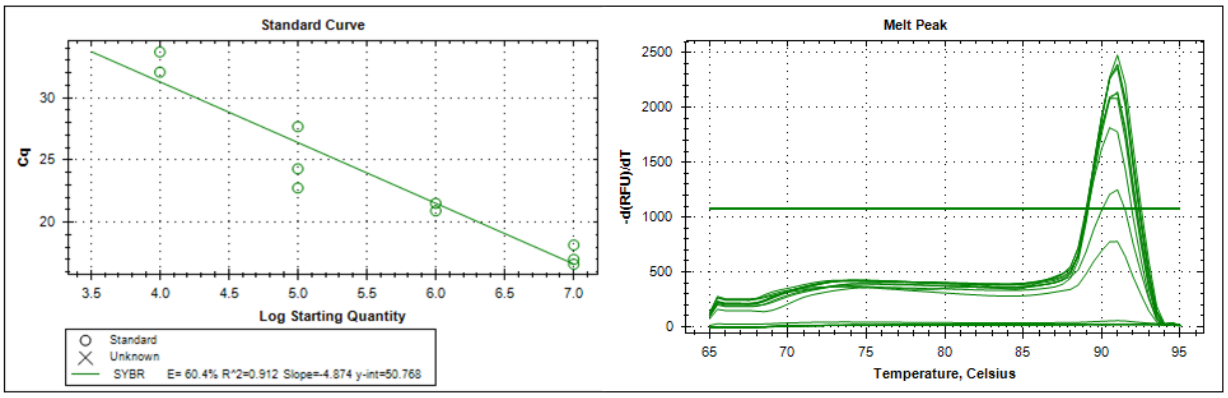

Appendix 9: Standard curve optimization post cloning with primer set DSRp2060F/Dsr4R

Test 1, Dilution series from 10^7 to 10^3 and primer concentration 0.5 µM.

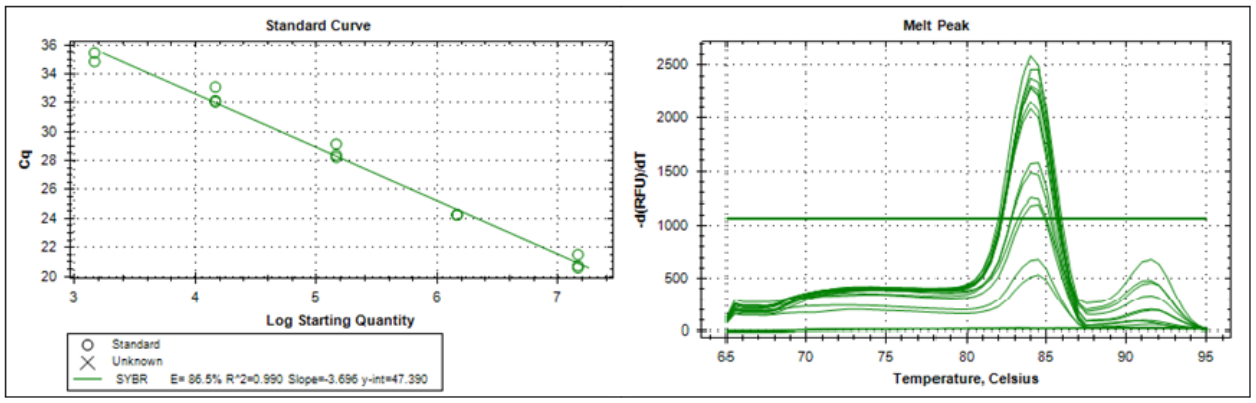

Test 4, Dilution series from 10^7 to 10^3 and primer concentration 0.5 µM.

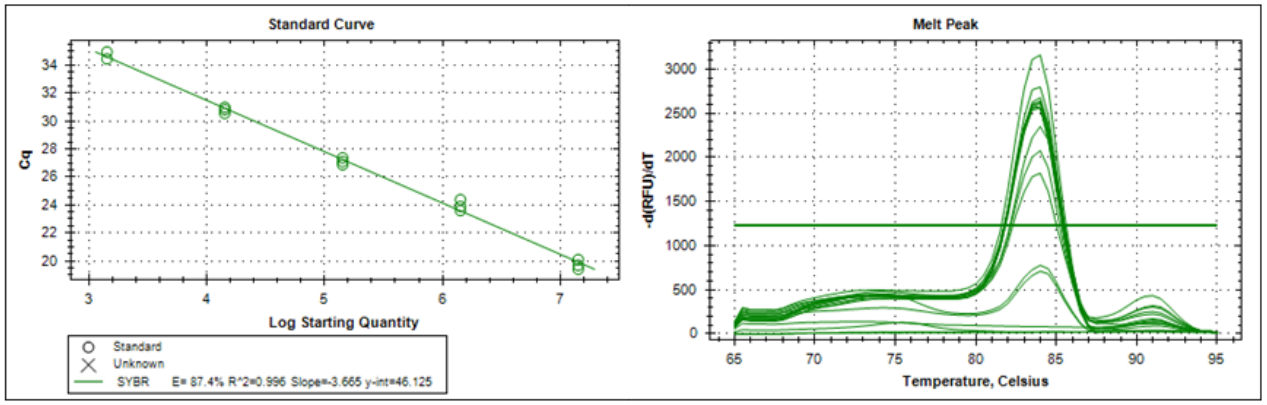

Appendix 10: Standard curve optimization post cloning with primer set DSRp2060F/Dsr4R and samples

Test 4, Dilution series from 10^8 to 10^3 and primer concentration 0.5 µM.

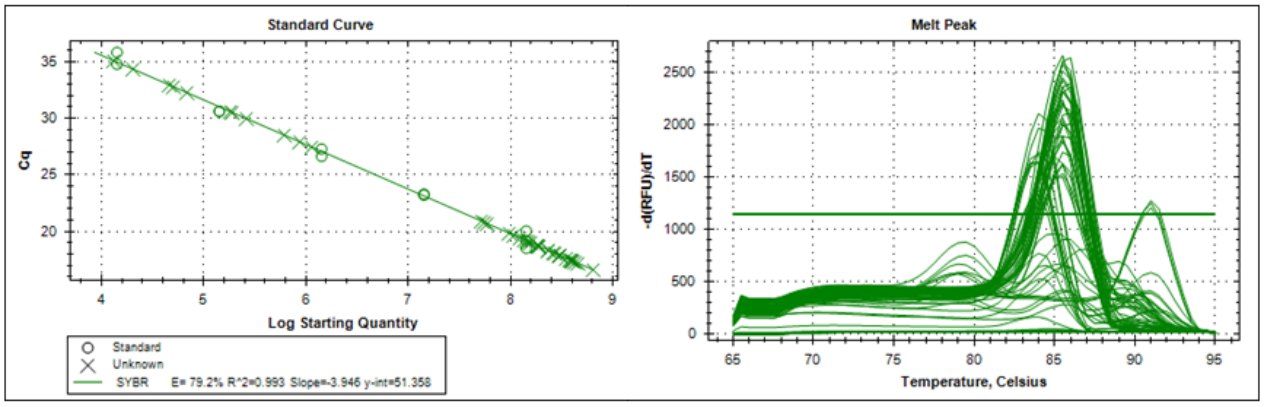

Appendix 11: Raw data for standard curve, quantified samples and raw melt data

	Samples	Cq	Starting Quantity (SQ)	Log Starting Quantity	SQ Standard deviation
Standards	10^8	18,01	1,42E+08	8,152	-
	10^8	18,59	1,42E+08	8,152	-
	10^8	17,79	1,42E+08	8,152	-
	10^7	22,28	1,42E+07	7,152	-
	10^7	21,01	1,42E+07	7,152	-
	10^7	20,77	1,42E+07	7,152	-
	10^6	24,6	1,42E+06	6,152	-
	10^6	24,68	1,42E+06	6,152	-
	10^6	24,49	1,42E+06	6,152	-
	10^5	28,97	1,42E+05	5,152	-
	10^5	29,33	1,42E+05	5,152	-
	10^5	28,21	1,42E+05	5,152	-
	10^4	31,78	1,42E+04	4,152	-
	10^4	33,02	1,42E+04	4,152	-
	10^4	32,22	1,42E+04	4,152	-
	10^3	33,8	1,42E+03	3,152	-
	10^3	34,92	1,42E+03	3,152	-
	10^3	35,63	1,42E+03	3,152	-
	NTC	N/A	N/A	N/A	-
	NTC	N/A	N/A	N/A	-
	NTC	N/A	N/A	N/A	-
November 2017	Ekofisk 2/4J-1	16,77	3,37E+08	8,528	1,06E+08
	Ekofisk 2/4J-1	16,15	5,13E+08	8,71	
	Ekofisk 2/4J-1	16,84	3,23E+08	8,509	
	Ekofisk 2/4J-2	17,44	2,16E+08	8,334	2,40E+07
	Ekofisk 2/4J-2	17,59	1,95E+08	8,29	
	Ekofisk 2/4J-2	17,26	2,43E+08	8,385	
	Ekofisk 2/4J-3	16,45	4,18E+08	8,621	7,43E+07
	Ekofisk 2/4J-3	16,43	4,25E+08	8,628	
	Ekofisk 2/4J-3	16,99	2,93E+08	8,466	
	Ekofisk 2/4J-4	17,3	2,38E+08	8,376	5,66E+07
	Ekofisk 2/4J-4	17,5	2,08E+08	8,317	
	Ekofisk 2/4J-4	18,22	1,28E+08	8,107	
	Ekofisk 2/4VB	28,55	1,28E+05	5,106	6,01E+04
	Ekofisk 2/4VB	28,16	1,66E+05	5,219	
	Ekofisk 2/4VB	30,02	4,79E+04	4,68	
December 2018	Ekofisk 2/4J-1	16,79	3,32E+08	8,522	5,84E+07
	Ekofisk 2/4J-1	17,31	2,35E+08	8,371	
	Ekofisk 2/4J-1	17,36	2,28E+08	8,358	
	Ekofisk 2/4J-2	18,78	8,80E+07	7,944	9,17E+06
	Ekofisk 2/4J-2	19,11	7,04E+07	7,848	
	Ekofisk 2/4J-2	18,85	8,38E+07	7,923	
	Ekofisk 2/4J-3	15,68	7,02E+08	8,846	1,42E+08
	Ekofisk 2/4J-3	16,34	4,50E+08	8,654	
	Ekofisk 2/4J-3	16,3	4,62E+08	8,664	
	Ekofisk 2/4J-4	17,68	1,84E+08	8,265	3,78E+07
	Ekofisk 2/4J-4	18,18	1,32E+08	8,119	
	Ekofisk 2/4J-4	18,44	1,11E+08	8,045	
	Ekofisk 2/4VB	27,42	2,73E+05	5,436	3,52E+06
	Ekofisk 2/4VB	22,72	6,33E+06	6,801	
	Ekofisk 2/4VB	28,04	1,80E+05	5,256	
Janaury 2018	Ekofisk 2/4J-1	17,19	2,55E+08	8,407	1,27E+07
	Ekofisk 2/4J-1	17,19	2,55E+08	8,406	
	Ekofisk 2/4J-1	17,32	2,33E+08	8,368	
	Ekofisk 2/4J-2	17,94	1,55E+08	8,19	7,64E+06
	Ekofisk 2/4J-2	17,81	1,69E+08	8,228	
	Ekofisk 2/4J-2	17,91	1,57E+08	8,197	
	Ekofisk 2/4J-3	18,8	8,70E+07	7,94	1,11E+07
	Ekofisk 2/4J-3	19,07	7,28E+07	7,862	
	Ekofisk 2/4J-3	19,23	6,52E+07	7,814	
	Ekofisk 2/4J-4	17,34	2,31E+08	8,364	1,94E+07
	Ekofisk 2/4J-4	17,46	2,13E+08	8,328	
	Ekofisk 2/4J-4	17,61	1,92E+08	8,284	
	Ekofisk 2/4VB	26,38	5,45E+05	5,736	2,00E+05
	Ekofisk 2/4VB	28,29	1,52E+05	5,182	
	Ekofisk 2/4VB	26,79	4,14E+05	5,617	
March 2018	Ekofisk 2/4VB	26,95	3,73E+05	5,572	1,02E+05
	Ekofisk 2/4VB	26,32	5,70E+05	5,756	
	Ekofisk 2/4VB	26,46	5,18E+05	5,714	

	Samples	Melt Temperature	Peak Height	Begin Temperature	End Temperature
Standards	10^8	84	2173,45	78,5	87,5
	10^8	84	2080,54	78,5	87,5
	10^8	84	2121,96	78,5	87
	10^7	84	2252,06	78	87,5
	10^7	84	2312,96	78	87,5
	10^7	84	2320,35	78,5	87,5
	10^6	84	2373,12	78	87,5
	10^6	84	2287,17	77,5	87,5
	10^6	84	2288,75	77,5	87,5
	10^5	84	2230,82	77,5	87,5
	10^5	84	2160,17	78	87,5
	10^5	84	2389,35	78,5	87,5
	10^4	84	1642,31	78,5	87,5
	10^4	84	1254,21	79	87,5
	10^4	84	1481,9	79	87,5
	10^3	None	None	None	None
	10^3	None	None	None	None
	10^3	None	None	None	None
	NTC	None	None	None	None
	NTC	None	None	None	None
	NTC	None	None	None	None
November 2017	Ekofisk 2/4J-1	86	2307,79	79	89
	Ekofisk 2/4J-1	86	2457,28	79	94
	Ekofisk 2/4J-1	85,5	2482,57	79	94
	Ekofisk 2/4J-2	86	2175,82	78,5	93,5
	Ekofisk 2/4J-2	86	2221,98	79,5	94
	Ekofisk 2/4J-2	86	2301,56	79,5	95
	Ekofisk 2/4J-3	86	2698,29	79	94
	Ekofisk 2/4J-3	86	2635,13	79	95
	Ekofisk 2/4J-3	85,5	2637,41	79	94
	Ekofisk 2/4J-4	85,5	2616,72	78,5	94
	Ekofisk 2/4J-4	86	2607,87	79	94
	Ekofisk 2/4J-4	86	2619,46	79	94
	Ekofisk 2/4VB	88	1150,07	82	95
	Ekofisk 2/4VB	88,5	1166,02	82	95
	Ekofisk 2/4VB	88	1154,15	82	95
December 2017	Ekofisk 2/4J-1	86	2088,96	78,5	93,5
	Ekofisk 2/4J-1	86	2112,98	78,5	93,5
	Ekofisk 2/4J-1	86	2114,82	78,5	93,5
	Ekofisk 2/4J-2	85,5	2033,81	78,5	89
	Ekofisk 2/4J-2	85,5	1943,38	79	88,5
	Ekofisk 2/4J-2	85,5	1979,35	78	88,5
	Ekofisk 2/4J-3	85,5	1824,79	79	88,5
	Ekofisk 2/4J-3	85,5	1750,43	79	88,5
	Ekofisk 2/4J-3	86	1668,5	79	88,5
	Ekofisk 2/4J-4	86	2433,09	79	94
	Ekofisk 2/4J-4	86	2564,68	79	94
	Ekofisk 2/4J-4	85,5	2688,8	79	93
	Ekofisk 2/4VB	None	None	None	None
	Ekofisk 2/4VB	85,5	2311,69	79	95
	Ekofisk 2/4VB	None	None	None	None
January 2018	Ekofisk 2/4J-1	86	2374,8	79	94
	Ekofisk 2/4J-1	86	2342,29	79	93,5
	Ekofisk 2/4J-1	86	2337,48	79	93,5
	Ekofisk 2/4J-2	85,5	2399,85	78,5	89
	Ekofisk 2/4J-2	85,5	2325,61	78,5	89
	Ekofisk 2/4J-2	85,5	2200,31	79	89
	Ekofisk 2/4J-3	86	2013,22	78,5	94
	Ekofisk 2/4J-3	85,5	2013,81	79,5	94
	Ekofisk 2/4J-3	85,5	2096,08	79	94
	Ekofisk 2/4J-4	85,5	2462,13	78,5	94
	Ekofisk 2/4J-4	85,5	2377,47	78,5	94
	Ekofisk 2/4J-4	85,5	2371,53	79	94
	Ekofisk 2/4VB	None	None	None	None
	Ekofisk 2/4VB	None	None	None	None
	Ekofisk 2/4VB	None	None	None	None
March 2018	Ekofisk 2/4VB	91	1471,58	85,5	95
	Ekofisk 2/4VB	91	1314,29	84	95
	Ekofisk 2/4VB	91	1282,6	84,5	95